Sentinel-6A : F06 Reprocessing Calval Assesment

Reference : SALP-RP-MAO-OP-17577-CN
Nomenclature : Sentinel-6A : F06 Reprocessing Calval Assesment
Issue : 02/ 00
Date : October 3, 2022

EUMETSAT
Eumetsat-Allee 1, D-64295 Darmstadt, Germany
Tel: +49 6151 807-7
Fax: +49 6151 807 555
http://www.eumetsat.int

Chronology Issues:		
Issue:	Date:	Reason for change:
1.0	2022-07-21	Creation
2.0	2022-09-06	Addition of tandem phase analysis, GMSL analysis and compliance status to system requirements.

People involved in this issue :				
	AUTHORS	**COMPANY**	**DATE**	**INITIALS**
Written by:	Bastien Courcol Emeline Cadier	CLS CLS		
Approved by:	François Bignalet-Cazalet	CNES		
Application authorised by:	C. Martin-Puig	EUMETSAT		

List of Tables

List of Figures

Applicable documents / reference documents

Contents

1. Introduction

Sentinel-6 is a collaborative Copernicus mission, implemented and co-funded by the European Commission, ESA, EUMETSAT and the USA through NASA and NOAA.

EUMETSAT is responsible for the Sentinel-6 operations as part of the Copernicus component of the EU Space Programme. The Sentinel-6 Quality Assessment reports are generated by CNES as per EUMETSAT-CNES agreement in the context of Copernicus.

This document presents the synthesis report concerning validation activities of Sentinel-6A PDAP 2022 reprocessing with Processing Baseline (PB) F06.

Since the launch of the Sentinel-6A satellite on 21st of November 2021, PDAP PB has been updated several times following the satellite commissionning activities. Sentinel-6A NTC (Non-Time Critical) products have been reprocessed using PB F06 until cycle 54 track 22. From cycle 54 track 23, PB F06 is used to compute operational NTC data.

This present global report deals with the complete reprocessed period of the Sentinel-6A mission, thanks to comparison with operational dataset, as well as comparison with Jason-3 over the tandem phase. This reprocessing present the first opportunity to assess Sentinel-6A data performance with an homogeneous PB version over the complete mission lifetime. The analysis is performed over ocean and using 1 Hz data.

This report is split into 6 main sections after this introduction describing the keys of the reprocessing campaign:

- first, the **data used** are presented.
- the **data coverage** and measurement validity issues are then presented.
- a synthetis of the **geophysical parameter derived from altimeter and radiometer** is exposed.
- a detailed comparison to Jason-3 over the **tandem phase**
- a GMSL analysis
- a compliance status to **system requirements**

2. Data used and processing

2.1. Sentinel-6A F06 reprocessed data

Sentinel-6A data has been reprocessed with Processing Baseline F06 (PB) for Non Time Critical (NTC) timeliness, for both LR (Low Resolution) and HR (High Resolution) modes.

The new baseline F06 only impacts HR data for all timeliness. The number of Doppler beams (a.k.a. looks) incoherently integrated within the stack to generate the multi-looked L1B power waveforms has been reduced, from 448 originally, to now 322 looks. This allows for not accounting undesired Doppler ambiguity effects within the stack observed from beginning of mission until present. With this new baseline, SWH differences between HR and LR are considerably reduced, and range differences between LR and HR are less dependent on SWH.

The reprocessed data spans from 2020/12/17 at 22:17:43 to 2022/04/28 at 01:29:52, corresponding to the period from cycle 4 track number 14 to cycle 54 track number 22.

The analysis is performed over ocean and using 1 Hz data. For LR and HR both ”ocean” retrackers were used, being MLE4 and SAMOSA, respectively.

A detailed description of the products can be found in the Sentinel-6A user handbook [1] and in the product notice [2].

2.2. Sentinel-6A operational data used for comparison

The operational data used for comparison has been corrected from the COG anomaly. This anomaly of 1.06m impacted the beginning of the mission and has been corrected on the 2021-02-09 (cycle 9 pass 114) for HR and on the 2021-02-15 (cycle 10 pass 005) for LR. To account for this anomaly in our analysis, 1.06 m was subtracted to the SSHA over the faulty period. The reason for this correction is to be able to compare the two datasets more adequatly without having the vertical scale shrinked or the beginning of the series out of bounds.

Accordingly, the validity flag was recomputed using the operational parameters on the corrected operational dataset. Otherwise, during the whole duration of the anomaly, all data would be edited. However, when this flag was computed for the HR mode, the cycle 54 was not yet available and so its 22 passes appear as edited. Please note that the 22 passes in Cycle 54 at the end of the reprocessing dataset have not been included in the comparisons with the operational data.

2.3. Jason-3 data used for comparison

Between 2020/12/17 to 2022/04/07 (cycle 4 to 51 for Sentinel-6A), Sentinel-6A and Jason-3 are flying in tandem formation on the same ground track with only 30 seconds apart, Jason-3 ahead of Sentinel-6A.

In this current report, Jason-3 GDR-F standard with MLE4 retracking was used to compare to Sentinel-6A reprocessed data. A detailed description of the products can be found in the Jason-3 product handbook [3].

Sentinel-6A F06 and Jason-3 GDR-F share the same standard in terms of geophysical corrections: same tide models, same mean surface height, etc. In particular :

- for the wind speed, Collard algorithm is used on both mission
- for the sea state bias, Sentinel-6A uses the same Sea State Bias parametrisation as Jason-3 GDR-f, both

in LR and in HR.

3. Data coverage and validity of measurements

This section consists in analysing the availability of data for level 2 NTC products before and after the re-processing. Futhermore the edited (invalidated) measurements are monitored and analysed.

The coverage of the PB F06 reprocessing is better than for the operational dataset, with 38 recovered passes in LR and 41 in HR, and **no new missing passes**.

3.1. Missing measurements

When looking directly at the data points, the differences between the two datasets are more significant. Table 1 lists the total number of passes in the reprocessed data, and the number of passes with a different number of points with respect to the operational dataset, with thresholds of 1 and 500 (i.e. 8min and 20s). About 4 to 18 % (for HR with at least 1 more missing point in reprocessed data) of passes have a different number of points. In HR, about 75% of the new missing points are located in non-RMC everywhere cycles. This table also includes

Parameter	LR	HR
Total number of passes in reprocessing	12622	12451
Number of passes with at least 1 more missing point wrt to operational dataset	592	2215
Number of passes with at least 1 less missing point wrt to operational dataset	559	463
Number of passes with at least 500 more missing points wrt to operational dataset	5	1
Number of passes with at least 500 less missing points wrt to operational dataset	42	41

Table 1 – Number of passes with a different number of missing points in reprocessed wrt operational. This includes passes that are entirely missing.

The major missing segments (more than 100 points or 1min40s) in reprocessed data that were available in operational data are listed below :

- 03/02/2021 : between 21:45:30 and 21:55:23 (C8 - P227) in LR
- 05/02/2021 : between 21:32:27 and 21:55:23 (C9 - P24) in LR
- 11/06/2021 : between 21:53:25 and 21:55:23 (C21 - P204) in LR
- 24/06/2021 : between 02:03:23 and 02:12:24 (C23 - P7) in LR
- 21/10/2021 : between 02:03:23 and 02:50:54 (C35 - P8) in LR and HR

Please note that the figures in this report have not been fully updated with all the available passes and are missing a few in the reprocessed dataset. In LR, theses passes are : c10 p1, c14 p254, c22 p169, c34 p138 to 151 and c37 p169. In HR, theses passes are : c22 p169, c34 p138 to 151 and c37 p169. The cyclic monitoring of available data for both dataset is presented in figure 1.

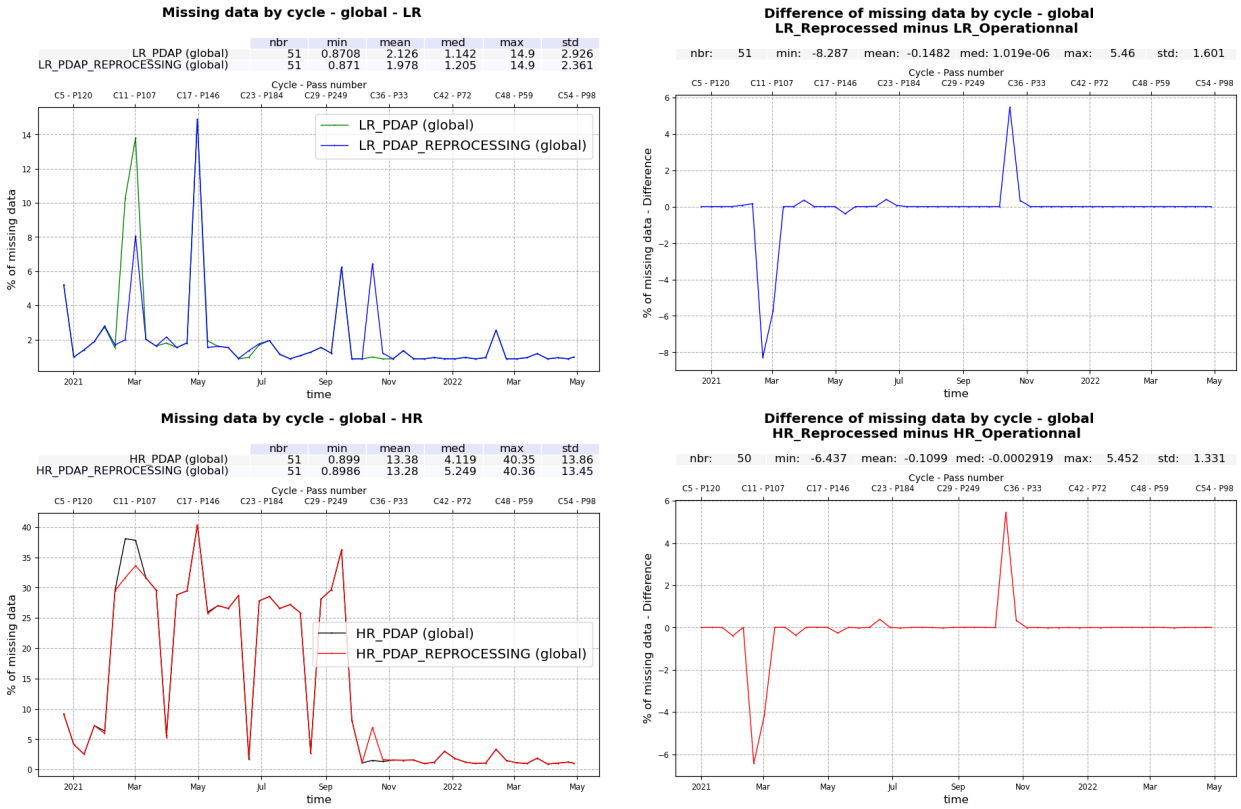

*Figure 1 – Percentage of missing data for the operational and reprocessed datasets (**left**) and their difference (**right**) for both LR (**top**) and HR (**bottom**). On the diffence plots, positive values represent a loss of data with the reprocessing and negative values a gain of data thanks to the reprocessing*

3.2. Edited measurements

3.2.1. Overview

The outlier detection or editing step of the Cal/Val process is applied to remove any measurement that is considered erroneous. Thus, it helps refining the various metrics which are provided in the specific sections dedicated to the performance over the ocean. The definition of an erroneous measurement, and of the accepted error level on the final sea level anomaly is of course a tradeoff between accuracy and data coverage. The monitoring of the percentage of valid and edited measurements also provides relevant information about the mission performances.
A series of editing criteria are used to detect outliers over ocean. This process is divided into 3 main parts:

- removal of all measurements affected by sea-ice.
- removal of all measurements which exceed defined thresholds on different parameters.
- further checks on along-track sla consistency.

For each step of the process, the number of outliers is routinely monitored at Cal/Val level. The number of removed data is used to detect processing anomalies which could be due to instrumental, geophysical or algorithmic changes. The process performed here is dedicated to ocean applications. Data over land are removed using a land/water mask prior to the analysis described in this section. The editing criteria have not been changed with the reprocessing.

The percentage of valid data per cycle after editing process for the operational and reprocessed dataset over ocean is monitored on figure 2. As expected, in both HR and LR, the number of edited points is closer and closer after each PDAP and PB updates (vertical dashed grey lines). The curves are visually identical after the last PB update (F05). In both LR and HR, there is a peak of edited measurements at cycle 13 that is caused by the anomaly during the PDAP v3.2 deployment, on NTC (and STC) C-band and MLE3 data due to incorrect mispointing. This anomaly was patched with the PDAP version 3.2.1. This peak is more significant in operational data compared to reprocessed data and is discussed in section 3.2.5..

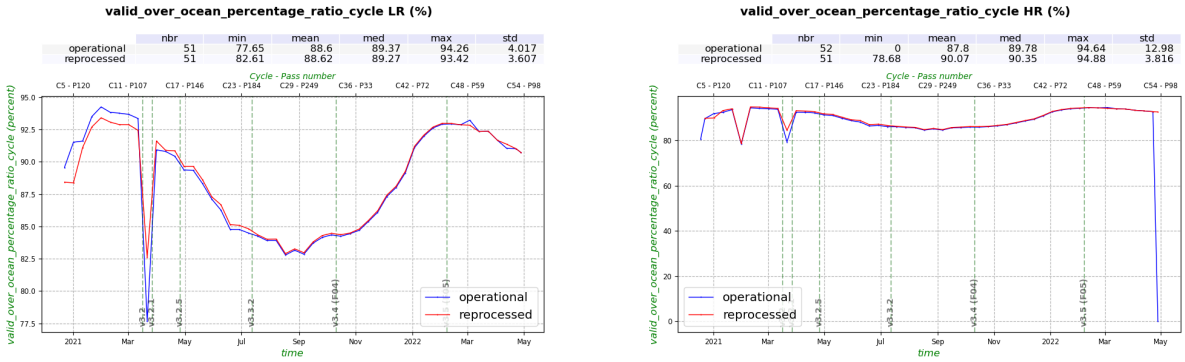

*Figure 2 – Percentage of valid measurement for the operational (blue) and reprocessed (red) datasets over ocean by cycle in LR (**left**) and HR (**right**)*

In LR, more points are edited in the reprocessed dataset before the cycle 13, because of the flag ice (cf section 3.2.2.), as opposed to the remainder of the time series.

In HR, the operational dataset is always more edited than the reprocessed except for the cycle 5. This is due to the dry tropospheric correction (cf section 3.2.4.). A second peak is observed at the cycle 8, with similar intensity in both datasets. This is due to a range anomaly (-9m on range) from passes 12 to 60 following a POS4 restart. All the data is edited in this time window.

3.2.2. Rejection on ice detection

The first step of the editing process includes the removal of points with ice detection. The ice flag (based on rad_sea_ice_flag within the products) is used to remove measurements affected by sea ice within the altimeter footprint.

The percentage of measurements edited on the ice flag criterium over ocean is monitored on the figure 3. In both LR and HR, the reprocessed ice flag edits slightly more before the cycle 13. This is linked to the AMR-C 24h warm target calibration that happened on the 17-18/03/2021 (on cycle 13 passes 20 to 45). The reprocessed flag ice is therefore more reliable. After the cycle 13, the percentage of edited data is similar in both datasets. Very small variations can be linked to differences in missing data.

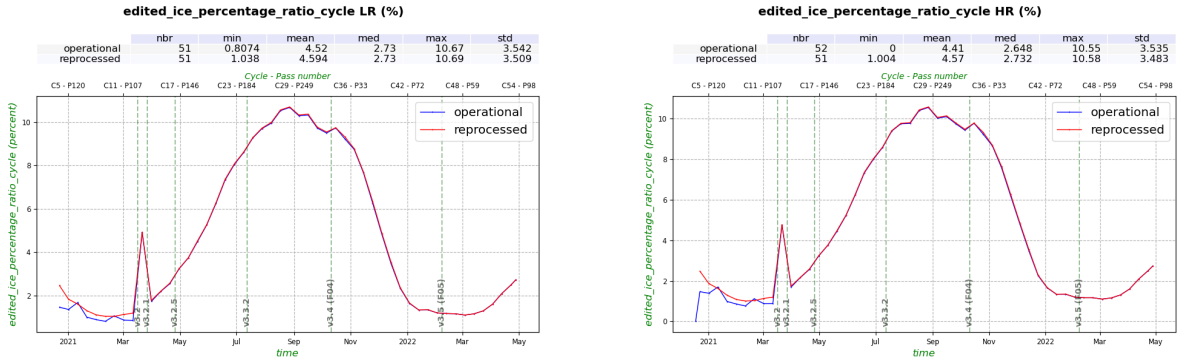

*Figure 3 – Percentage of edited measurements on ice detection for the operational (blue) and reprocessed (red) datasets over ocean by cycle in LR (**left**) and HR (**right**)*

3.2.3. Rejection on threholds criteria

Once the measurements corrupted by sea ice surfaces are identified, the quality of the parameters retrieved by the altimeter, as well as that of the geophysical corrections are checked with respect to defined thresholds. These thresholds and the corresponding percentage of corrupted measurements are detailed in table 2. For each of the listed parameters, the percentage of detected outliers is closely monitored cycle by cycle, day by day and pass by pass by CLS Cal/Val routines.

Parameters	Min threshold	Max threshold	Unit	% rejected	
				LR	HR
Sea surface height anomaly	-2	2	m	4.3/3.9	4.3/3.9
Sea surface height	-130	100	m	2.6/2.6	0.0/0.0
Nb measurements of range	10	N/A		2.9/2.9	0.0/0.0
Std. deviation of range	0	See (*)	m	3.6/3.6	1.8/1.8
Backscatter coefficient	LR: 7 HR: 10	LR: 30 HR: 35	dB	2.4/2.5	1.0/0.9
Nb measurements of sigma0	10	N/A		2.9/3.0	0.0/0.0
Std. deviation of sigma0	0	1	dB	4.6/4.9	3.2/3.2
Significant wave height	0	LR: 11 HR: N/A	m	3.0/3.0	0.0/0.0
Altimeter wind speed	0	30	m.s-1	3.1/3.0	2.4/2.0
Sea State Bias	-0.5	0	m	2.3/2.3	0.0/0.1
Ionospheric correction filtered	-0.4	0.04	m	3.9/3.2	3.8/3.2
Square off nadir angle	-0.2	0.64	deg2	2.3/2.4	N/A
Equilibrium tide	-0.5	0.5	m	0.0/0.0	0.0/0.0
Combined atmospheric correction	-2	2	m	0.0/0.0	0.0/0.0
Dry tropospheric correction	-2.5	-1.9	m	0.0/0.1	0.0/0.1
Internal tide	-5	5	m	0.0/0.0	0.0/0.0
Ocean tide	-5	5	m	0.0/0.0	0.0/0.0
Pole tide	-15	15	m	0.0/0.0	0.0/0.0
Earth tide	-1	1	m	0.0/0.0	0.0/0.0
AMR wet tropospheric correction	-0.5	-0.001	m	0.3/0.4	0.3/0.4
Global statistics of edited measurements by thresholds (%)				6.9/6.7	5.9/5.3

Table 2 – Table of parameters used for editing and the corresponding percentages of edited measurements for each parameter for Sentinel-6A LR and HR in the operational and reprocessed datasets respectively

(*) The maximum threshold for range standard deviation is set as function of significant wave height as follow:

- In LR:
  - for SWH $\leq$ 2m : 0.192
  - for SWH $>$ 2m : 0.018 * SWH + 0.156
- In HR:
  - for SWH $\leq$ 2m : 0.187
  - for SWH $>$ 2m : 0.033 * SWH + 0.121

As table 2 shows, the percentage of edited points at this step is decreased for both LR (-0.2% at 6.7%) and HR (-0.6% at 5.3%) in the reprocessed dataset. This is mainly driven by the SSHA (-0.4% in both LR and HR) and ionospheric correction (-0.7% in LR and -0.6% in HR). Additionally, in HR mode only, the wind speed is a main contributor as well (-0.4%), with a lesser number of edited points at the beginning of the time series before the cycle 17 when a PDAP update (v3.2.5) changed the HR configuration and the wind speed.

It is worth noting that parameters at default values are included in these threshold statistics, for they fail the boolean tests. Additionally, the majority of all edited points come from these default values rather than actual out of bound values, as can be seen in the cyclic monitoring of figure 4. For both types of edited points, the two datasets draw closer with the PDAP updates.

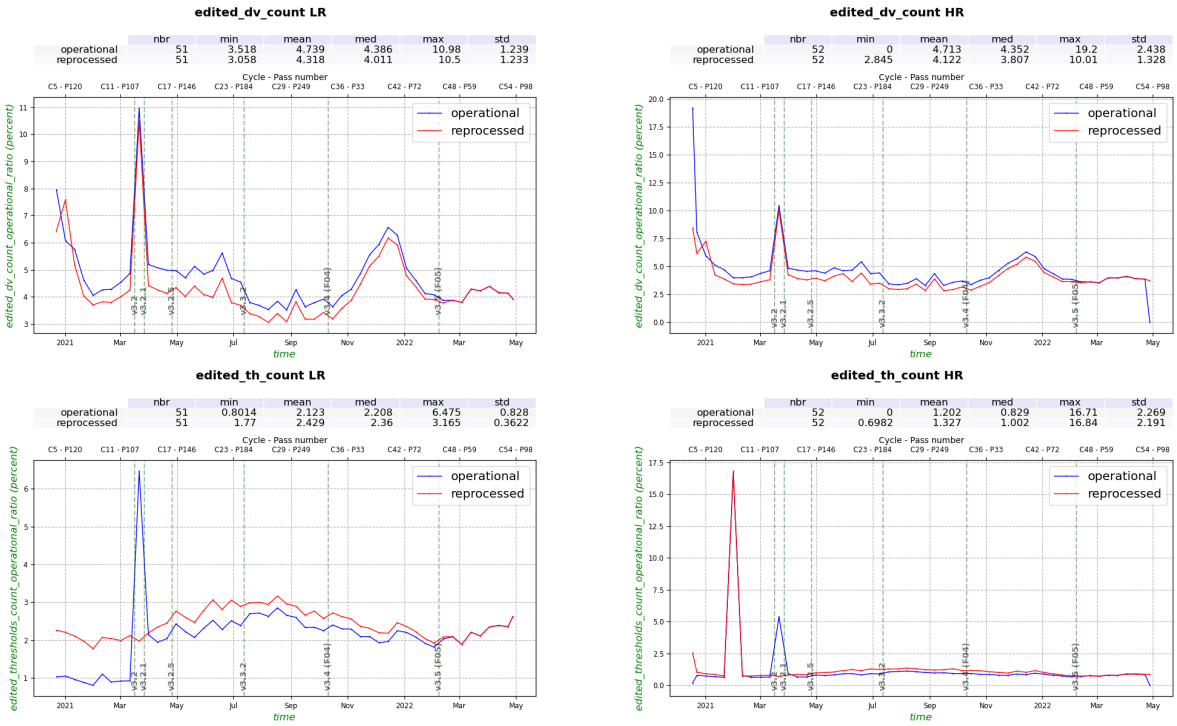

*Figure 4 – Percentage of edited measurements for the operational (blue) and reprocessed (red) datasets over ocean by cycle based on parameters at default value (**top**) and out of bounds (**bottom**) for both LR (**left**) and HR (**right**).*

The four following subsections will focus on the editing parameters with relevant differences between the operational and reprocessed datasets.

3.2.4. Details on dry tropospheric correction editing

The percentage of edited points on the dry tropospheric correction is presented in figure 5 (top). The only notable feature is a peak at cycle 5 in the reprocessed data. From passes 121 to 126 (included) of this cycle (from 01-01-2021 00:31:12.0 to 06:08:28.0), the dry tropospheric correction is set to default value in the products(cf Figure 5 bottom). There is no matching event. This was caused by a missing meteo file.

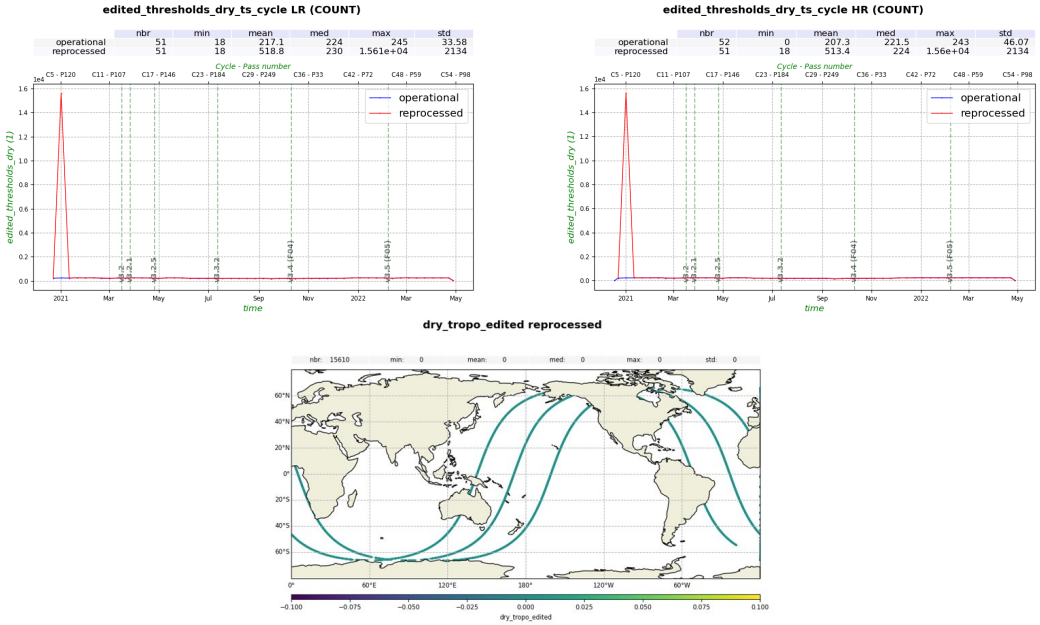

*Figure 5 – Percentage of edited measurements on dry troposhperic thresholds for the operational and reprocessed datasets over ocean by cycle in LR (**top left**) and HR (**top right**) and edited measurements over the cycle 5 (**bottom**)*

3.2.5. Details on filtered ionospheric correction editing

The percentage of edited points on the filtered ionospheric correction is presented in figure 6. The top panels include only the points at default value and the bottom panels include only the points that are out of bounds. Prior to PB F05 deployment that fixed a bug in the computation of the filtered ionospheric correction, more points are set to default value in the operational dataset. The recovered points are mainly located in the Antarctica and near Indonesia, as can be seen in the example shown in figure 7. Concerning the out of bounds ionospheric correction, the main feature is the peak at cycle 13 corresponding to the PDAP v3.2 anomaly, in operational data only. This is expected as the anomaly impacted the C band. Other small variations can be linked to differences in missing data.

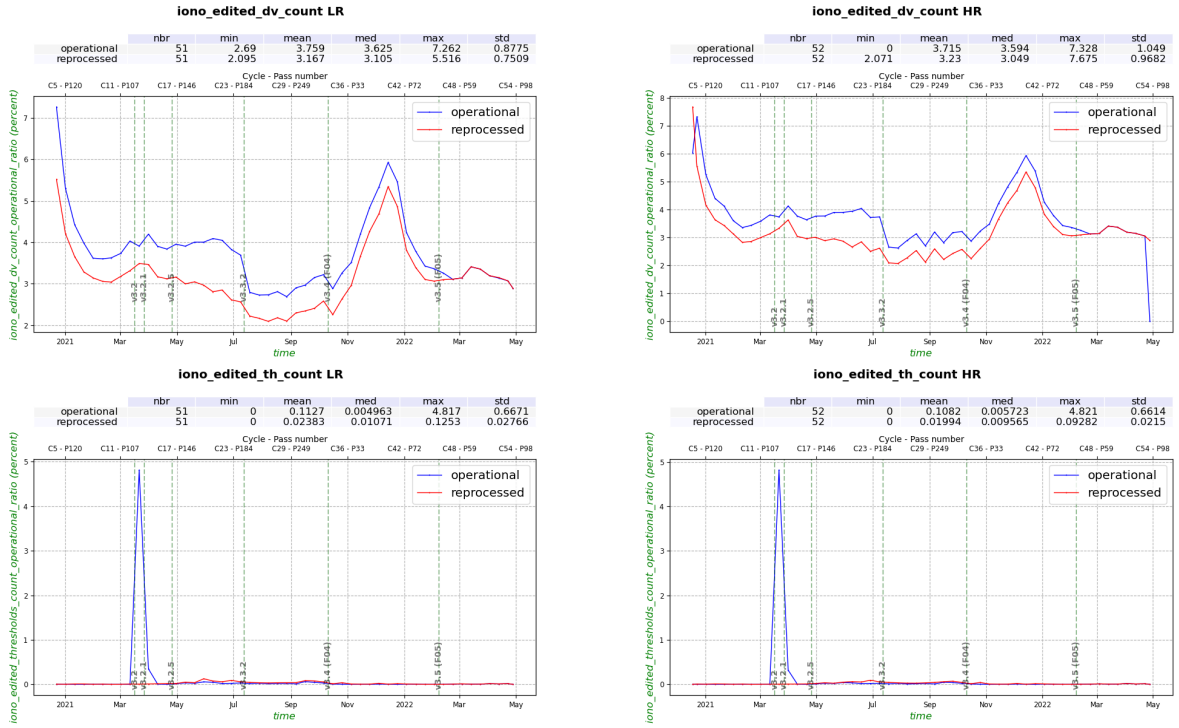

*Figure 6 – Percentage of edited measurements for the operational and reprocessed datasets over ocean by cycle based on filtered ionospheric correction at default value (**top**) and out of bounds (**bottom**) for both LR (**left**) and HR (**right**).*

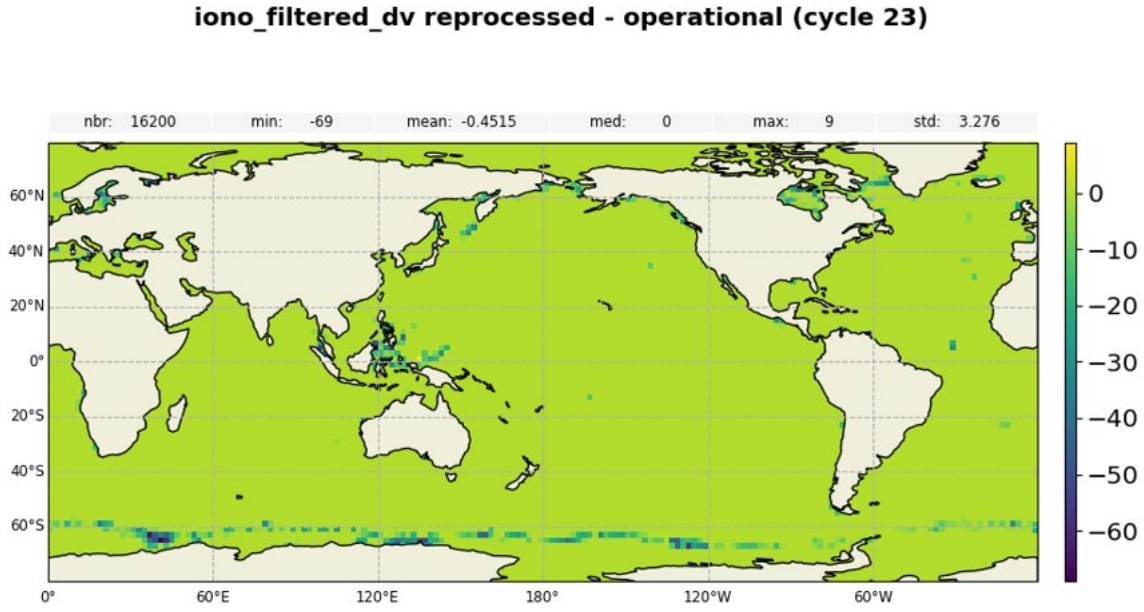

*Figure 7 – Map of the difference in the number of filtered ionospheric correction at default value (reprocessed - operational) for the cycle 23 counted in boxes of 2*2 degrees.*

3.2.6. Details on SSB editing (HR)

The percentage of edited points on the SSB being at default value in HR is presented in figure 8 (top). Cycles with RAW/RMC masks are more edited in the reprocessed dataset. These lost points are located in coastal regions, as it can be seen in the example from cycle 16 shown in the bottom panel. It can be explained by the reduced number of looks implemented in PB F06 for HR processing: the very first and last measurement at the start or end of a section of HR data can be lost while the switch between RAW and RMC is performed. Note that after cycle 23, when the Mode Mask was switched to ”LRMC everywhere”, the number of SSB points at default value is similar in both datasets.
There is no out of bounds SSB in both datasets.

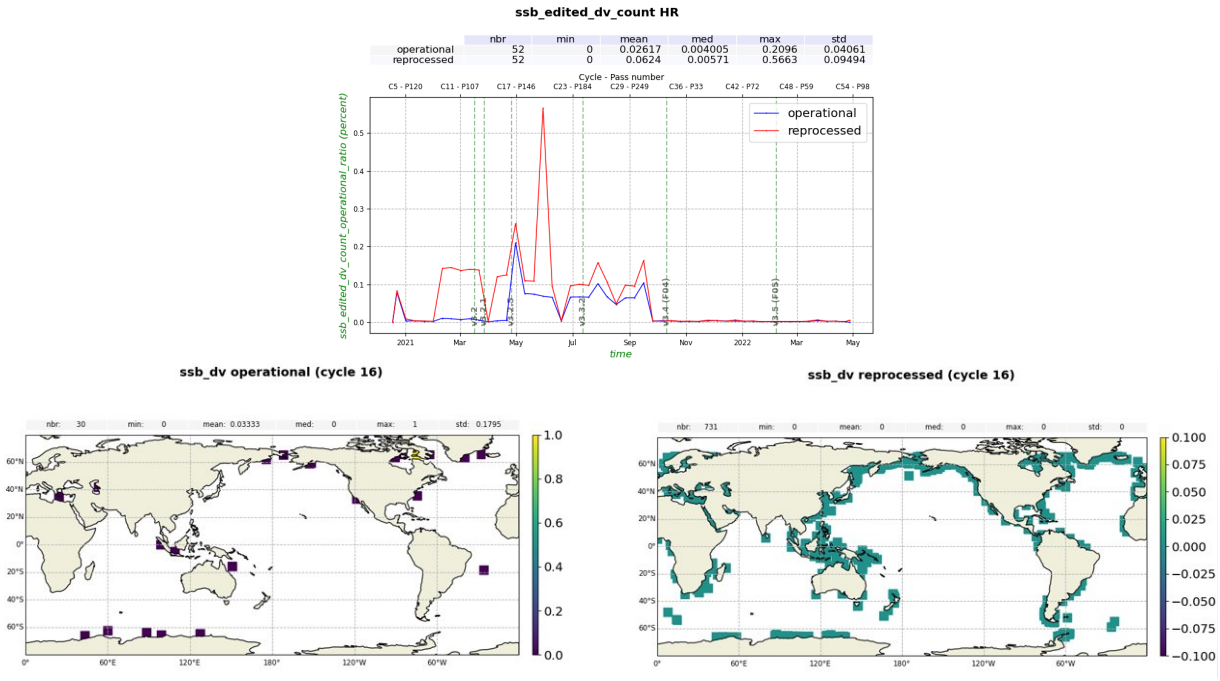

*Figure 8 – Percentage of edited measurements based on SSB at default value for the operational (blue) and reprocessed (red) datasets over ocean by cycle in HR (**top**) maps of SSB at default value for the cycle 16 in the operational (**bottom left**) and reprocessed datasets (**bottom right**) (one rectangle represents a single point).*

3.2.7. Details on SSHA editing

The percentage of edited points on the SSHA is presented in figure 9. The top panels include only the points at default value and the bottom panels include only the points that are out of bounds. Prior to PB F05 deployment, more points are at default value in the operational dataset. These points are recovered thanks to the filtered ionospheric correction (cf section 3.2.5.). Concerning the out of bounds SSHA, the number of edited points is far less compared to the default values ones. More points are edited in the reprocessed dataset between the PDAP v3.2 and PB F05 deployment. However, these additional points are at default value in the operational dataset, again because of the filtered ionospheric correction.

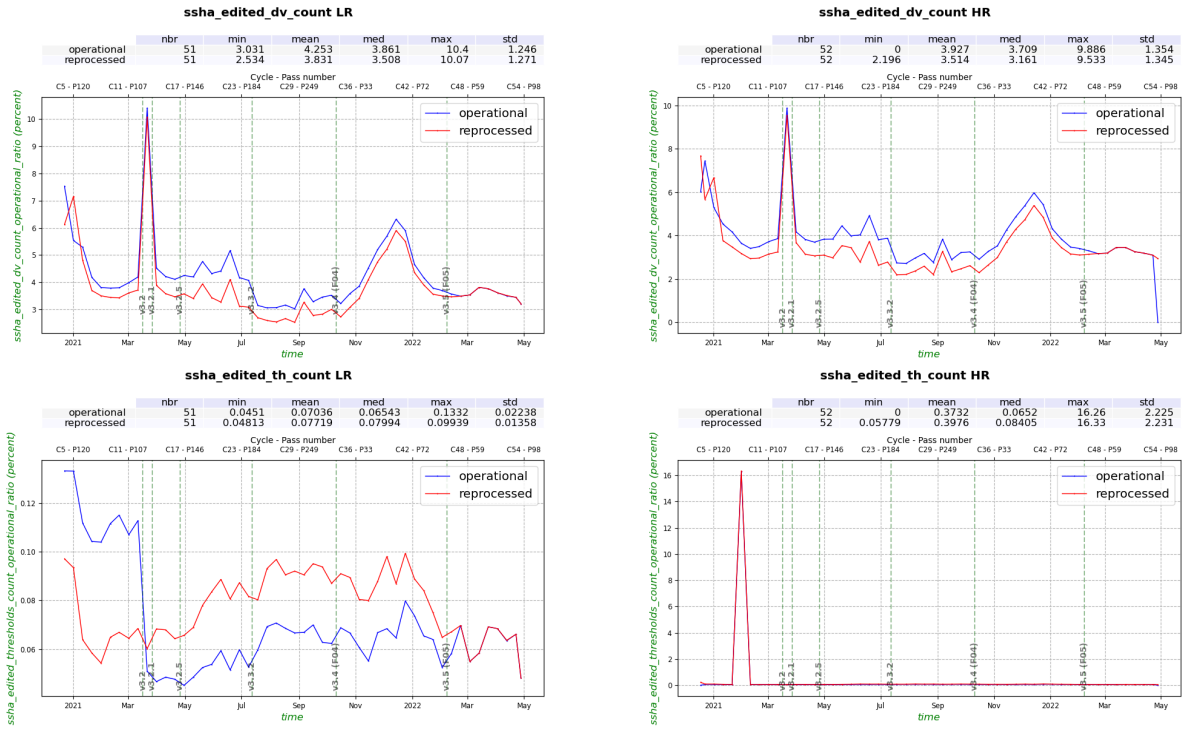

*Figure 9 – Percentage of edited measurements for the operational (blue) and reprocessed (red) datasets over ocean by cycle based on SSHA at default value (**top**) and out of bounds (**bottom**) for both LR (**left**) and HR (**right**).*

3.2.8. Along-track SSHA consistency

Once the thresholds editing is applied, the consistency of the along-track sea surface height anomaly is checked. The statistics of the SSHA by pass are computed, with a selection that excludes zones of geophysical varibility. If the mean or the standard deviation is higher than a given threshold, the entired pass is edited. This process is repeated for a stricter set of selection and thresholds. The details are listed in table 3.

The percentage of edited points based on SSHA pass statistic is presented in figure 9. There is only one occurence of this happening, at the cycle 20.
In LR, only one pass is edited in the operational dataset : p182 (01-06-2021 03:18:11.0 to 04:14:23.0). In the reprocessed dataset, a second pass is also edited : p183 (01-06-2021 04:14:24.0 to 05:10:35.0). The editing of this extra pass is still being investigated.

In HR, in the operational data set, the same pass 182 is edited. In the reprocessed dataset, the SSHA is at default value for the two passes 182 and 183 and therefore do not appear in this diagnostic. No matching events have been found at these dates.

Parameters	Set 1	Set 2
Selection		
Bathymetry	<-1000m	<-1000m
Coastal distance	>100km	>100km
Oceanic variability	<0.3m	<0.1m
Min number of measurements	3	200
Thresholds		
Mean (absolute value)	0.3m	0.15m
STD	0.4m	0.2m

Table 3 – Table of parameters used for the editing on the SSHA pass statistics. These parameters are identical in HR and LR.

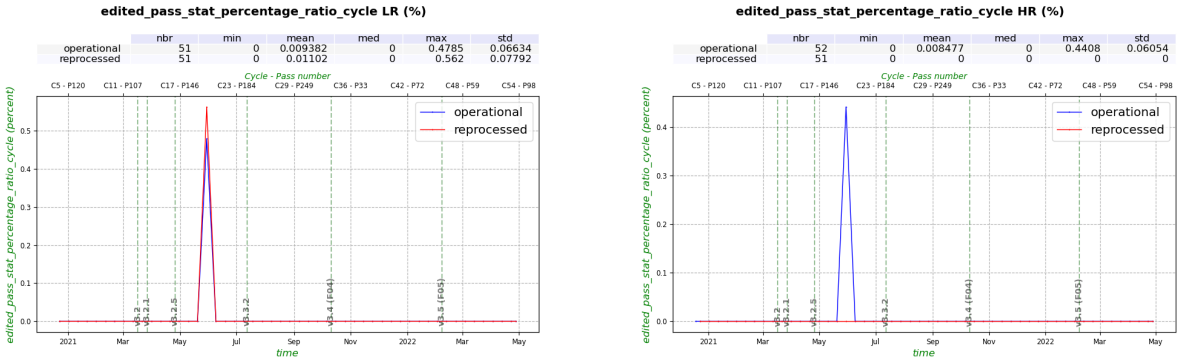

*Figure 10 – Percentage of edited measurements on SSHA pass statistics for the operational (blue) and reprocessed (red) datasets over ocean by cycle in LR (**left**) and HR (**right**)*

4. Geophysical parameters

4.1. Altimeter parameter

Parameters derived from POS-4 altimeter are monitored in this section.

4.1.1. Significant Wave Height

Comparison between operational and reprocessed data

The time monitoring of LR Ku-band Significant Wave Height (SWH) over the complete reprocessing period is presented in figure 11, for both operational (blue) and reprocessed (red) datasets. Dashed vertical lines represent the different updates of the operational processing.

Comparison between the two datasets hightlights differences up to PDAP v3.2 deployement in April 2021. In this PDAP version, LR configuration has been reviewed with, in particular, the update of the skewness parameter in the retracking to 0.1 (as for Jason-3), the update of the tracking window and of the instrument correction. After this update, no differences are observed between operational and reprocessed LR SWH, both in mean and standard deviation.

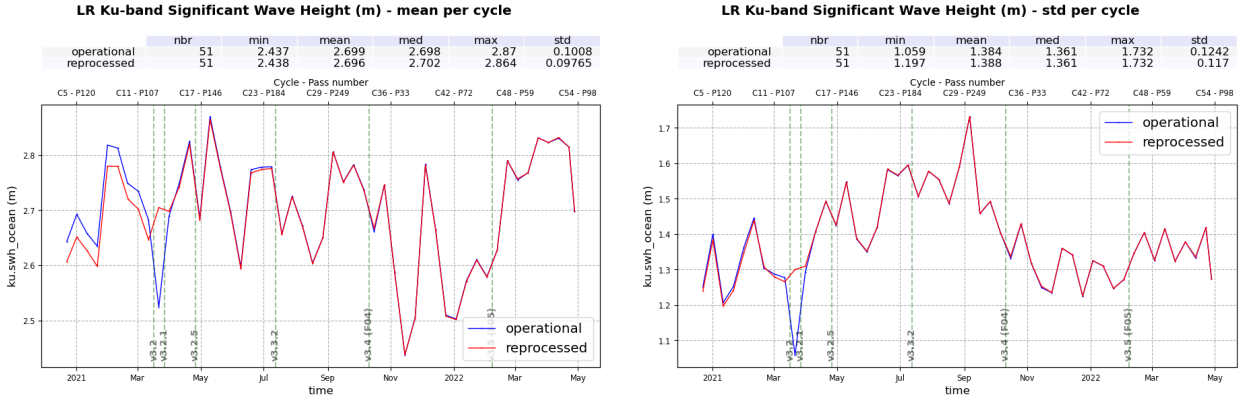

Figure 11 – Time monitoring of Sentinel-6A LR Ku-band Significant Wave Height in meters, before reprocessing (blue) and after reprocessing (red). Left: mean per cycle, Right: standard deviation per cycle

HR SWH monitorings highlight expected significant difference between operational and reprocessed data (figure 12). This is expected and is mainly due to PB F06 (see section 2.1. for more details). With the reprocessed data, a decrease is oberved in mean (-17 cm) and in standard deviation (-4.8 cm).

The monitoring of SWH difference between HR and LR data (figure 13) shows the reduction of the bias between the two retrievals thanks to the reprocessing and PB F06 update on HR processing. It is now centred around 23.4 cm. Furthermore, we do not observe any drift between LR and HR SWH.

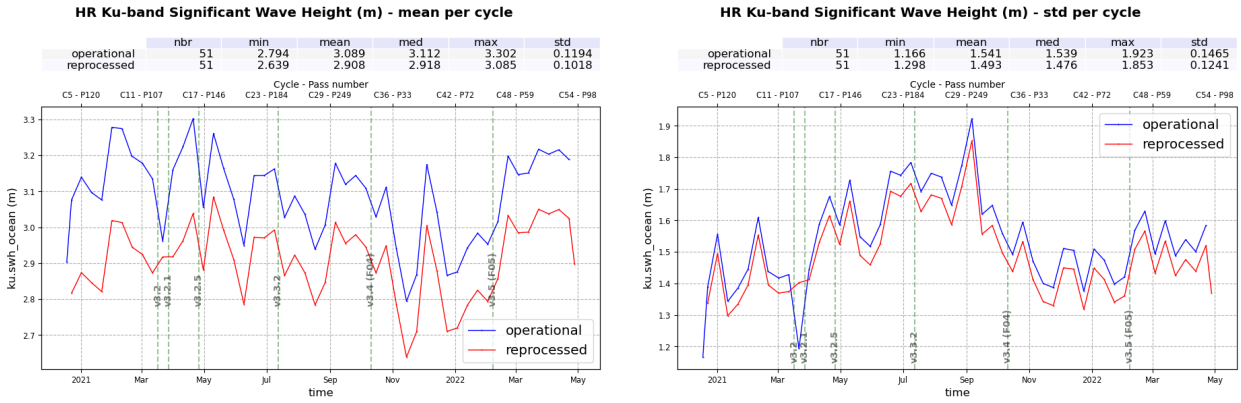

Figure 12 – Time monitoring of Sentinel-6A HR Ku-band Significant Wave Height in meters, before reprocessing (blue) and after reprocessing (red). Left: mean per cycle, Right: standard deviation per cycle

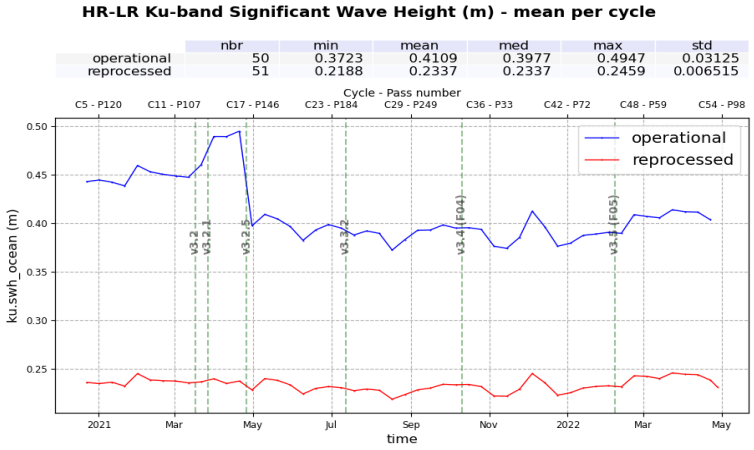

Figure 13 – Time monitoring of Sentinel-6A Ku-band Significant Wave Height difference : HR - LR. Mean per cycle in meters before reprocessing (blue) and after reprocessing (red).

Impact of PB F06

Over the cycles 47 to 53, Sentinel-6A operational data have been processed with PB F05. PB update from F05 to F06 only impacts HR data through HR processing update (reduction of the number of Doppler beams incoherently integrated within the stack, to generate the multi-looked L1B power waveforms). Comparing F05 and F06 data allows to directly quantify the impact of such an update.

The histogram of the HR SWH difference between PB F05 and F06 (figure 14) shows a HR SWH reduction of 16.5 cm in average with PB F06.
Looking at differences between HR and LR SWH for F05 and F06 data (figure 15), a strong reduction of the bias and its dependency to SWH over the complete SWH spectrum is achieved with PB F06. As expected, we observe here a reduction and not a complete correction of these ocean vertical velocity impacts on HR data. Still, the impacts are strongly reduced with PB F06 : the bias between HR and LR SWH ranges from 9 to 42 cm between 1 and 7m-wave with PB F06 instead of from 18 to 76 cm with PB F05.

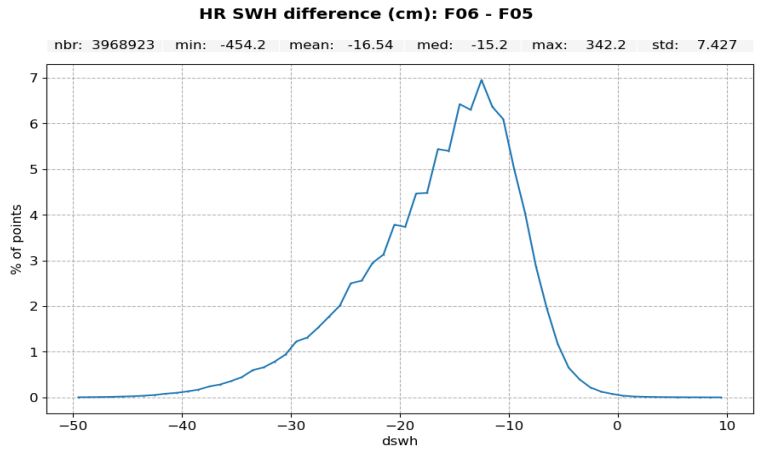

Figure 14 – Histogram of HR SWH difference between reprocessed and operational F05 data, computed over cycles 47 to 53.

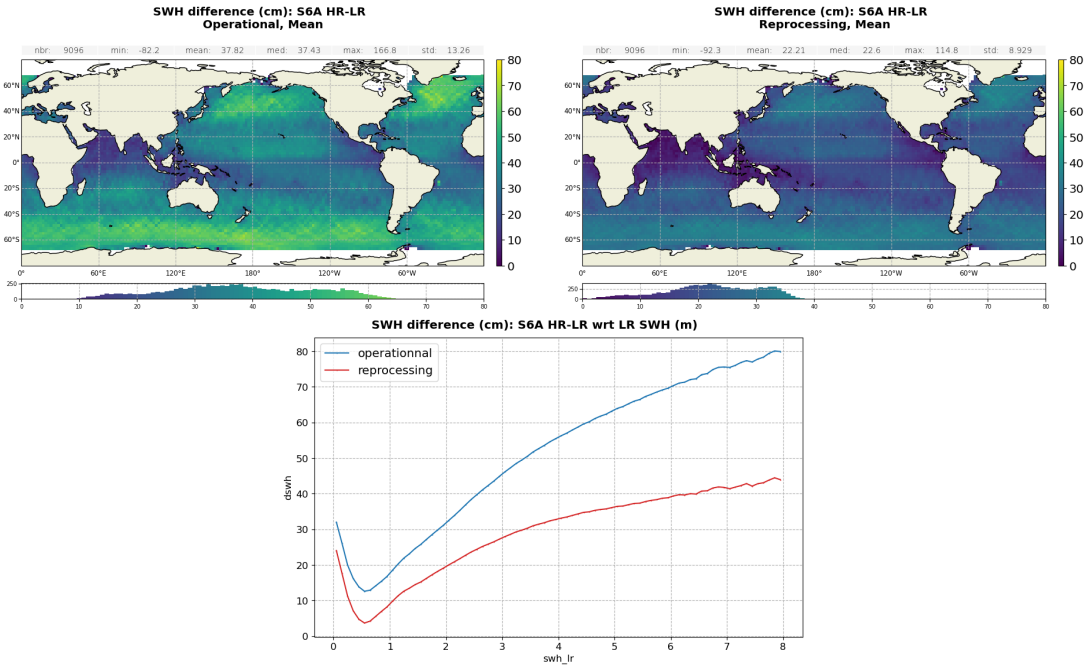

Figure 15 – HR - LR SWH difference over cycles 47 to 53 (PB F05 in operational) : Gridded map for operational data (top left) and for reprocessed data (top right), Difference function of LR SWH (bottom)

Reprocessed data

After reprocessing, LR SWH is centred around 2.70 m, which is in line with Jason-3 (figure 16). Note that the histogram of Sentinel-6A LR data is virtually the same as for Jason-3, except at very low wave heights, where Sentinel-6A performs better, due to its improved handling of low wave heights in the Level 2 processing.

Due to the remaining impact of ocean vertical velocity, HR SWH is centred around 2.91 m.

Maps of SWH averaged over the reprocessing period show the same geographical patterns between Jason-3 and Sentinel-6A LR and HR (figure 17).

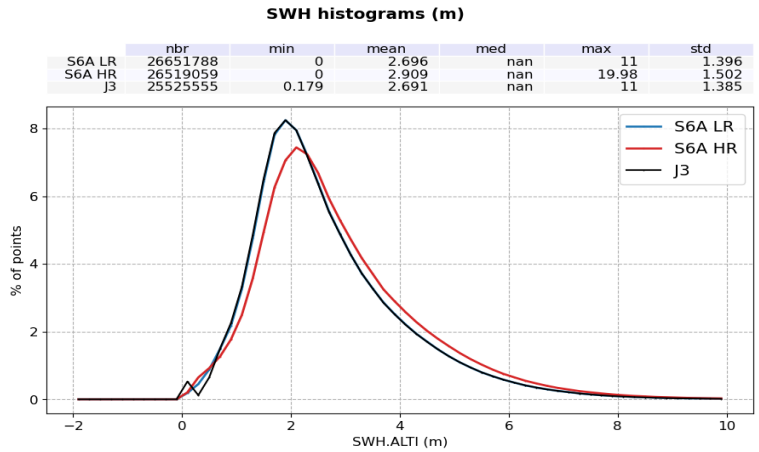

Figure 16 – Histogram of Ku-band SWH for Jason-3 (black), reprocessed S6A LR (blue) and reprocessed S6A HR (red). Computed over the completed reprocessed period. S6A LR blue curve is overlaid with Jason-3 black curve.

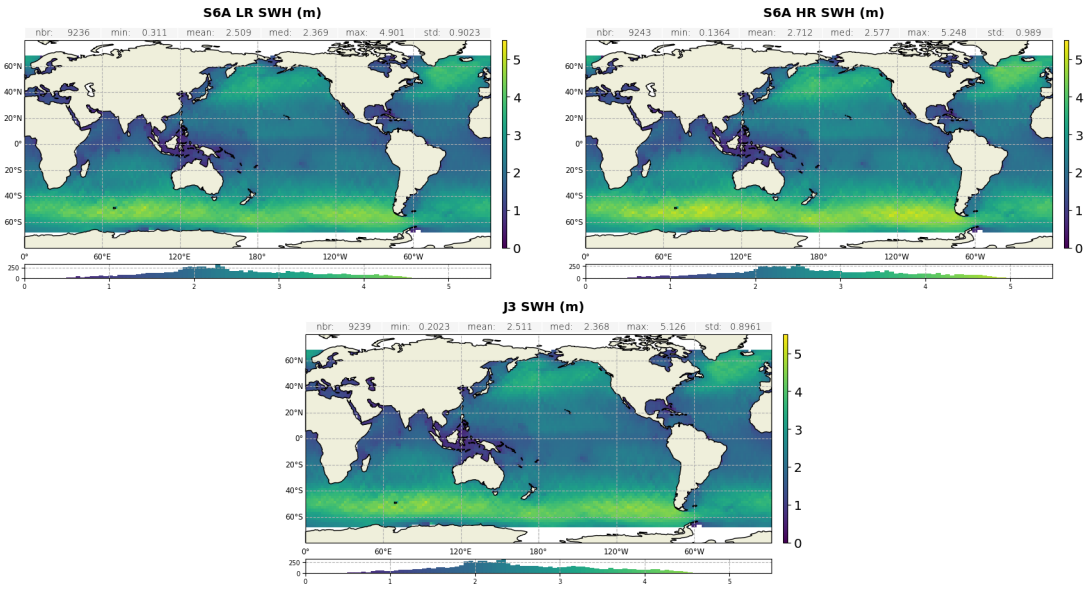

Figure 17 – Map of Ku-band SWH for reprocessed S6A LR (top left), reprocessed S6A HR (top right), and Jason-3 (bottom). Computed over the completed reprocessed period.

4.1.2. Range

Comparison between operational and reprocessed data

HR versus LR range bias is monitored in figure 18. Left pannel exhibits a peak over cycle 9 on the operational dataset. This is linked to the COG correction anomaly impacting both LR and HR data and resulting in a constant bias of 1.06 m on the range. This anomaly has been corrected from the 2021-02-09 in NTC HR and from the 2021-02-15 in NTC LR. This non concomitant correction induces the peak on cycle 9.
Zooming on the y-axis, the impact of PDAP v3.2 (LR configuration update) is clearly visible. After PDAP v3.2, the bias observed between reprocessed and operational curves is due to HR processing update in PB F06.

Looking more closely at HR versus LR range bias for the reprocessing, no significant drift can be identified

(figure 19).

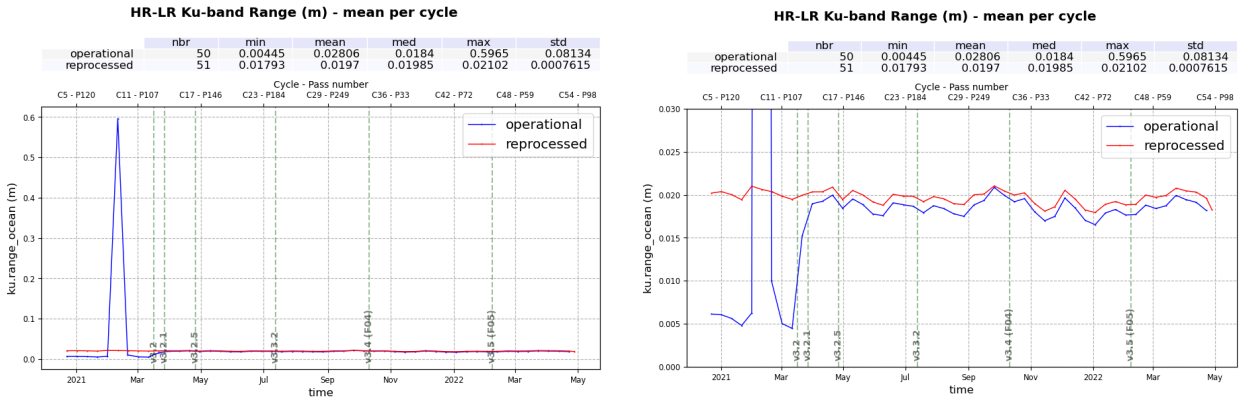

Figure 18 – Time monitoring of Sentinel-6A Ku-band Range difference : HR - LR. Mean per cycle in meters before reprocessing (blue) and after reprocessing (red). Right pannel : same figure zoomed in on y-axis.

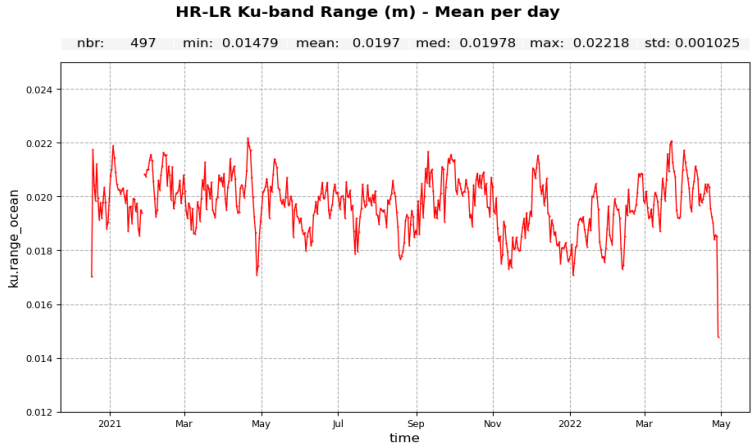

Figure 19 – Time monitoring of Sentinel-6A Ku-band Range difference : HR - LR. Mean per day in meters after reprocessing.

Impact of PB F06

Ranges from PB F05 and F06 are compared on figure 20. The range bias between the two processings is centred around 1.2 mm in average, meaning that HR range has increased by 1.2 mm with PB F06 update.

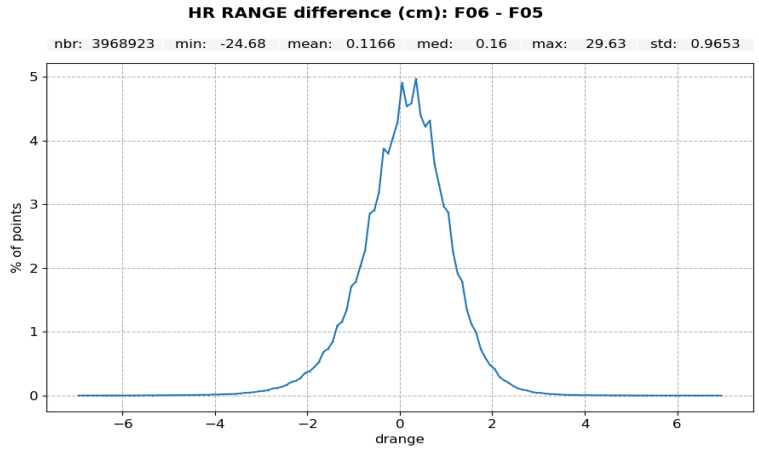

Figure 20 – Histogram of HR Range difference between reprocessed and operational F05 data, computed over cycles 47 to 53.

HR versus LR range bias is compared over PB F05 time period (figure 21). As for SWH, the range bias correlation to SWH is reduced. With PB F06 (red curve in bottom plot), the increase of the bias is of 3.8 cm between 1 and 7-m wave, while it was of 4.7 cm over the same wave interval for PB F05 (blue curve). Note here that such comparison between LR and HR range highlights the skewness difference between LR and HR processings.

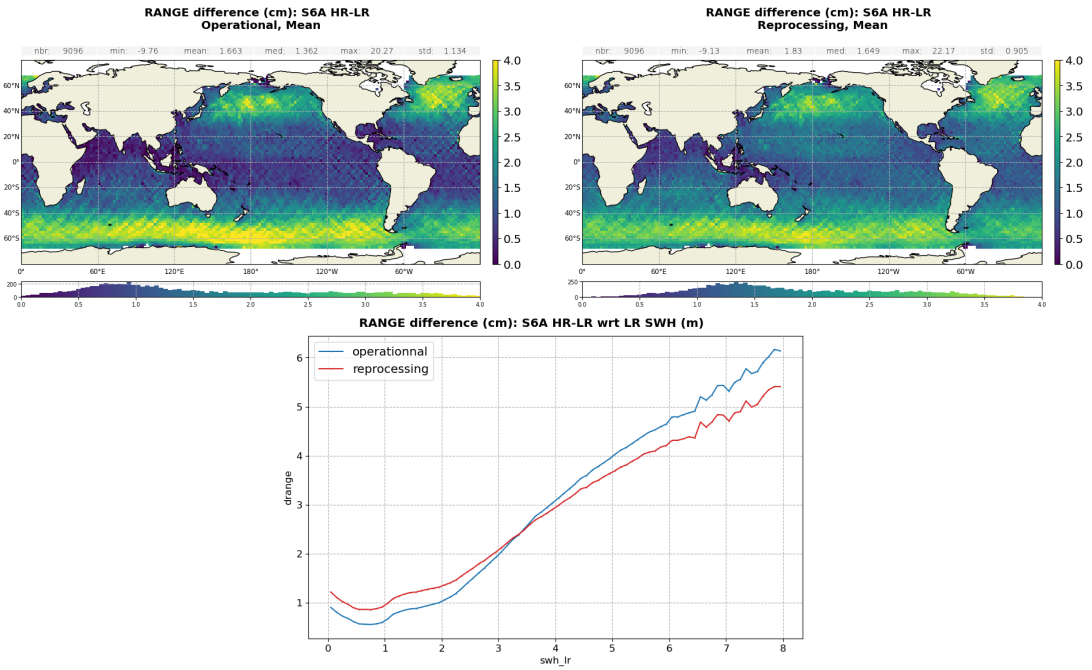

Figure 21 – HR - LR Range difference over cycles 47 to 53 (PB F05 in operational) : Gridded map for operational data (top left) and for reprocessed data (top right), Difference function of LR SWH (bottom)

Along track wind has a known impact on HR data and more particularly on HR range. To highlight this

impact, two gridded maps of HR versus LR range difference are drawn, one for ascending tracks and the other one for descending tracks. Next, the difference between these two maps is computed (ascending minus descending). Such process allows to remove all systematic error on the bias (such as waves) and to only highlight HR variations with respect to LR that depend on track orientation.

Figure 22 shows the resulting maps for both F05 (operational) and F06 (reprocessed) data. A clear improvement is brought by PB F06 with a reduction of the amplitude of the wind pattern. It ranges between -1.5 and 1.5 cm with PB F05 data ans between -1 and 1 cm with PB F06 data.

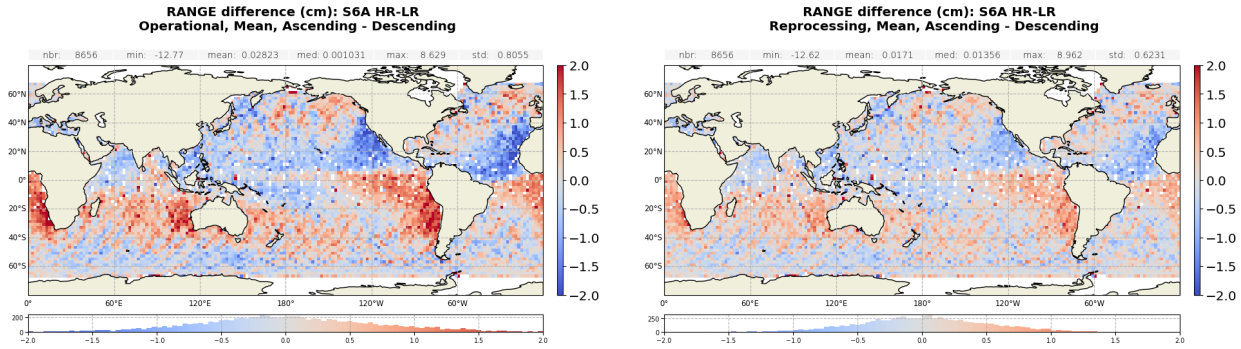

Figure 22 – Maps of Ascending versus Descendings tracks maps of HR versus LR range bias, computed over cycles 47 to 53 (PB F05 in operational). Left pannel: for operational data. Right panel: for reprocessed data.

4.1.3. Backscater coefficient

Comparison between operational and reprocessed data

Operational and reprocessed LR Ku-band backscatter coefficient (sigma0) are in line from PB F04 deployement, both in mean and in standard deviation (figure 23). The two curves are brought together in two steps. First with the PDAP v3.2 updating LR configuration and then with PB F04 where a correction has been applied in the handling of calibration files.

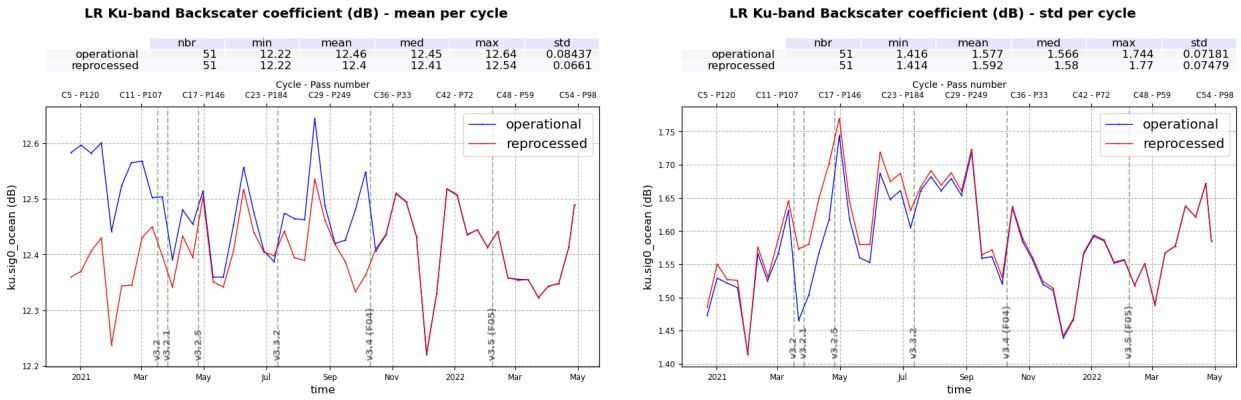

Figure 23 – Time monitoring of Sentinel-6A LR Ku-band Backscater coefficient in dB, before reprocessing (blue) and after reprocessing (red). Left: mean per cycle, Right: standard deviation per cycle

As for LR, operational and reprocessed HR Ku-band backscatter coefficient seem to be in line from PB F04 deployement, both in mean and in standard deviation (figure 24). Again, the two curves are brought together in two steps. First with the PDAP v3.2.2 (PB F03) and then with PB F04. Looking more closely, the two lines are not exactly overlaid from PB F04. The small bias observed is detailed in the next paragraph.

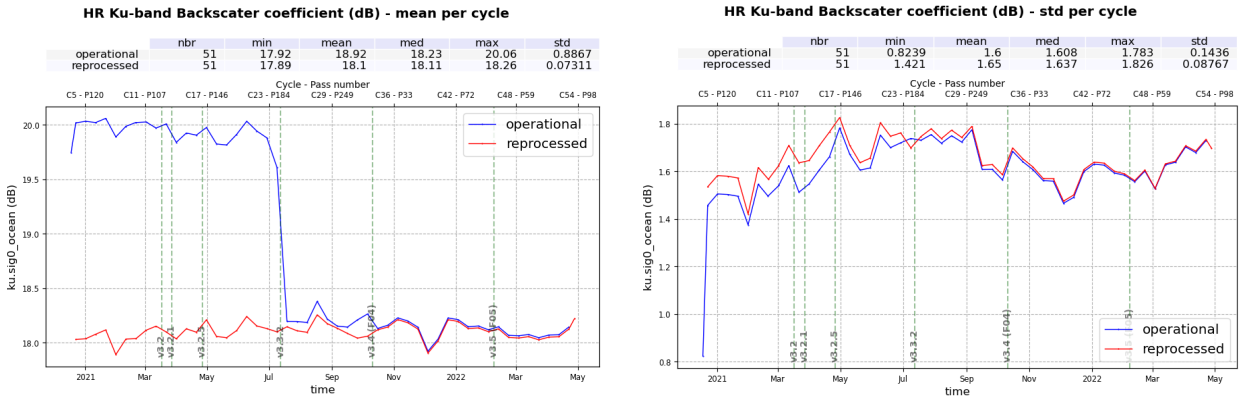

Figure 24 – Time monitoring of Sentinel-6A HR Ku-band Backscatter coefficient in dB, before reprocessing (blue) and after reprocessing (red). Left: mean per cycle, Right: standard deviation per cycle

Impact of PB F06

With PB F06, HR backscatter coefficient has slightly decreased by 0.02 dB (see figure 25), which is in line with the bias observed in figure 24. This bias should be taken into account for the calibration bias applied on sigma0 for the wind speed computation. Further details on the sigma0 calibration bias can be found in sections 5.2.1. and 5.3.3. of the tandem phase analysis.

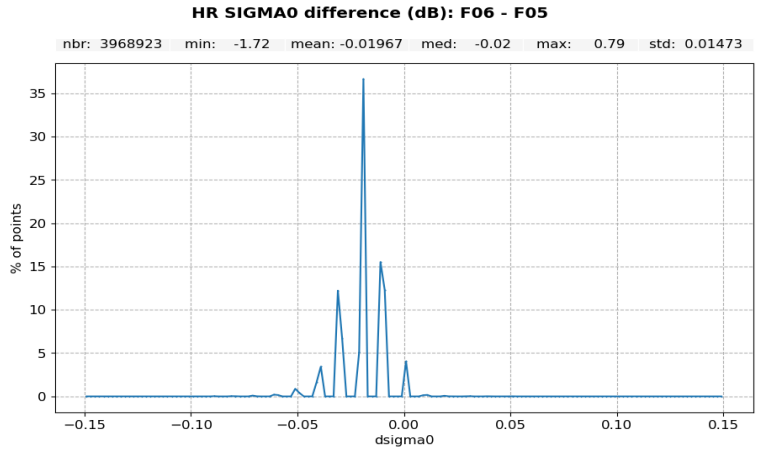

Figure 25 – Histogram of HR Backscatter coefficient difference between reprocessed and operational F05 data, computed over cycles 47 to 53.

Comparison to LR backscatter coefficient highlights once again a reduction of the correlation to SWH (see figure 26).

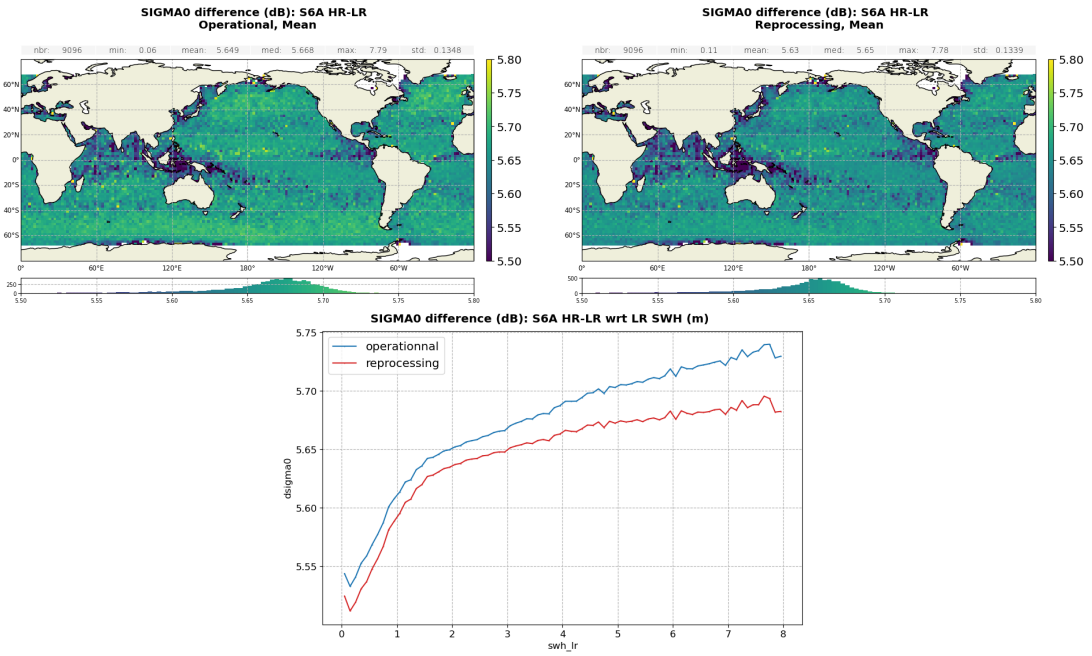

Figure 26 – HR - LR Backscatter coefficient difference over cycles 47 to 53 (PB F05 in operational) : Gridded map for operational data (top left) and for reprocessed data (top right), Difference function of LR SWH (bottom)

Reprocessed data

After reprocessing, LR Sigma0 is centred around 12.4 dB, which is slightly smaller than Jason-3 (13.6 dB). HR Sigma0 is centred around 18.1 dB (figure 27). Maps of Sigma0 averaged over the reprocessing period show the same geographical patterns between Jason-3 and Sentinel-6A LR and HR (figure 28).

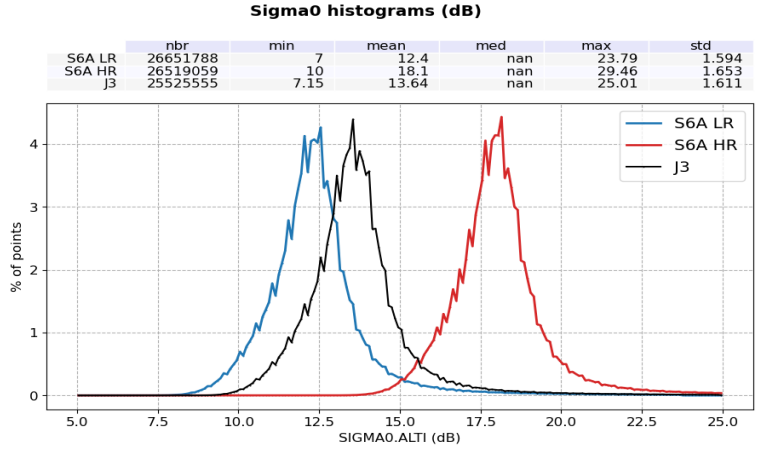

Figure 27 – Histogram of Ku-band Backscatter coefficient for Jason-3 (black), reprocessed S6A LR (blue) and reprocessed S6A HR (red). Computed over the completed reprocessed period.

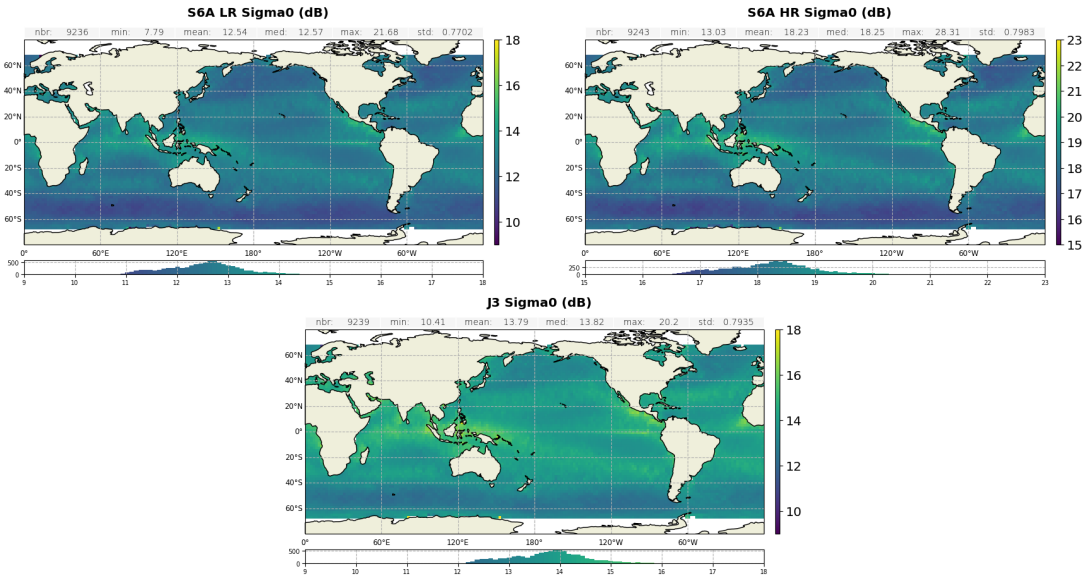

Figure 28 – Map of Ku-band Backscatter coefficient for reprocessed S6A LR (top left), reprocessed S6A HR (top right), and Jason-3 (bottom). Computed over the completed reprocessed period.

4.1.4. Altimeter Wind-Speed

Comparison between operational and reprocessed data

As for the backscatter coefficient, operational and reprocessed LR altimeter wind-speed are in line from PB F04 (figure 29).

For HR, we observe a small reduction with reprocessed wind-speed (figure 30). Comparing to F05 operational data, HR wind-speed decreases by 12 cm/s in the reprocessing. This is linked to the backscatter coefficient increase with PB F06 (see section 4.1.3.).

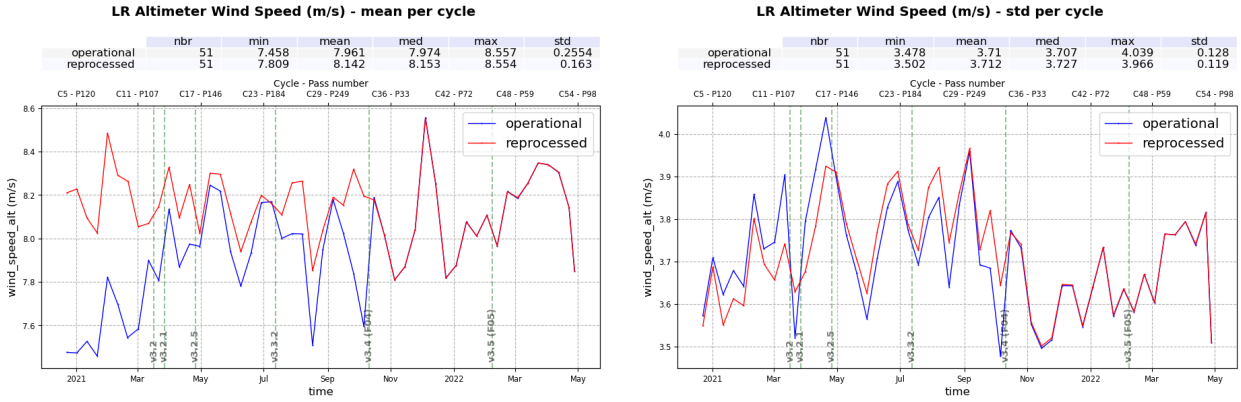

Figure 29 – Time monitoring of Sentinel-6A altimeter wind-speed in m/s, before reprocessing (blue) and after reprocessing (red). Left: mean per cycle, Right: standard deviation per cycle

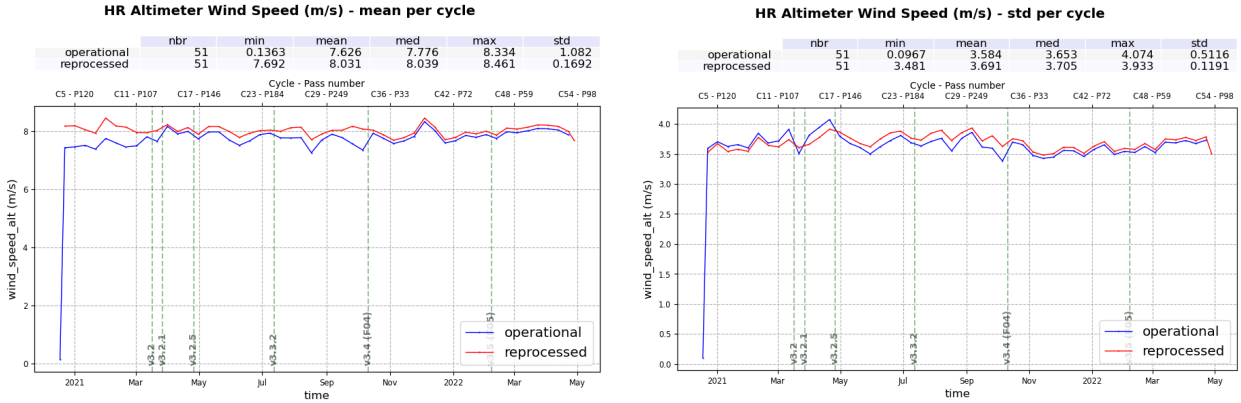

Figure 30 – Time monitoring of Sentinel-6A altimeter wind-speed in m/s, before reprocessing (blue) and after reprocessing (red). Left: mean per cycle, Right: standard deviation per cycle

Reprocessed data

After reprocessing, LR wind-speed is centred around 8.15 m/s, which is of the same order as Jason-3 (8.13 m/s). HR wind-speed is centred around 8.04 m/s (figure 31). Maps of altimeter wind-speed averaged over the reprocessing period show the same geographical patterns between Jason-3 and Sentinel-6A LR and HR (figure 32).

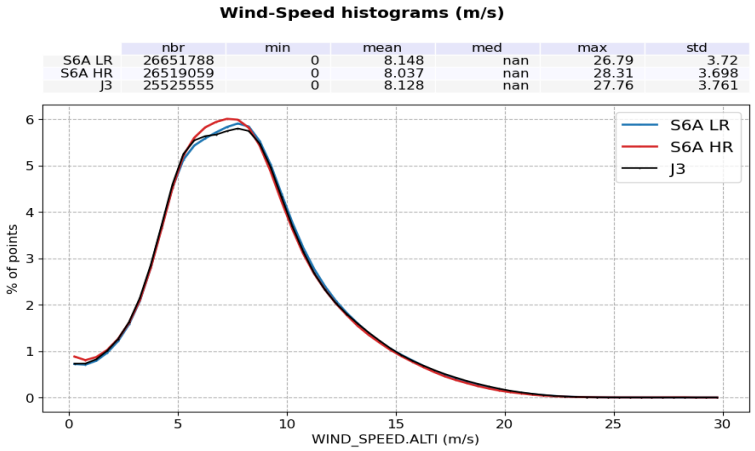

Figure 31 – Histogram of altimeter wind-speed for Jason-3 (black), reprocessed S6A LR (blue) and reprocessed S6A HR (red). Computed over the completed reprocessed period.

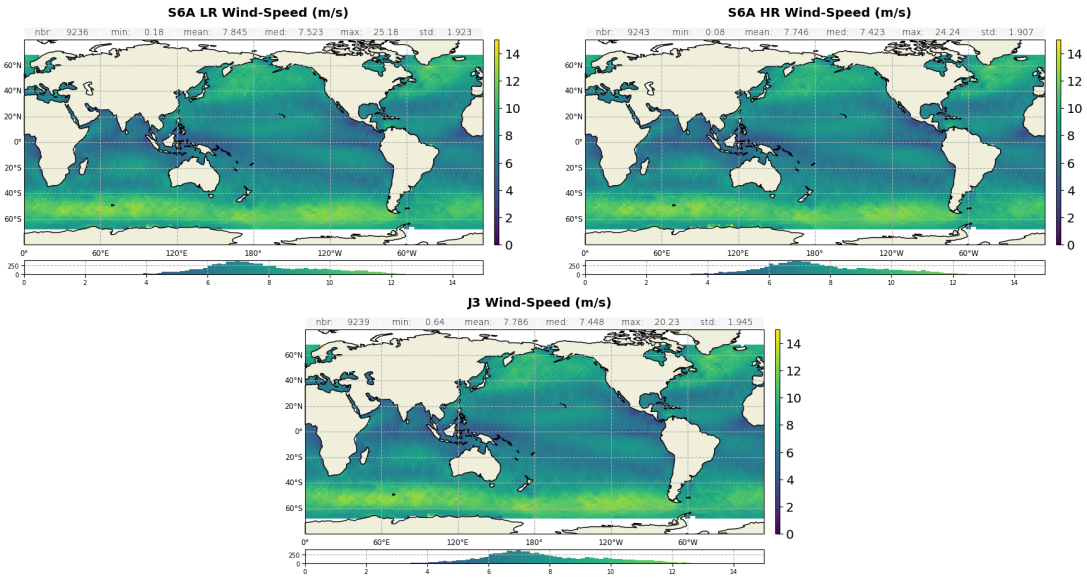

Figure 32 – Map of altimeter wind-speed in m/s for reprocessed S6A LR (top left), reprocessed S6A HR (top right), and Jason-3 (bottom). Computed over the completed reprocessed period.

4.1.5. Sea State Bias

Comparison between operational and reprocessed data

As for the backscatter coefficient and wind-speed, operational and reprocessed LR Ku-band Sea State Bias (SSB) are in line from PB F04 (figure 33).

For HR, we observe a reduction with reprocessed SSB (figure 34). Comparing to F05 operational data, HR SSB decreases by 4.8 mm in the reprocessing. This is linked to the impact of PB F06 on both HR backscatter coefficient and HR SWH.

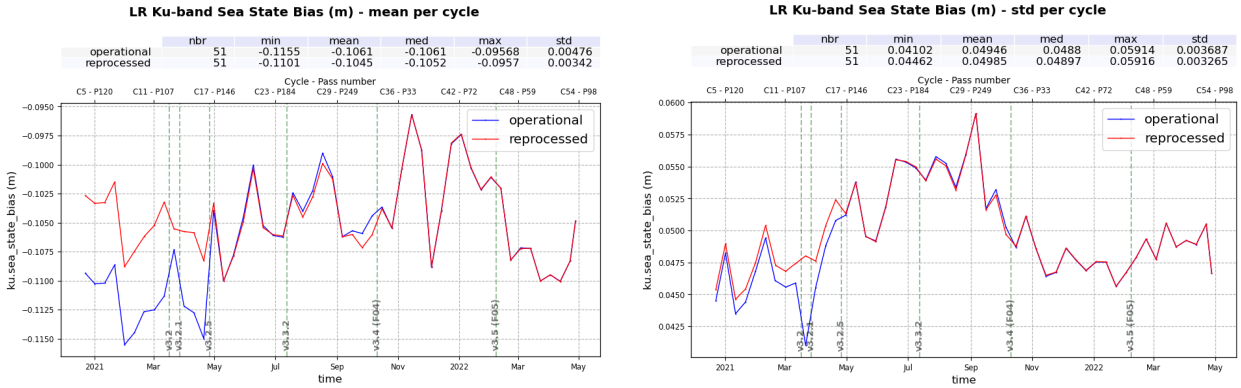

Figure 33 – Time monitoring of Sentinel-6A Ku-band Sea State Bias in meters, before reprocessing (blue) and after reprocessing (red). Left: mean per cycle, Right: standard deviation per cycle

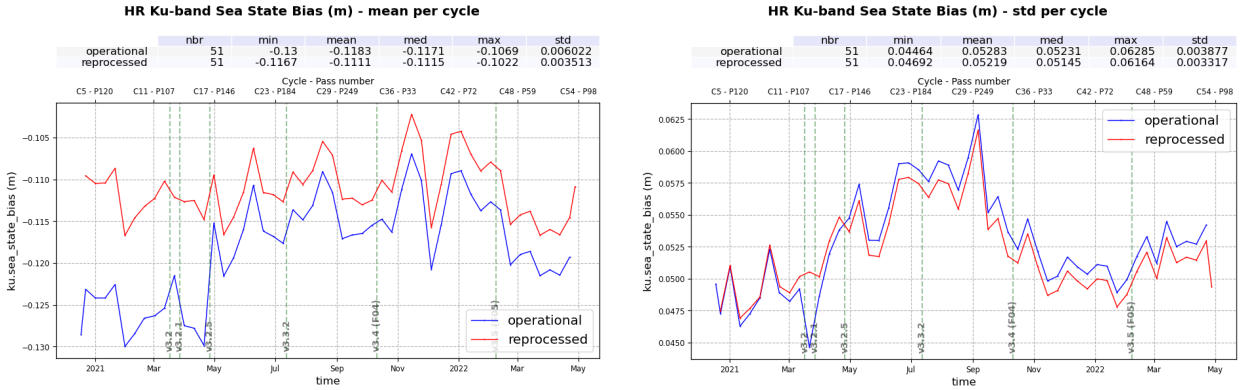

Figure 34 – Time monitoring of Sentinel-6A Ku-band Sea State Bias in meters, before reprocessing (blue) and after reprocessing (red). Left: mean per cycle, Right: standard deviation per cycle

Reprocessed data

After reprocessing, LR Ku-band SSB is centred around -10.5 cm, which is in line with Jason-3 (-10.4 cm). HR SSB is centred around -11.1 cm (figure 35). Maps of Ku-band SSB averaged over the reprocessing period show the same geographical patterns between Jason-3 and Sentinel-6A LR and HR (figure 36).

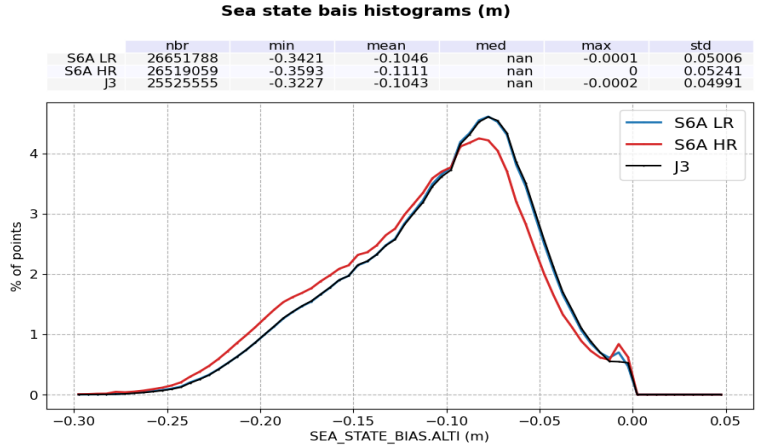

Figure 35 – Histogram of Ku-band Sea State Bias for Jason-3 (black), reprocessed S6A LR (blue) and reprocessed S6A HR (red). Computed over the completed reprocessed period.

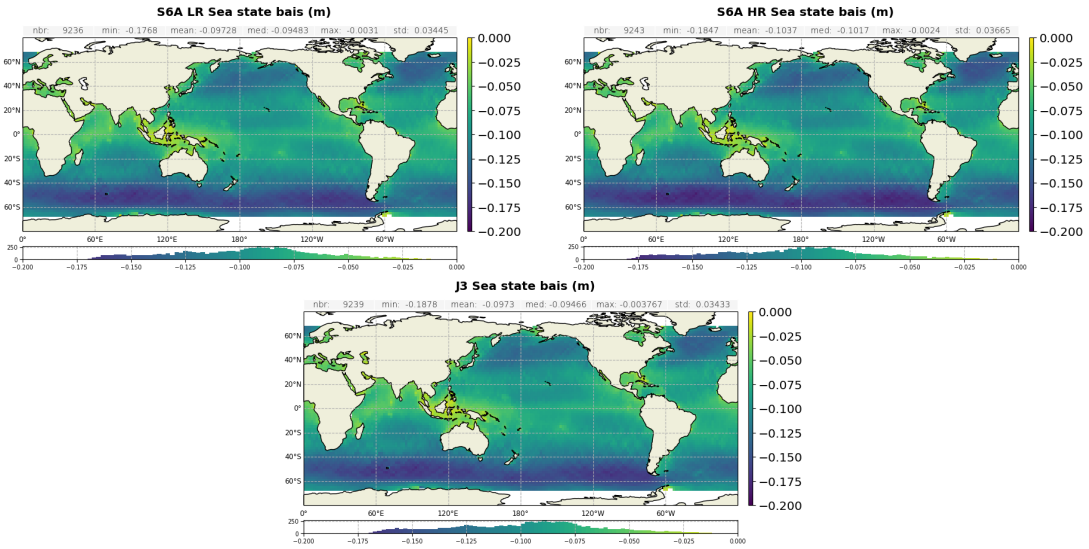

Figure 36 – Map of Ku-band Sea State Bias for reprocessed S6A LR (top left), reprocessed S6A HR (top right), and Jason-3 (bottom). Computed over the completed reprocessed period.

4.1.6. Altimeter ionosphere correction

Comparison between operational and reprocessed data

Sentinel-6A altimeter ionosphere correction is derived from LR data, in Ku and C band. The ionosphere correction in HR products is copied from LR products and thus identical. Filtred ionosphere correction from altimeter is analysed in this section.

Operational and reprocessed ionosphere corrections are in line from PB F04 deployement, both in mean and in standard deviation (figure 37). On this monitoring, a decrease of the ionosphere correction is visible from September. This behavior is observed on ionosphere corrections derived from other altimeters (as Jason-3) and on GIM retrieval. This is an expected behavior of the ionosphere correction.

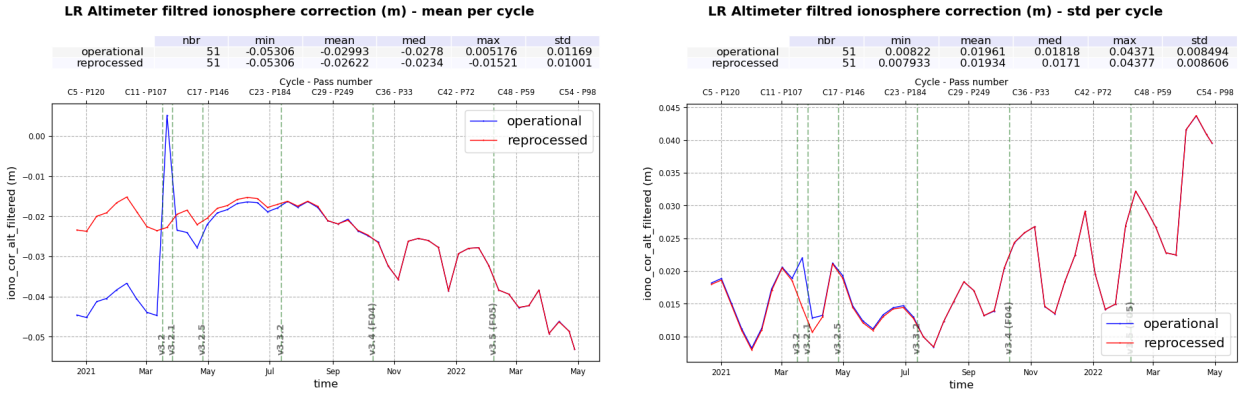

Figure 37 – Time monitoring of Sentinel-6A LR Altimeter filtred ionospehere correction in meters, before reprocessing (blue) and after reprocessing (red). Left: mean per cycle, Right: standard deviation per cycle

Reprocessed data

After reprocessing, Sentinel-6A ionosphere correction is centred around -2.6 cm, which is slightly smaller than Jason-3 (-2.1 cm), see figure 38. The corresponding maps show the same geographical patterns between Jason-3 and Sentinel-6A LR (figure 39).

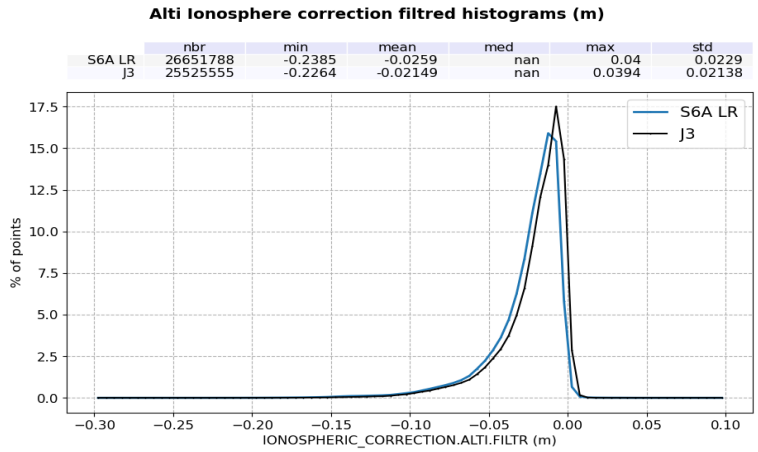

Figure 38 – Histogram of altimeter filtred ionospehere correction for Jason-3 (black) and reprocessed S6A LR. Computed over the completed reprocessed period.

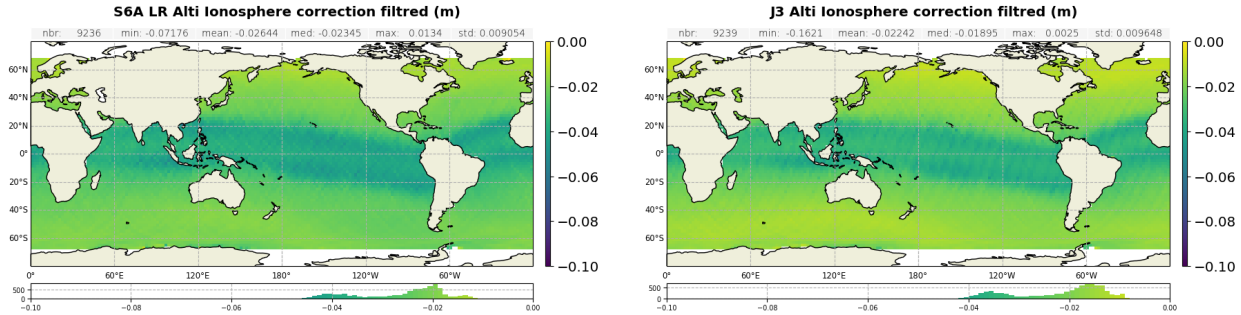

Figure 39 – Map of altimeter filtred ionospehere correction for reprocessed S6A LR (left) and Jason-3 (right). Computed over the completed reprocessed period.

Reprocessed Sentinel-6A altimeter ionosphere correction shows in average a better consistency to GIM model than Jason-3. The bias with respect to GIM is centred around 0.8 cm for Sentinel-6A data while 1.2 cm for Jason-3 (figure 40). Howerver, looking at the corresponding maps of altimeter versus GIM difference (figure 41), the amplitude of the difference is stronger for Sentinel-6A than Jason-3. This behavior can be linked to the reduced smoothing in Sentinel-6A ionosphere correction filtering, thus giving more accurate reflection of the peaks and troughs in the ionospheric content.

4.1.7. Mispointing

Comparison between operational and reprocessed data

In this section is analysed the square of the off-nadir angle derived from the MLE4 waveform retracking from LR dataset. Thanks to the reprocessing, the mispointing is more stable in time as the LR configuration updated with PDAP v3.2 is applied over the complete dataset (figure 42).

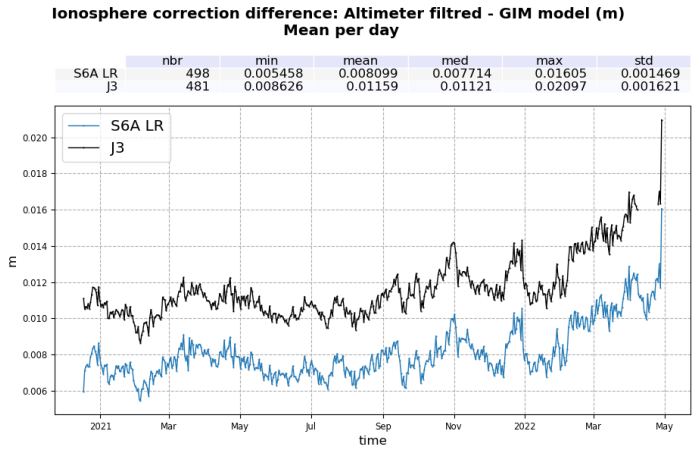

Figure 40 – Time monitoring of the ionosphere correction difference : Altimeter Filtred minus GIM model (m), for Jason-3 (black) and Sentinel-6A LR reprocessed data (blue)

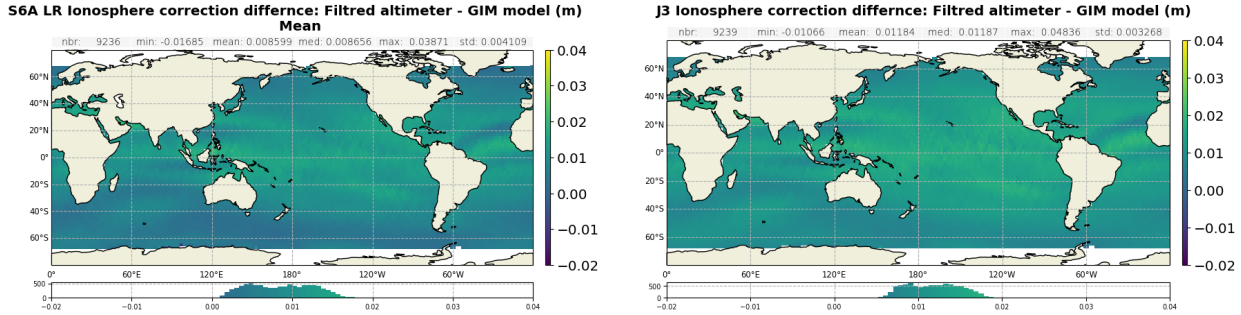

Figure 41 – Map of ionosphere correction difference : Altimeter Filtred minus GIM model (m). For reprocessed S6A LR (left) and Jason-3 (right). Computed over the completed reprocessed period.

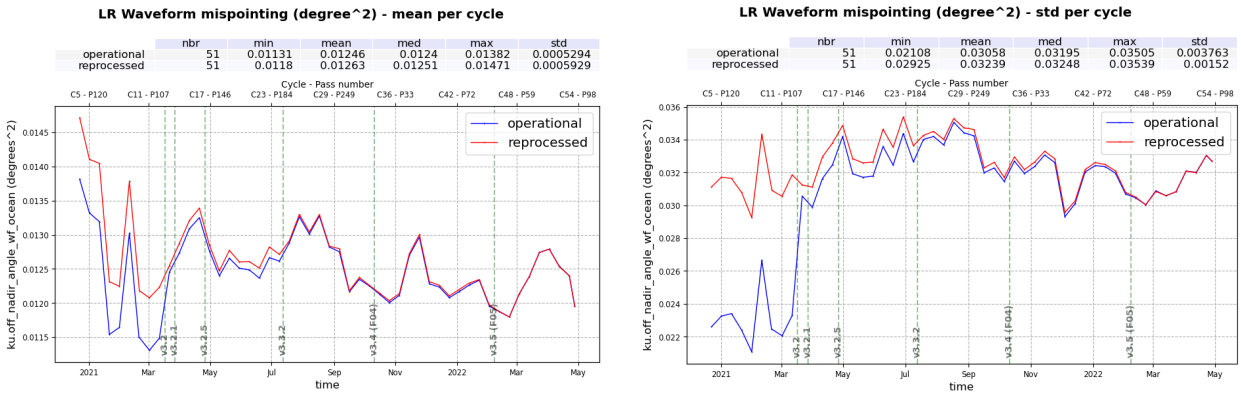

Figure 42 – Time monitoring of Square of the off-nadir mispointing angle in $degree^2$, before reprocessing (blue) and after reprocessing (red). Left: mean per cycle, Right: standard deviation per cycle

Reprocessed data

Reprocessed Sentinal-6A mispointing is centred around 0.0126 $degree^2$. It shows a bias with respect to Jason-3 mispointing which is more centred around 0. The corresponding maps show the same geographical patterns between Jason-3 and Sentinel-6A LR (figure 44). For Sentinel-6A, tracks with higher mispointing are due to manoeuvres occuring over the Phase-E1 of the satellite.

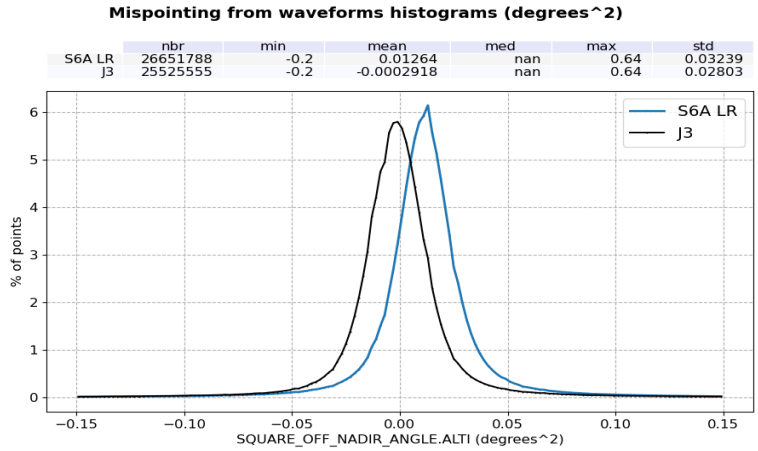

Figure 43 – Histogram of Square of the off-nadir mispointing angle for Jason-3 (black) and reprocessed S6A LR. Computed over the completed reprocessed period.

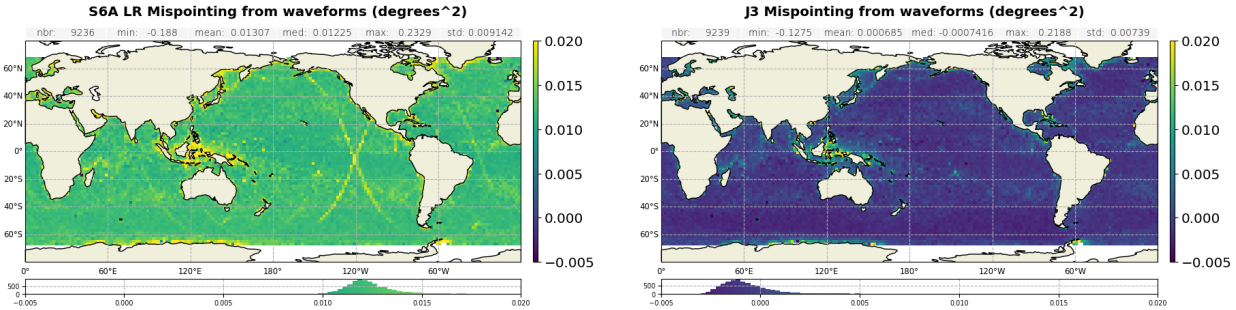

Figure 44 – Map of Square of the off-nadir mispointing angle for reprocessed S6A LR (left) and Jason-3 (right). Computed over the completed reprocessed period.

4.2. Wet tropospheric correction from AMR-C

Comparison between operational and reprocessed data

Wet Troposheric Correction (WTC) derived from radiometer is monitored and especially its coherence to WTC from ECMWF model.
Monitoring of the differences between radiometer and model WTC allows to highlight any jump or drift between the two retrievals. For operational data, radiometer WTC is impacted by various updates and calibrations (see figure 45, blue curve). In particular, on the 17-18th March 2021, the AMR-C has undergone a 24h warm target calibration. After this calibration, the bias between radiometer and ECMWF WTC has been strongly reduced from about - 4.5 mm to about -1 mm.

Thanks to the reprocessing of radiometer parameters, bias between radiometer and ECMWF WTC is more stable in time as shown on the red curve of figure 45. The jump induced by the warm target calibration is not present anymore. Howerver, we still observe two changes of behavior: from October 2021 (differences go from -1 mm to 1 mm), and from February 2022 (differences go from 1 mm to around 0 mm).

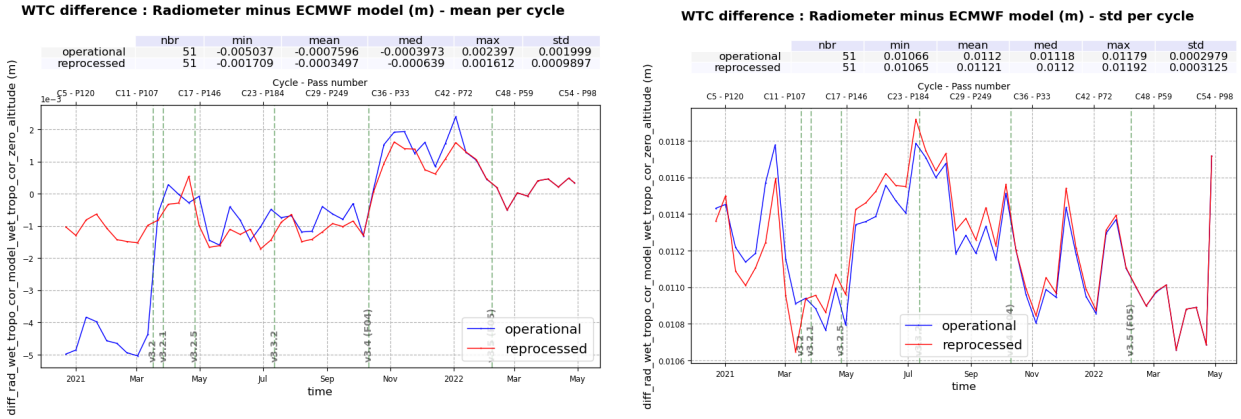

Figure 45 – Time monitoring of wet tropospheric correction difference (m): WTC from radiometer minus WTC from ECMWF model. Before reprocessing (blue) and after reprocessing (red). Left: mean per cycle, Right: standard deviation per cycle

Reprocessed data

Looking more closely to S6A reprocessed data, the monitoring per day of the bias between radiometer and model highlights four phases induced by three events (figure 46 left panel):

- on 27-28 April 2021, a jump of -4 mm is observed in the bias preceded by a progressive increase of the bias (from beginning of March 2021) by the same amplitude. The jump visible on 27-28 April 2021 is concumitent with a satellite restart and is not observed in Jason-3 time series (figure 46 right panel). The potential link between the satellite restart and this jump is under investigation.
- on 13 October 2021, a jump of +2 mm is observed on both Sentinel-6A and Jason-3 monitoring. It is linked to an update in the ECMWF model (see [4] for more details).
- around mid-February 2022, one last change is observed on Sentinel-6A monitoring. This change is more progressive and spanned over about 3 days. Over this period, Jason-3 and Sentinel-6 monitorings split from one-another and comparison cannot be done. The origin of this small change (-1 mm) on Sentinel-6A is under investigation.

The corresponding maps (figure 47) does not highlight strong discrepencies between S6A and J3 retrievals.

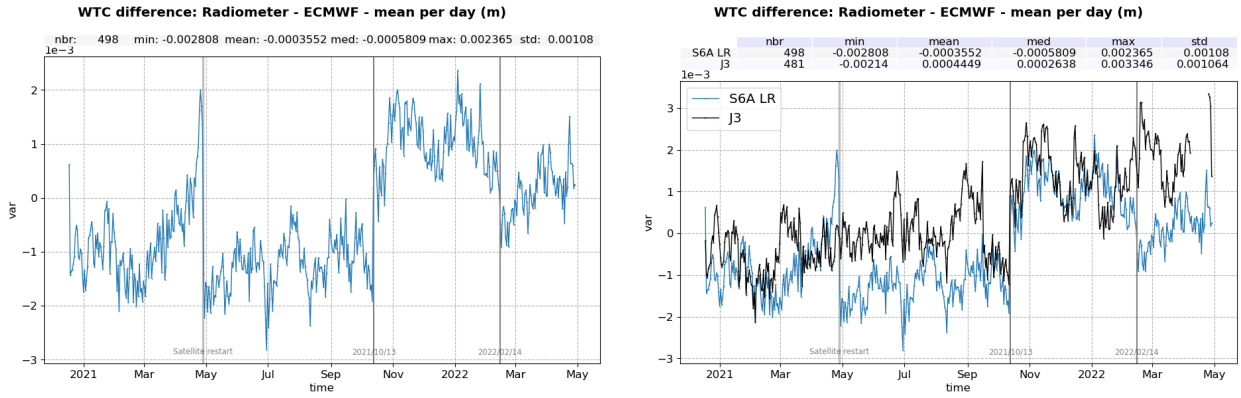

Figure 46 – Mean per day of wet tropospheric correction difference: WTC from radiometer minus WTC from ECMWF model. For Sentinel-6A reprocessed data only (left panel) and for S6A and J3 on the same plot (right panel).

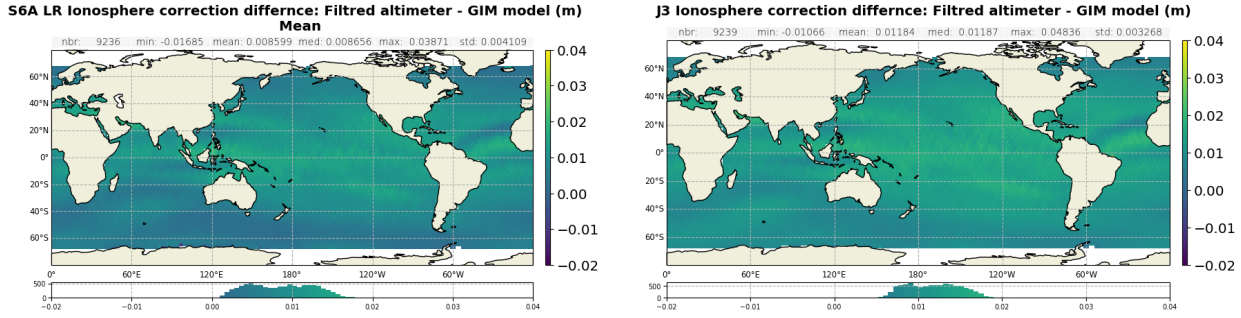

Figure 47 – Map of WTC difference : Radiometer minus ECMWF model (m). For reprocessed S6A LR (left) and Jason-3 (right). Computed over the completed reprocessed period.

After reprocessing, Sentinel-6A radiometer WTC is centred around -15.0 cm, which in line with Jason-3 (-15.0 cm), see figure 48. The corresponding maps show the same geographycal patterns between Jason-3 and Sentinel-6A (figure 49).

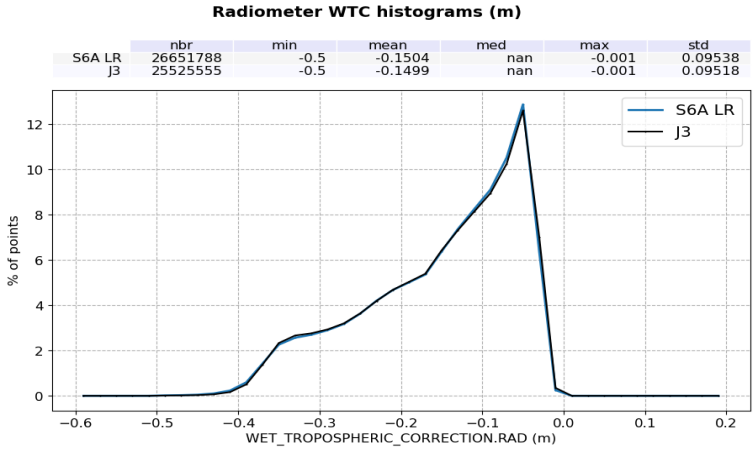

Figure 48 – Histogram of radiometer WTC for Jason-3 (black) and reprocessed S6A. Computed over the completed reprocessed period.

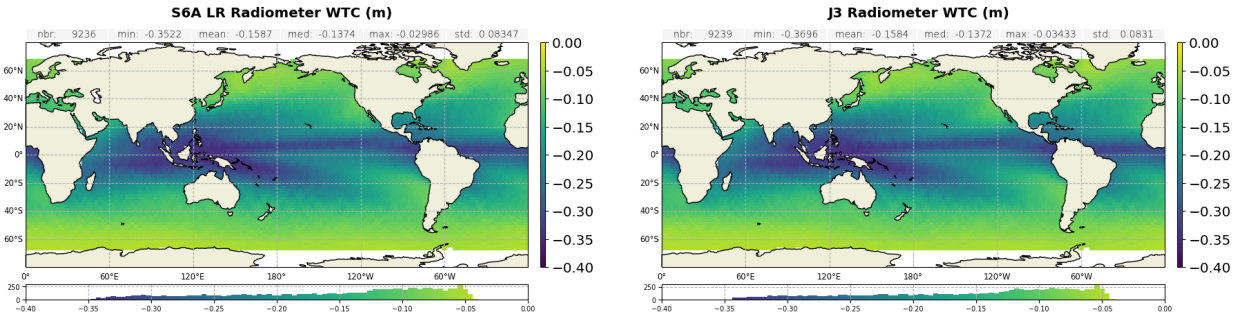

Figure 49 – Map of radiometer WTC for reprocessed S6A LR (left) and Jason-3 (right). Computed over the completed reprocessed period.

4.3. Sea Level Performances

The Sea Surface Height Anomaly is the most well-known parameter estimated from altimetry. It corresponds to the elevation of sea surface, with respect to a reference called Mean Sea Surface (MSS), generated by oceanic variability and climatic phenomena (such as Gulf stream current, El Nino, ...). It is computed as follow:

$$SSHA = Orbit - AltimeterRange - \sum(GeophysicalCorrections) - MeanSeaSurface$$

The details of the geophysical corrrections can be found in Sentinel ALT Level 2 Product Generation Specification available at https://www.eumetsat.int/media/48266.

4.3.1. Along-track analysis

Comparison between operational and reprocessed data

Comparison between operational and reprocessed datasets does not highlight any differences for LR SSHA after PB F05, both in mean and in standard deviation (figure 50). From July 2021 to February 2022 (i.e. between PDAP v3.2 and PB F05), the standard deviation of SSHA is slightly higher with reprocessed data. This is due to the update of the ionosphere correction filtering implemented in PB F05 (see section 3.2.5. for more details). As some points have been recovered in the Antartica and Indonesia regions, the standard deviation of the SSHA has slightly increased with the reprocessing.

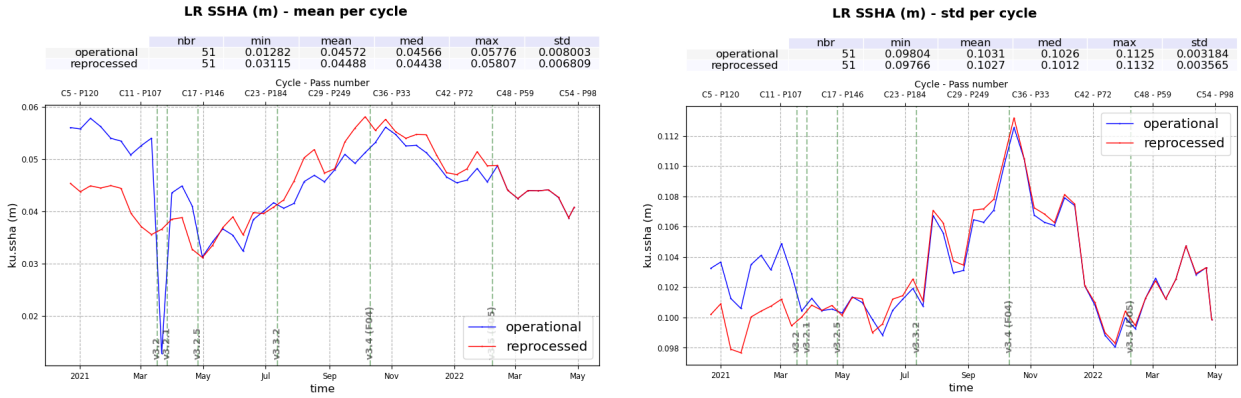

Figure 50 – Time monitoring of Sentinel-6A SSHA in meters, before reprocessing (blue) and after reprocessing (red). Left: mean per cycle, Right: standard deviation per cycle

Impact of PB F06

In HR, the reprocessed SSHA is impacted by PB F06 update at several levels:

- via the impact on the range (+ 1.2 mm)
- via the impact on the SSB through the SWH and the range (+ 4.8 mm)

The resulting impact on SSHA is of - 6 mm, as shown by the HR SSHA difference between F06 and F05 data presented on figure 52.

Thanks to the reprocessing, HR SSHA standard deviation has decreased.

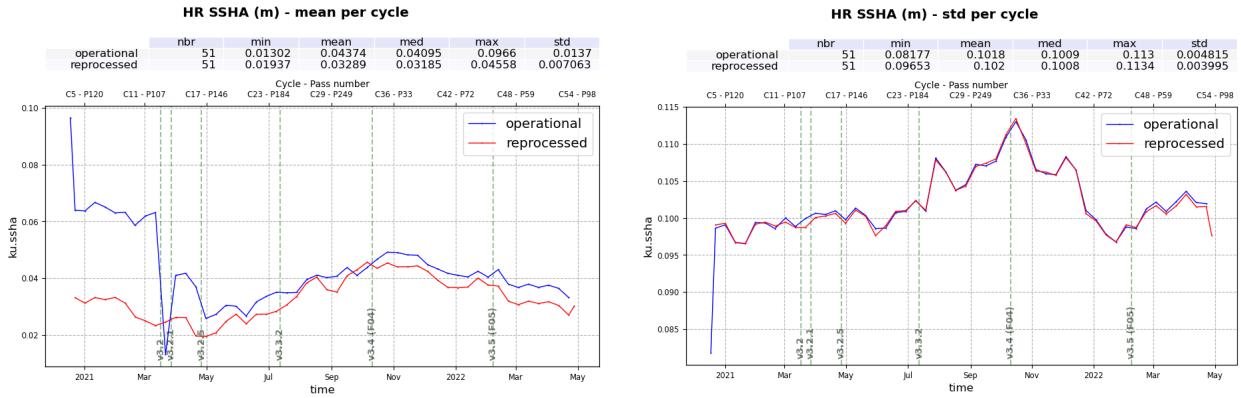

Figure 51 – Time monitoring of Sentinel-6A SSHA in meters, before reprocessing (blue) and after reprocessing (red). Left: mean per cycle, Right: standard deviation per cycle

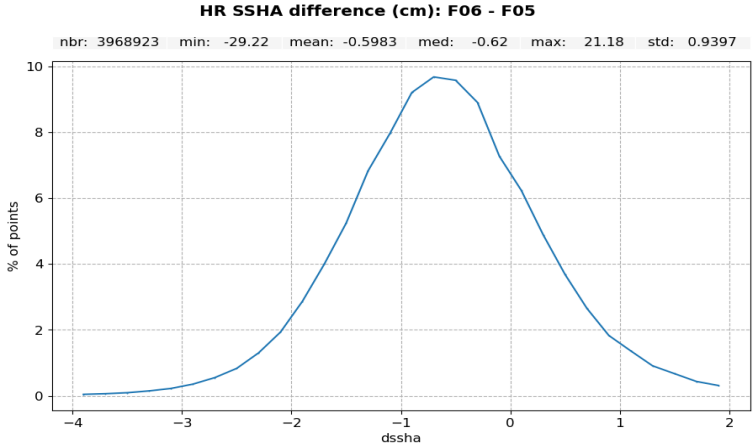

Figure 52 – Histogram of HR SSHA difference between reprocessed and operational F05 data, computed over cycles 47 to 53.

HR versus LR range bias is compared over PB F05 time period (figure 53). The SSHA bias correlation to SWH is reduced. With PB F06 (red curve in bottom plot), the bias decreases of 3.5 cm between 1 and 7-m wave height, while it was of 4 cm over the same wave height interval for PB F05 (blue curve). This is again due to the impact of F06 HR configuration update on range and SWH (through SSB). Note here that such comparison between LR and HR SSHA highlights the skewness difference between LR and HR processing, which will be dealt with in a future evolution of the HR processing and subsequent reprocessing.

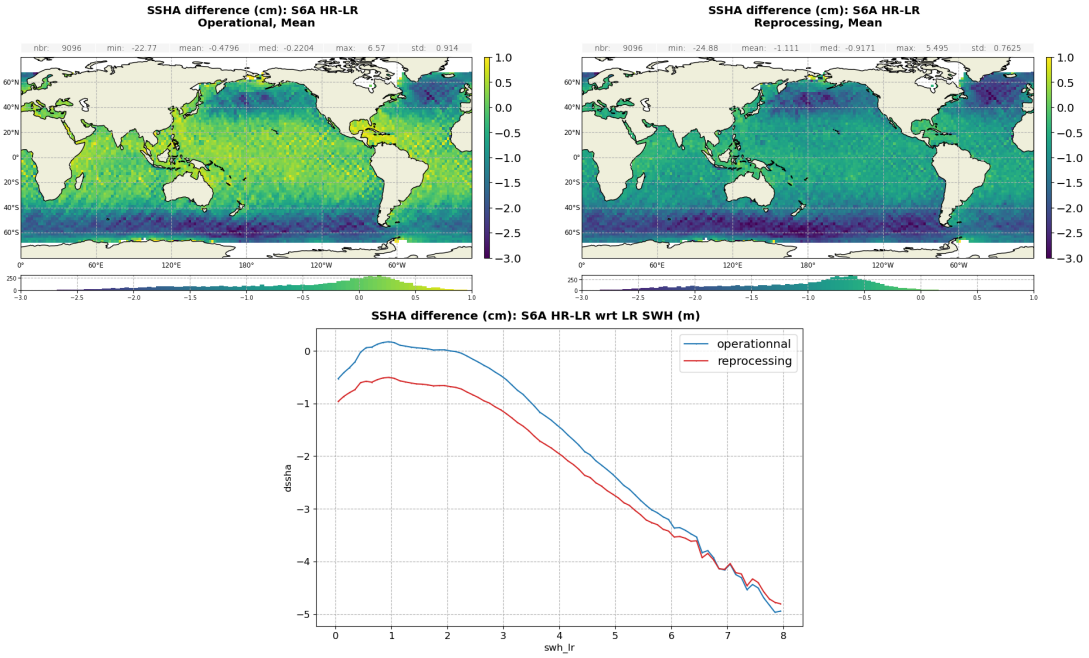

Figure 53 – HR - LR SSHA difference over cycles 47 to 53 (PB F05 in operational) : Gridded map for operational data (top left) and for reprocessed data (top right), Difference function of LR SWH (bottom)

Reprocessed data

After reprocessing, product SSHAs are centred around 4.5 cm for S6A LR and 3.3 cm for S6A HR, as for Jason-3 (figure 54). Maps of SSHA averaged over the reprocessing period show the same geographical patterns between Jason-3 and Sentinel-6A LR and HR (figure 55).

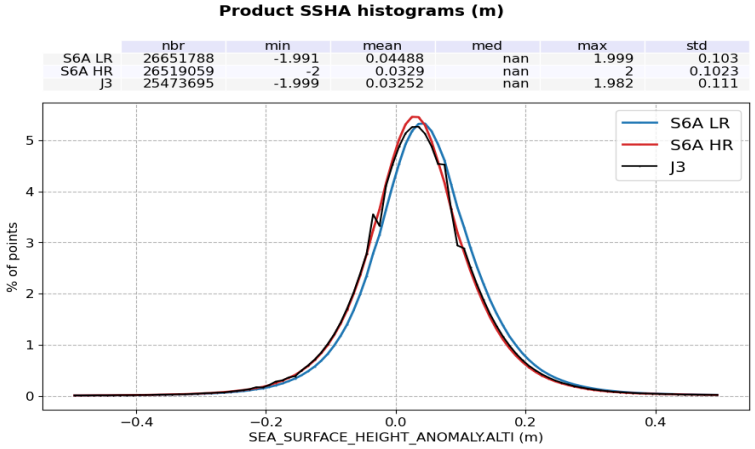

Figure 54 – Histogram of product SSHA for Jason-3 (black), reprocessed S6A LR (blue) and reprocessed S6A HR (red). Computed over the completed reprocessed period.

As shown on the temporal monitoring (figure 56), Jason-3, Sentinel-6A LR and HR SSHAs follow the same temporal variation, in term of mean and standard deviation. The standard devation is similar for S6A LR and HR and is centred around 10 cm, which is 1 cm smaller than Jason-3. In addition, J3 SSHA standard deviation shows greater temporal variations, while S6A LR and HR standard deviation is more stable in time. These discrepancies are still under investigation.

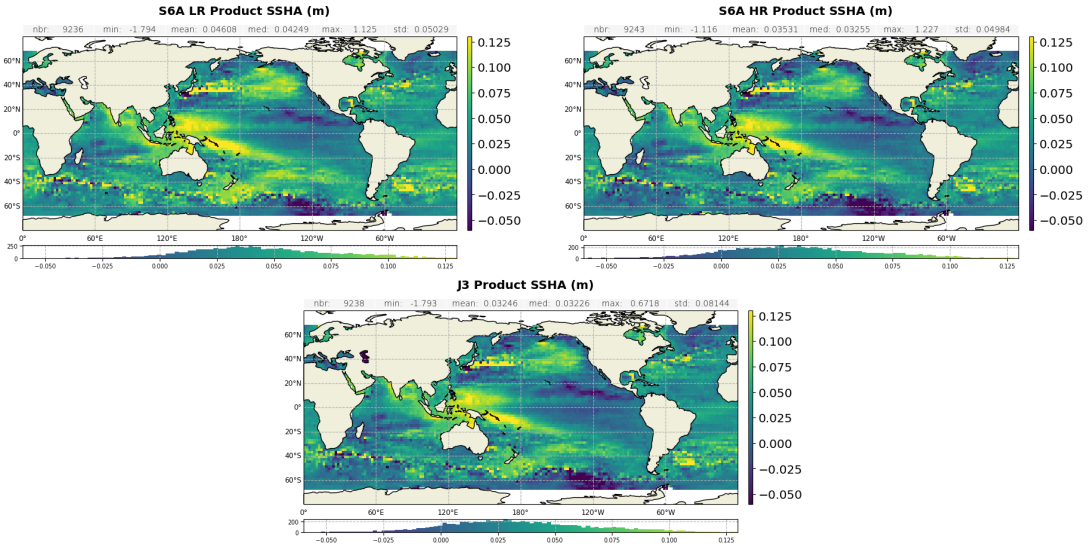

Figure 55 – Map of product SSHA in meters for reprocessed S6A LR (top left), reprocessed S6A HR (top right), and Jason-3 (bottom). Computed over the completed reprocessed period.

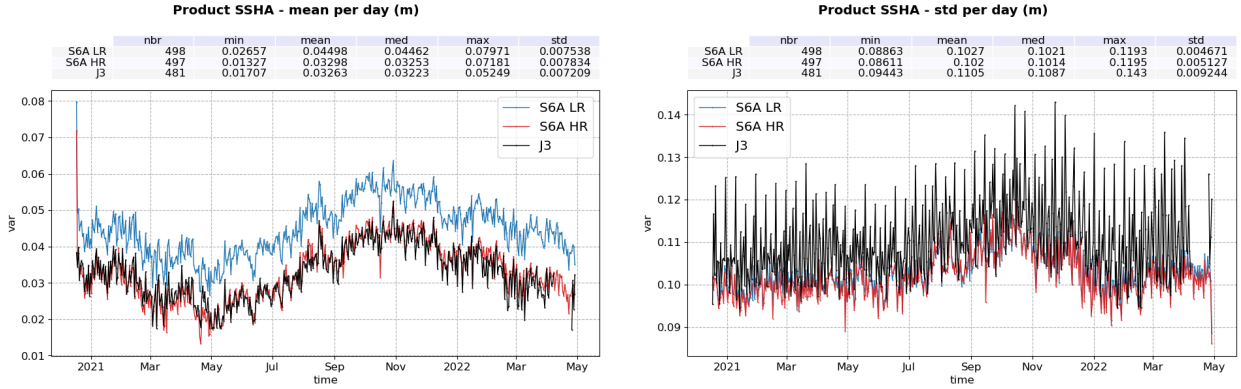

Figure 56 – Time monitoring of Sentinel-6A SSHA in meters, before reprocessing (blue) and after reprocessing (red). Left: mean per cycle, Right: standard deviation per cycle

4.3.2. Crossover analysis

Sea Surface Height crossover differences are the SSH differences between ascending and descending passes where they cross each other. Crossover differences are systematically analyzed to estimate data quality and the Sea Surface Height (SSH) performances. SSH crossover differences are computed from the valid data set on a one cycle basis, with a maximum time lag of 10 days, in order to limit the effects of ocean variability which are a source of error in the performance estimation. The mean SSH crossover differences should ideally be close to zero and standard deviation should ideally be small.

Nevertheless SLA varies also within 10 days, especially in high variablity areas. Furthermore, due to lower data availability (due to seasonal sea ice coverage), models of several geophysical corrections are less precise in high latitude. Therefore an additional geographical selection - removing shallow waters, areas of high oceanic variability and high latitudes ($> |50|$ deg) - is applied for cyclic monitoring.

Thanks to the reprocessing, the mean SSH difference at crossover is more stable in time, as shown on figure

57 left panel. Mean values are now in line with Jason-3 (properly centred around 0) and follow the same variation in time (figure 57 right panel).

Looking at standard deviation of the SSH difference at crossovers, we see again the improvement in stability brought by the reprocessing (figure 58). In addition, the HR configuration update implemented in PB F06 induces a reduction of the noise in HR of about 1 mm. After reprocessing, the SSH difference standard deviation is of 4.7 cm for S6A LR and 4.5 cm for S6A HR. This is smaller than Jason3 (4.8 cm).

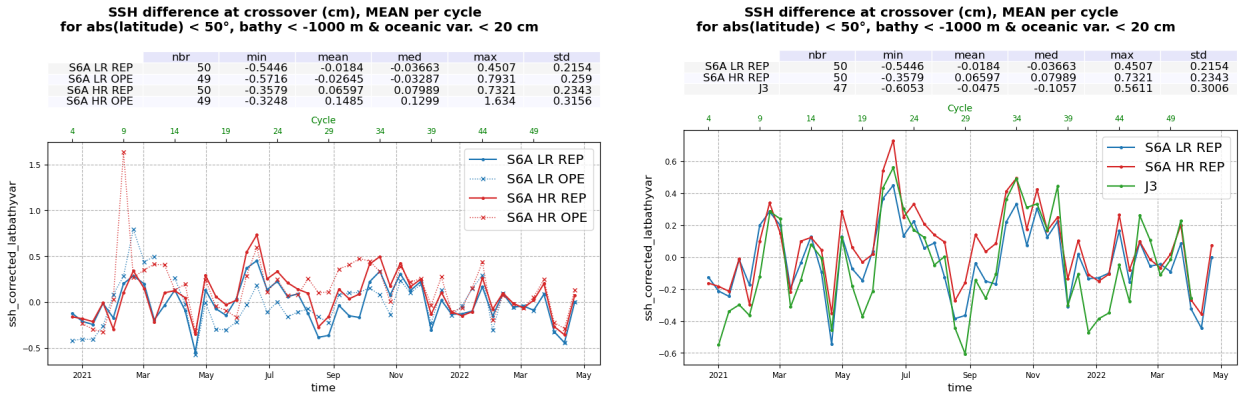

Figure 57 – Monitoring of the mean of SSH difference at mono-mission crossover for each cycle. Left panel: comparison before (dashed line) and after reprocessing (solid line). Right panel : comparison between Jason-3 and S6A reprocessed data

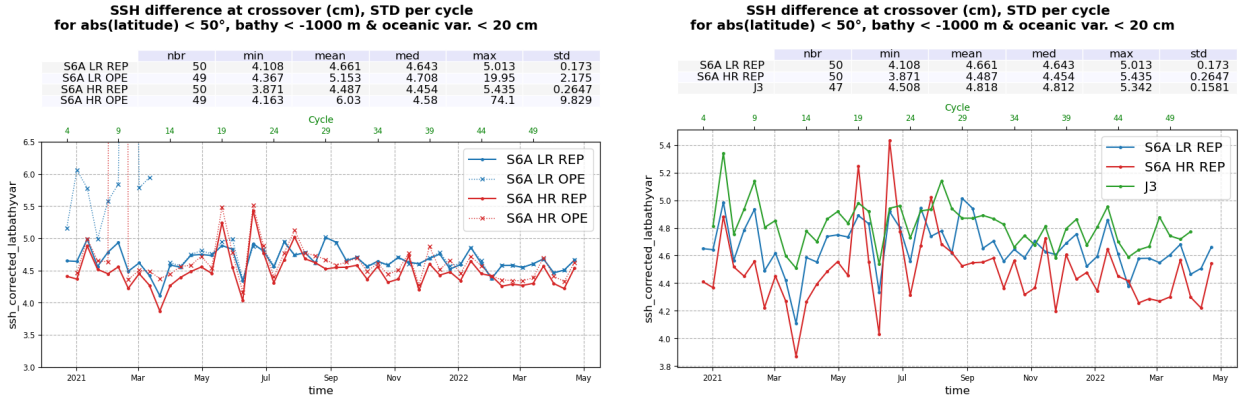

Figure 58 – Monitoring of the standard deviation of SSH difference at mono-mission crossover for each cycle. Left panel: comparison before (dashed line) and after reprocessing (solid line). Right panel : comparison between Jason-3 and S6A reprocessed data

Maps of LR SSH difference at crossover are smooth and does not hightlight any strong discrepancies between ascending and descending tracks in terms of SSH (figure 59).

Maps of HR SSH difference at crossover highlight patterns correlated to along-track wind (figure 60). It is linked to the impact of along-track wind on HR data an more particularly on HR range. These patterns are reduced in the reprocessed data, as already exposed in section 4.1.2..

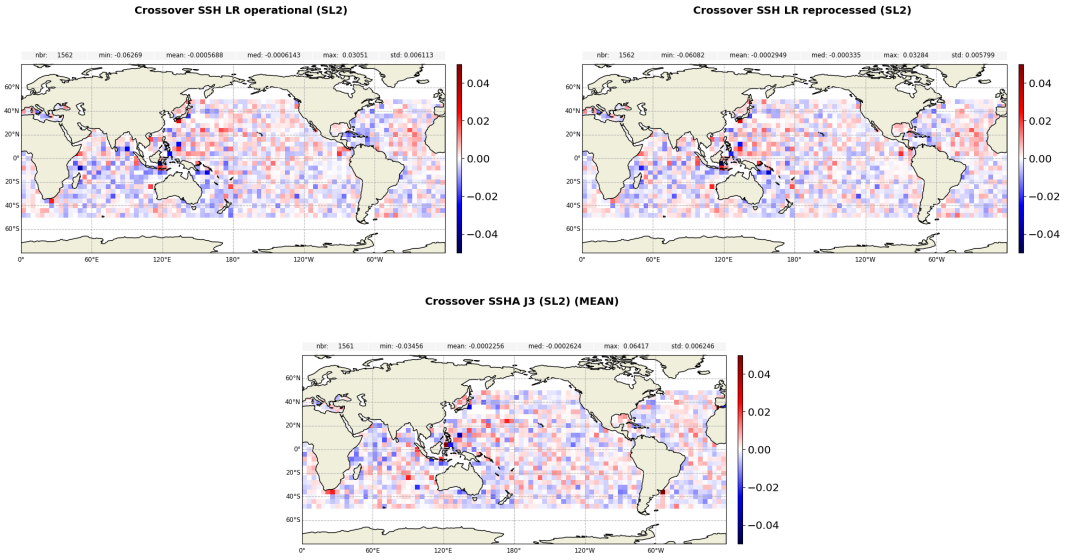

Figure 59 – Mean SSH difference at crossovers for S6A LR operational data (top left), S6A LR reprocessed data (top right) and J3 (bottom). Computed over the complete reprocessing period.

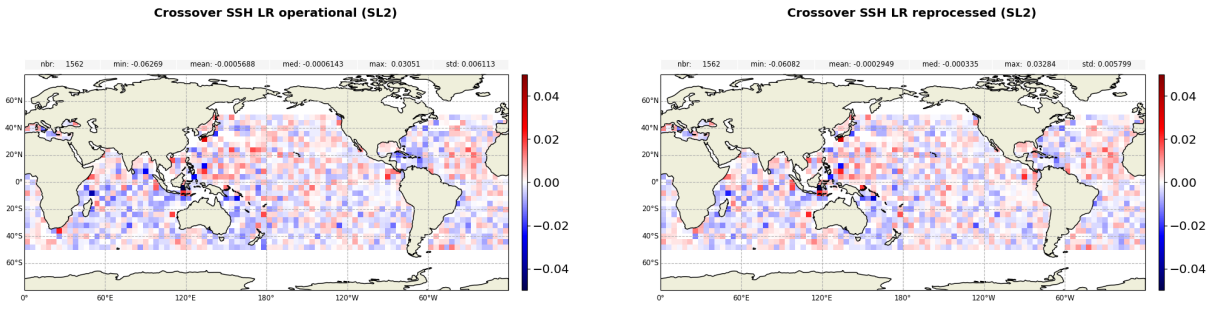

Figure 60 – Mean SSH difference at crossovers for S6A HR operational data (left) and S6A HR reprocessed data (right). Computed over the complete reprocessing period.

5. Analysis of the tandem flight with Jason-3

Between the 2020/12/17 and 2022/04/07 (Sentinel-6A cycles 4 to 51), Sentinel-6A and Jason-3 were flying in tandem formation on the same ground track with only 30 seconds apart, Jason-3 ahead of Sentinel-6A. This section is dedicated to the precise comparison between Sentinel-6A and Jason-3 data over this tandem flight.

To perform such analysis, Sentinel-6A and Jason-3 data are co-loacted by interpolation onto their common theorical ground-track. This allows to perform point to point differences over the complete tandem flight period and thus to give precise comparison metrics.

In this section, we focus on parameters involved in the SSHA computation. A particular attention is given to POS-4 switch to B-side (2021-09-14). Only reprocessed Sentinel-6A data are considered here.

5.1. Radiometer parameters

The WTC derived from radiometer are compared between Sentinel-6A (AMR-C) and Jason-3 (AMR). In average, the bias between the two retrieval is well centred around 0 (below 1 mm bias). Differences range between -1 and 1 cm with clear correlaction to wet troposhere content itself (figure 61).

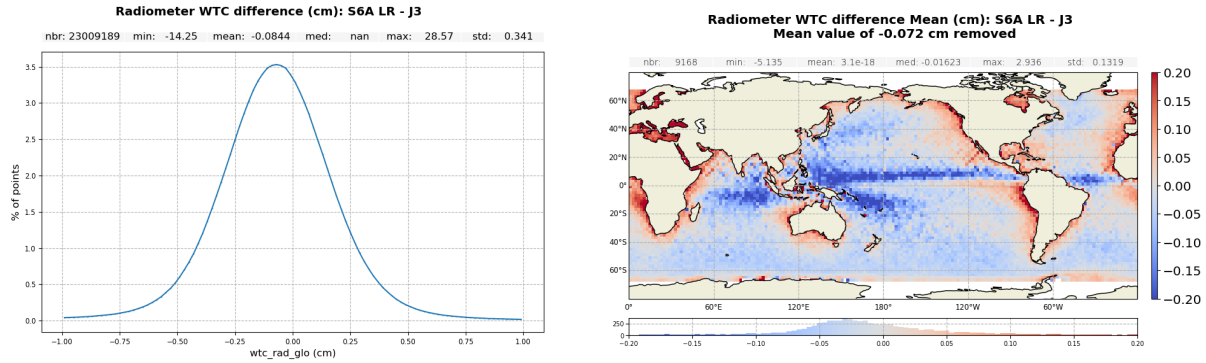

Figure 61 – Radiometer WTC difference : Sentinel-6A AMR-C minus Jason-3 AMR. Histogram (left) and gridded map (right) computed over the complete tandem period.

Looking at time monitoring of Sentinel-6A versus Jason-3 bias, two distinct changes can be observed (figure 62):

- on 27-28 April 2021, a jump of -4 mm is observed in the bias, preceded by a progressive increase of the bias (from beginning of March 2021) by the same amplitude. The same behavior was observed on Sentinel-6A radiometer WTC comparison to ECMWF model (see section 4.2.). The jump visible on 27-28 April 2021 is concomitent with a satellite restart. The potential link between the satellite restart and this jump is under investigation. The AMR-C jump is between two calibration sequencies and will therefore be difficult to remove.
- from the beginning of 2022, Sentinel-6A and Jason-3 radiometer WTC derived from one another to reach 3.3 mm bias around mi-february. The origin of this behavior is for the moment unknown and cannot be affected to neither Sentinel-6A AMR-C nor to Jason-3 AMR.

Generally, S6A and J3 AMR are being calibrated completely independently of each other for operational processing, so such a bias is possible. S6A AMR-C calibration shall be superior to the J3 AMR since S6 is

calibrated using the SCS, while J3 AMR is calibrated using the historical vicarious references. For the S6A AMR-C, each calibration brings the radiometer back to a nominal baseline with an uncertainty of about 2mm (1-sigma). As for future re-processing, a target could be to remove these differences between J3 and S6A, by calibrating J3 AMR to S6A AMR-C.

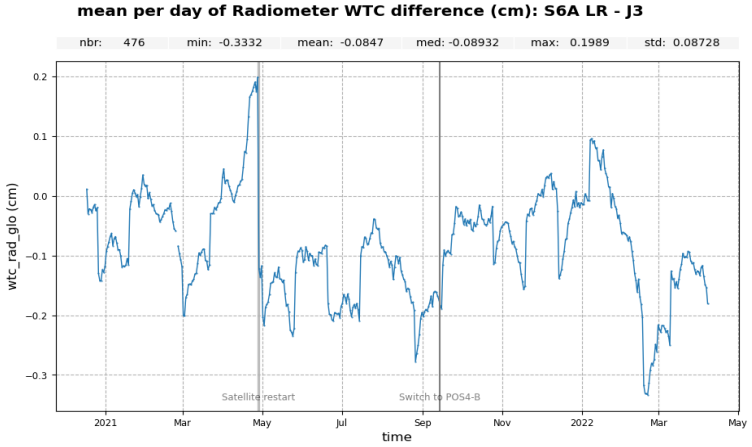

Figure 62 – Time monitoring of Radiometer WTC difference : Sentinel-6A AMR-C minus Jason-3 AMR. Mean per day computed over the complete tandem period.

5.2. LR

In this section, Sentinel-6A LR data is compared to Jason-3.

5.2.1. Ku-band

LR Ku-band SWH

Ku-band SWH bias between S6A LR and J3 is centred around -1.29 cm (figure 63). The mean daily bias varies between -0.7 and -2 cm with time with a standard deviation of 15.5 cm stable in time (figure 64). Note that the peak of standard deviation visible on the 27-28 April 2021 is linked to the satellite switch-off, leading to a data loss and thus to an increase in standard deviation.

A small difference is observed between POS4-A and POS4-B (-0.36 cm). It is hard to say here if it is due to the switch to POS-4 B-side or simply to sea state condition variations.

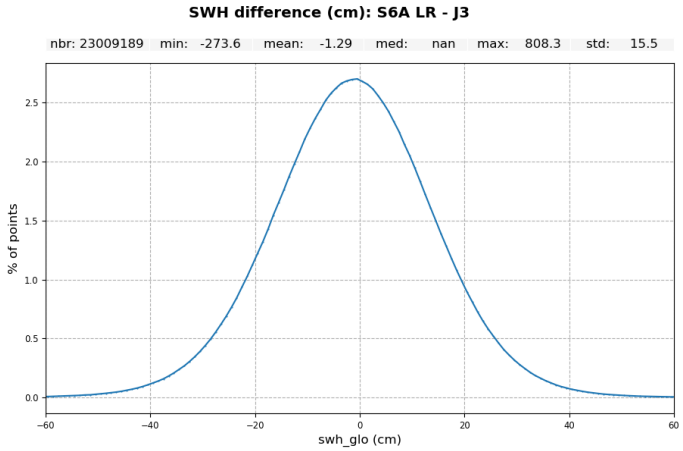

Figure 63 – Histogram of Ku-band SWH difference: Sentinel-6A LR minus Jason-3. Computed over the complete tandem period.

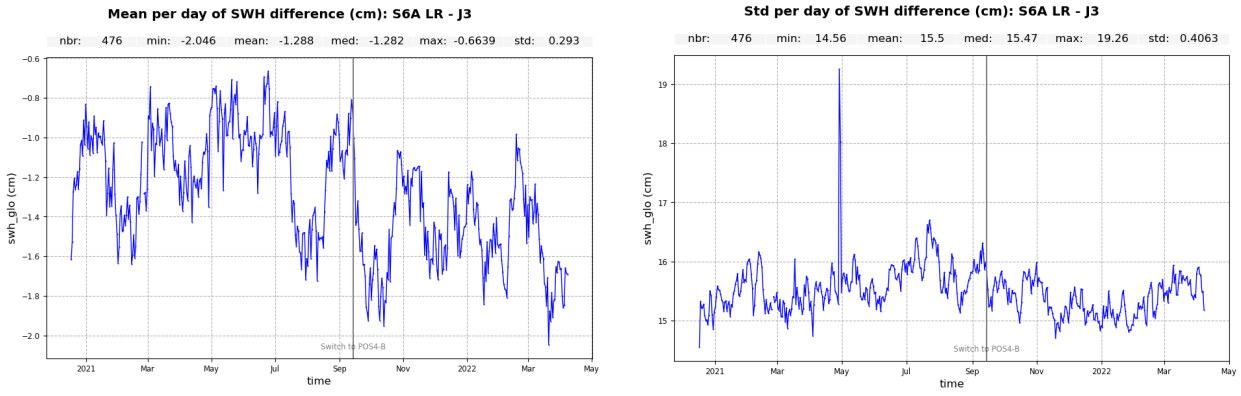

Figure 64 – Time monitoring of Ku-band SWH difference: Sentinel-6A LR minus Jason-3. Mean per day (left) and standard deviation per day (right) computed over the complete tandem period.

The map of SWH difference (figure 65) mainly shows a good consistency between the two missions, except in small waves areas where the bias is higher. The root cause of this higher bias is the improved handling of

low wave heights in Sentinel-6A Level 2 processing, as already explained in section 4.1.1.: S6A processing allows negative SWH values while it is not the case for Jason-3. It can lead to differences up to -9 cm for very low SWH (below 0.5 m). For SWH $>$ 1 m, Sentinel-6A LR and Jason-3 SWH are in line, with differences within 2 cm in absolute value.

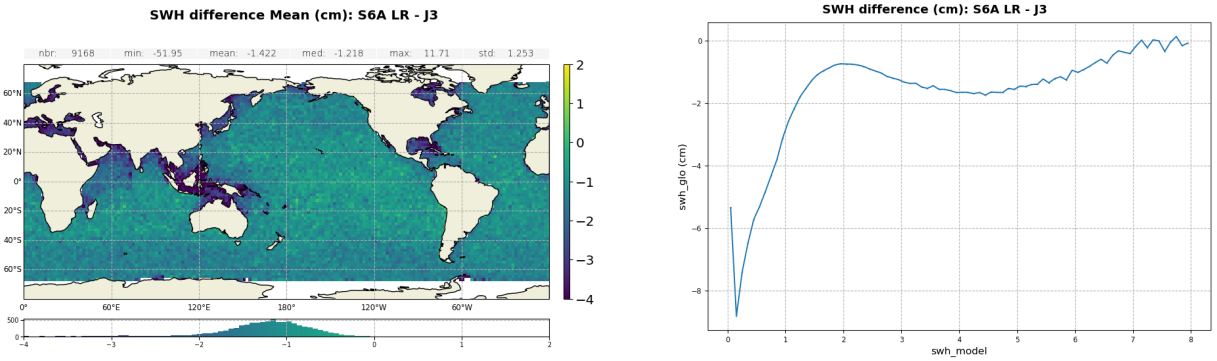

Figure 65 – Ku-band SWH difference: Sentinel-6A LR minus Jason-3 computed over the complete tandem period. Gridded map (left panel) and difference function of ERA5 SWH (right panel).

LR Ku-band Range

To compare ranges between the two missions, we do not perform a direct difference of the two ranges, because of the strong variation in time of range values. Instead, we compare (orbit - range - MSS).

Figure 66 highlights the consitency between the two satellites with an average bias of 0.76 cm. The time monitoring of the difference depicts a small drift in time of +2 to 3 mm over the entire tandem phase (figure 67).

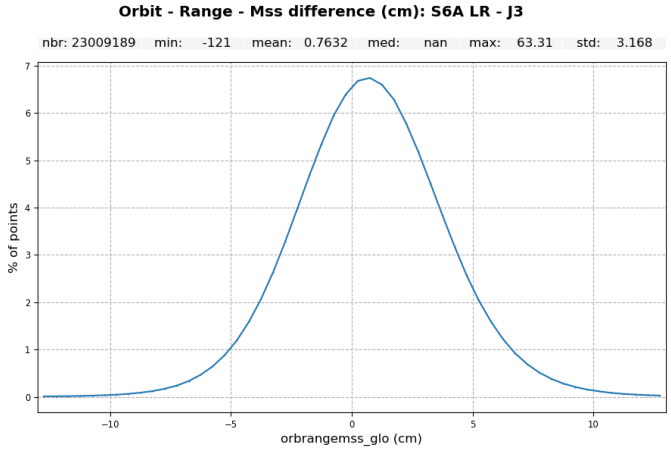

Figure 66 – Histogram of Orbit - Ku-band range - MSS difference : Sentinel-6A LR minus Jason-3. Computed over the complete tandem period.

The map of the difference (figure 68 left panel) presents a clear correlation to SWH. The bias increases of 0.7 cm between 2 and 7 m-wave, as shown on figure 68 right panel. Studies have shown that part of this correlation in linked to instrumental LUT applied on S6A range. It will be corrected thanks to the future numerical retracking where no intrumental LUT are applied. Part of the observed correlation to SWH will remain. Some can be linked to pulse to pulse correlation effect, not taken into account in the processing yet. An equatorial band of 5 mm amplitude is also clearly visible on the map. Investigations have shown that this behavior is most likely coming from Jason-3. The root cause is still to be identified.

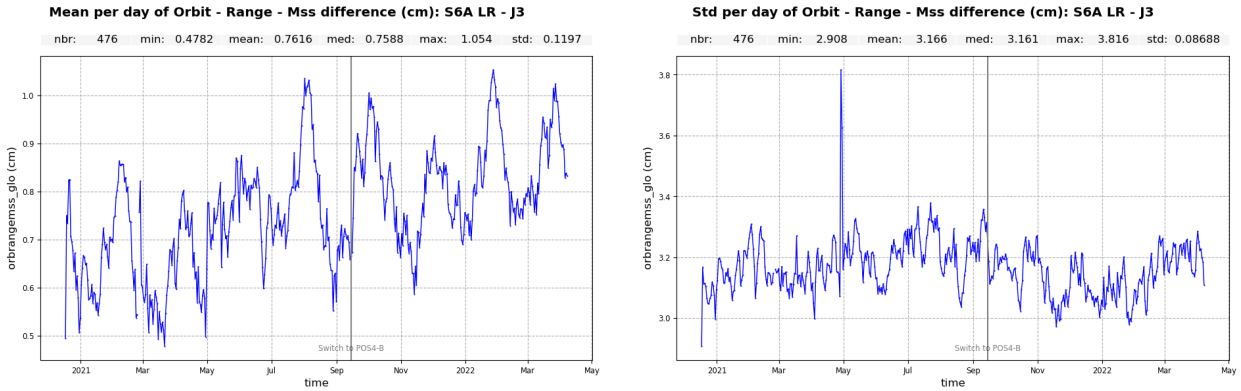

Figure 67 – Time monitoring of Orbit - Ku-band range - MSS difference: Sentinel-6A LR minus Jason-3. Mean per day (left) and standard deviation per day (right) computed over the complete tandem period.

At the beginning of S6A mission, hemispheric patterns were detected on the range difference map when splitting ascending and descending tracks. Thanks to POE-F orbit updates, it has been corrected and these patterns are not visible anymore on reprocessed data (figure 69).

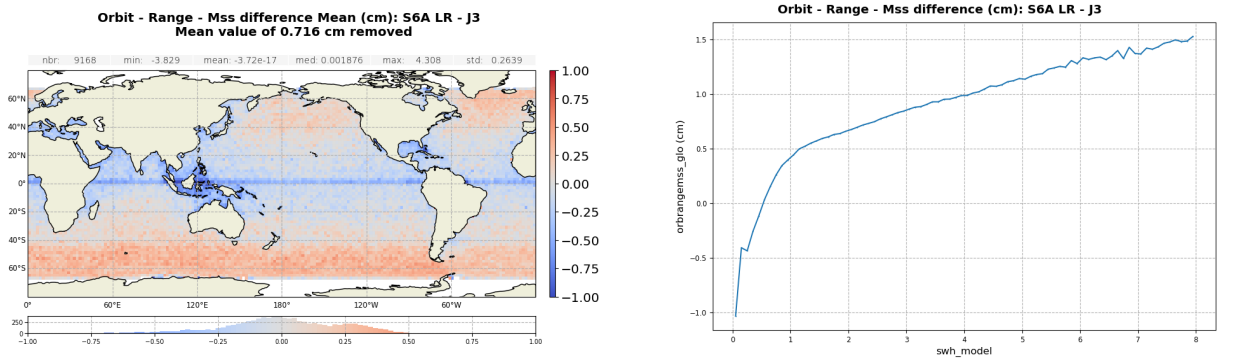

Figure 68 – Orbit - Ku-band range - MSS difference: Sentinel-6A LR minus Jason-3 computed over the complete tandem period. Gridded map (left panel) and difference function of ERA5 SWH (right panel).

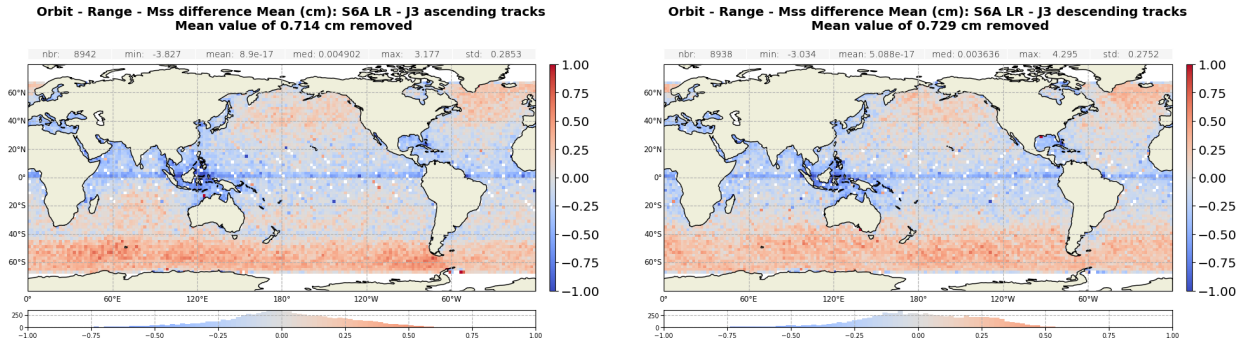

Figure 69 – Gridded map of Orbit - Ku-band range - MSS difference: Sentinel-6A LR minus Jason-3 computed over the complete tandem period. Ascending tracks (left panel) and descending tracks (right panel).

LR Ku-band backscatter coefficient

Figure 70 (left panel) shows the distribution of the difference in sigma0 over the complete period, with a bias of -1.23 dB. On the right panel, the distribution is splitted between POS4 sides. Values are not identical: -1.24 dB for side A and -1.21 dB for side B. This change can also be observed in the time monitoring (figure 71) with an increase of the bias at the switch to POS4-B. Apart from this, the sigma0 bias between the two missions is stable in time with a standard deviation of 0.12 dB.

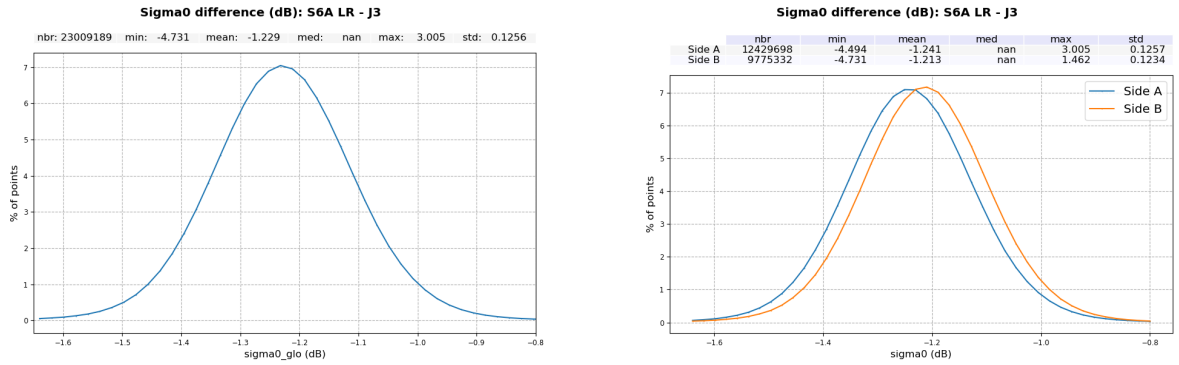

Figure 70 – Histogram of Ku-band backscatter coefficient difference: Sentinel-6A LR minus Jason-3. Computed over the complete tandem period (left panel) and over POS-4 side A and side B periods (right panel).

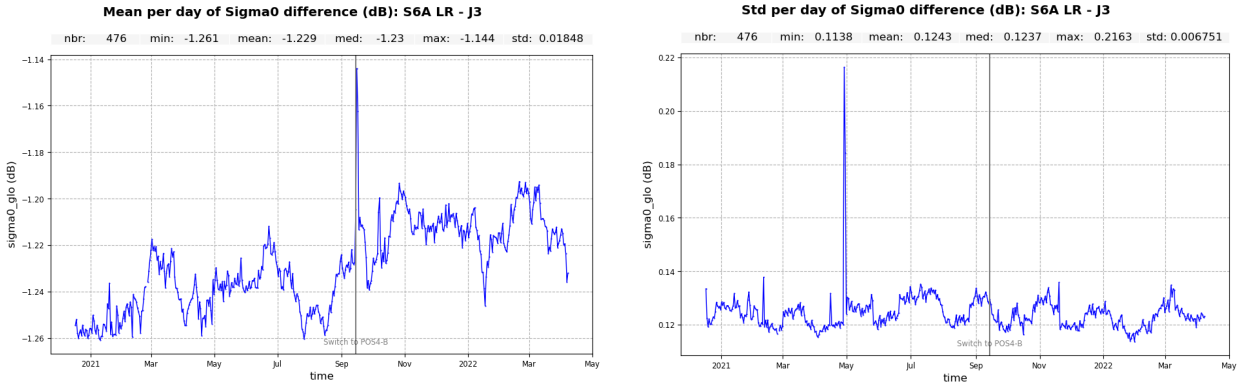

Figure 71 – Time monitoring of Ku-band backscatter coefficient difference: Sentinel-6A LR minus Jason-3. Mean per day (left) and standard deviation per day (right) computed over the complete tandem period.

The map of the sigma0 difference is presented in figure 72, left panel. As confirmed with the difference plot as function of SWH on the right panel, we observe a small SWH dependency : +0.08 dB between 2 and 7 m wave.

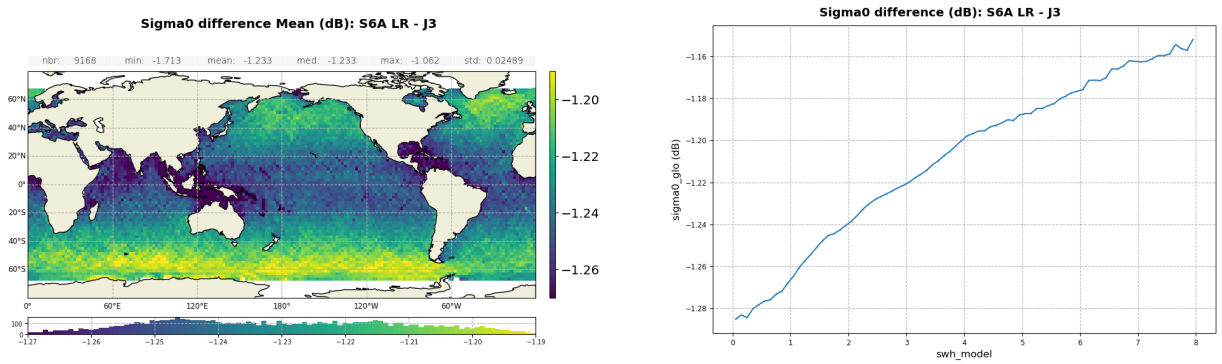

Figure 72 – Ku-band backscatter coefficient difference: Sentinel-6A LR minus Jason-3 computed over the complete tandem period. Gridded map (left panel) and difference function of ERA5 SWH (right panel).

LR Altimeter Wind-Speed

As can be seen on the histogram in figure 73, the differences in wind speed are well centred around 0 over the complete tandem period. Looking more closely at the evolution in time (figure 74), the bias is not constant, with different values between POS4-A (3 cm/s) and POS4-B (-6 cm/s). This result shows that the calibration bias applied on sigma0 for the wind speed computation (+1.29 dB) is not fully adjusted and different biases should be applied according to POS4 side.

For Sentinel-6A wind speed computation, the same algorithm as for Jason-3 GDR-F is applied (Collard). Sentinel-6A sigma0 in input of the computation should then be calibrated the same way as Jason-3. For Jason-3, the sigma0 calibration bias equals to 0.06 dB. Sentinel-6A sigma0 calibration should be calculated as the sum of J3/S6A sigma0 bias and J3 sigma0 calibration bias (0.06 dB).

For Sentinel-6A LR wind speed computation, the calibration bias applied on sigma0 should be :

- for POS4-A : + 1.30 dB (= 1.24 + 0.06)
- for POS4-B : + 1.27 dB (= 1.21 + 0.06)

We recommend to use these values for the next S6A reprocessing campaign.

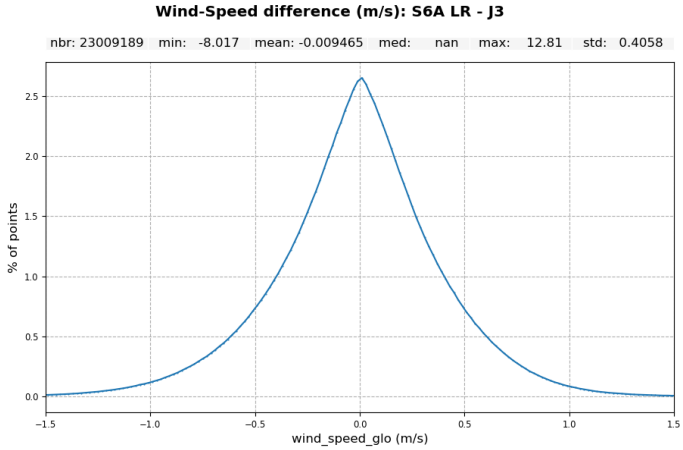

Figure 73 – Histogram of altimeter Wind-Speed difference: Sentinel-6A LR minus Jason-3. Computed over the complete tandem period.

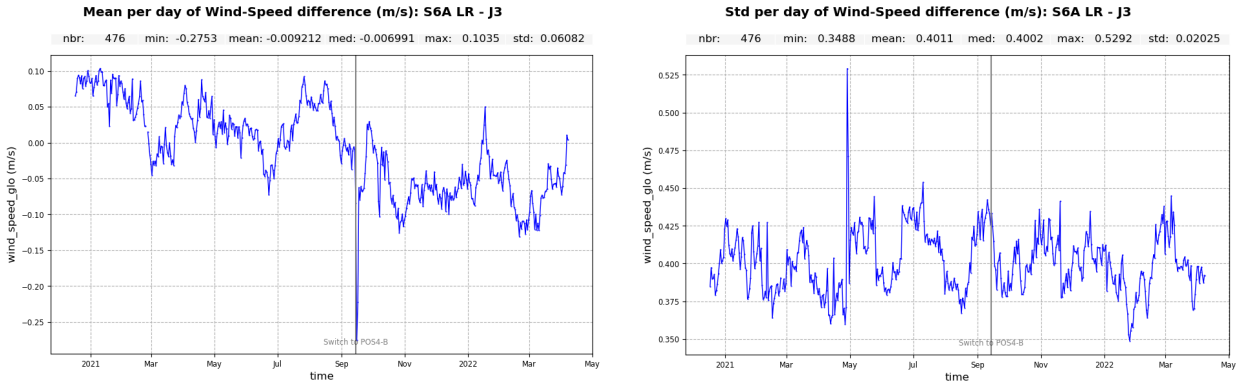

Figure 74 – Time monitoring of Ku-band Wind-Speed difference: Sentinel-6A LR minus Jason-3. Mean per day (left) and standard deviation per day (right) computed over the complete tandem period.

The map of altimeter wind-speed difference is presented in figure 75, left panel. As confirmed with the difference plot as function of SWH on the right panel, we observe a small SWH dependency : -0.31 m/s between 2 and 7 m wave. This is consistent with Ku-band sigma0 analysis.

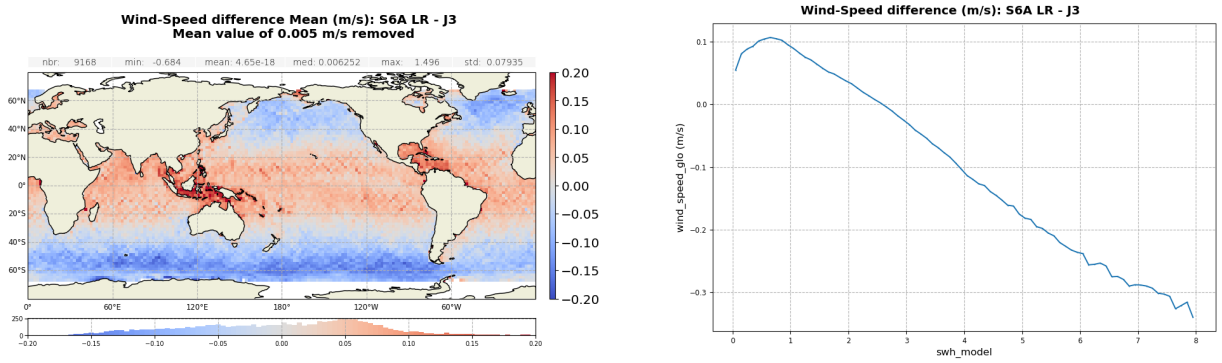

Figure 75 – Altimeter Wind-Speed difference: Sentinel-6A LR minus Jason-3 computed over the complete tandem period. Gridded map (left panel) and difference function of ERA5 SWH (right panel).

LR Ku-band Sea State Bias

Figure 76 shows the distribution of the differences in SSB over the complete period, with a bias of 0.4 mm. The time monitoring of these differences is presented in figure 77. A jump is visible at the switch to POS4-B due to the change in wind speed, from 0.2 to 0.6 mm in average. For each side, the SSB is otherwise stable.

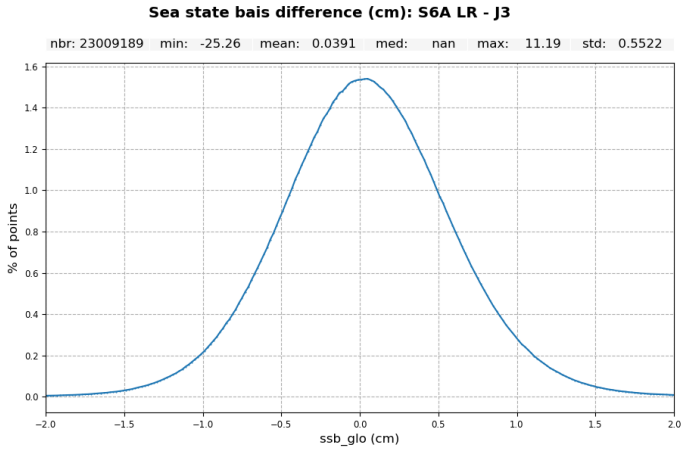

Figure 76 – Histogram of Ku-band SSB difference: Sentinel-6A LR minus Jason-3. Computed over the complete tandem period.

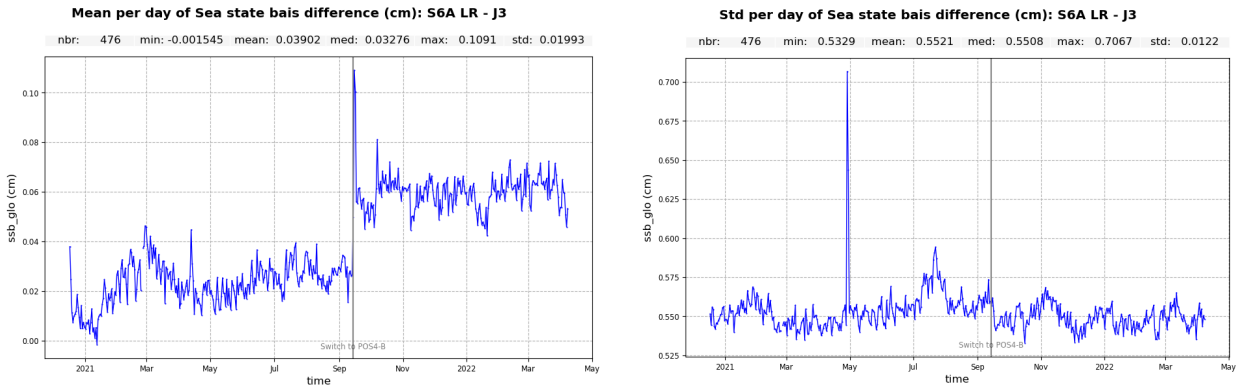

Figure 77 – Time monitoring of Ku-band SSB difference: Sentinel-6A LR minus Jason-3. Mean per day (left) and standard deviation per day (right) computed over the complete tandem period.

The map of the SSB difference is presented in figure 78, left panel. The differences are mostly located in low SWH areas. It is in line with what is observed for SWH differences in Figure 65 and is due to the difference in low SWH management between Sentinel-6A and Jason-3 processing.

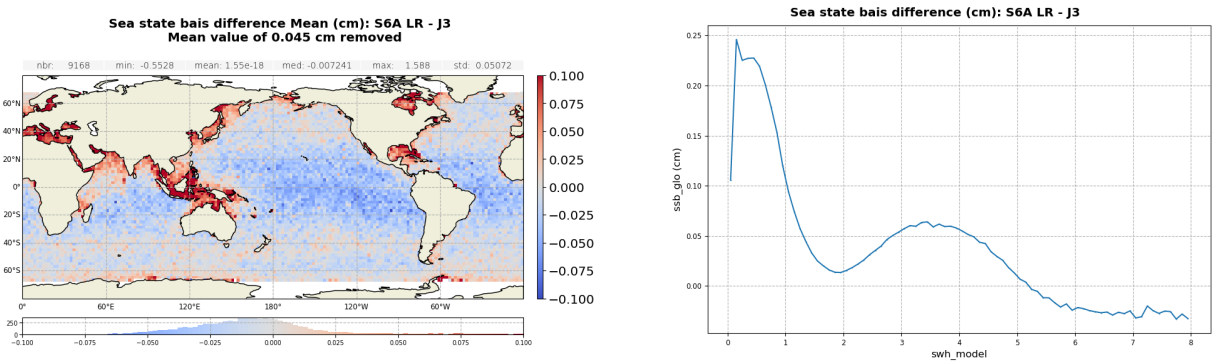

Figure 78 – Ku-band SSB difference: Sentinel-6A LR minus Jason-3 computed over the complete tandem period. Gridded map (left panel) and difference function of ERA5 SWH (right panel).

LR Mispointing

In this paragraph, difference of the square of the off-nadir angle derived from the MLE4 waveform retracking from LR dataset are compared between Jason-3 and Sentinel-6A. A bias of 0.013 degree^2 is detected (figure 79). Analysis presented in section 4.1.7. shows that this bias is coming from Sentinel-6A, as Jason-3 off-nadir angle is well cendred around 0. This bias is stable in time (figure 80). Manoeuvres perfomed on Sentinel-6A during the commissionning activities are visible on both the time monitoring and the map (figure 81).

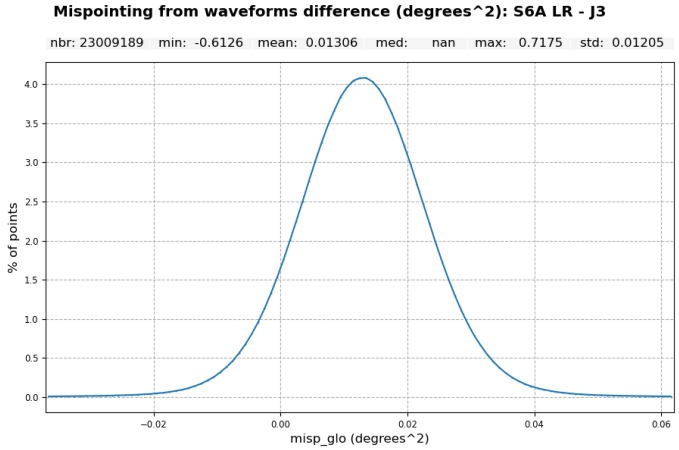

Figure 79 – Histogram of mispointing difference: Sentinel-6A LR minus Jason-3. Computed over the complete tandem period.

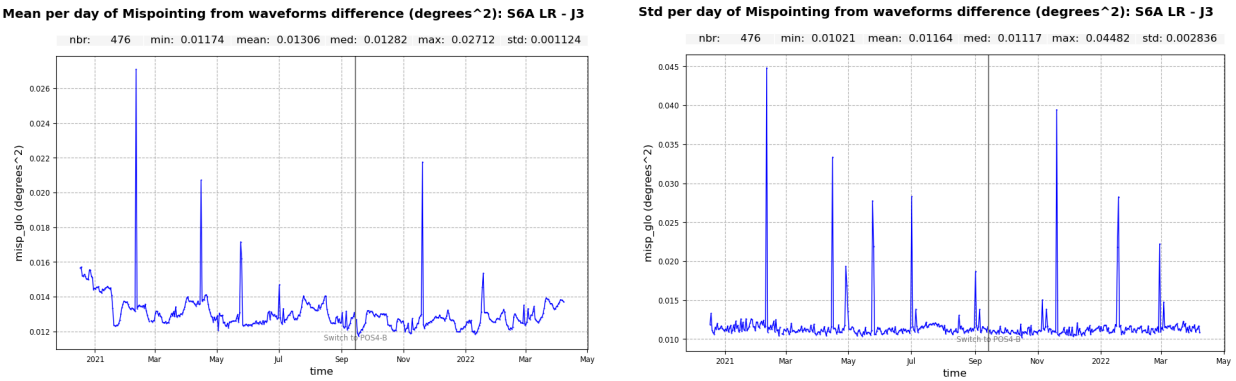

Figure 80 – Time monitoring of mispointing difference: Sentinel-6A LR minus Jason-3. Mean per day (left) and standard deviation per day (right) computed over the complete tandem period.

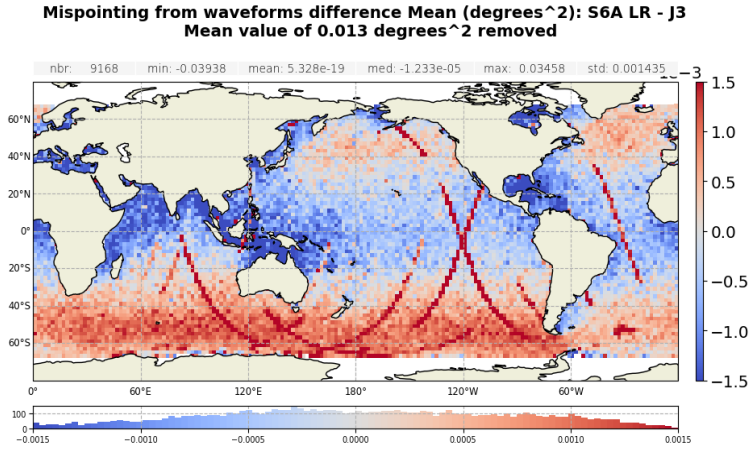

Figure 81 – Mispointing difference: Sentinel-6A LR minus Jason-3 computed over the complete tandem period. Gridded map (left panel) and difference function of ERA5 SWH (right panel).

5.2.2. C-band

LR C-band SWH

Please note that the C-band SWH is not used in the SSHA computation process.

C-band SWH difference between Sentinel-6A LR and Jason-3 show a large bias of -20 cm (figures 82 and 83), with a standard deviation of 80 cm. This behavior is expected and understood. It is due to POS4 design: the number of pulses in POS4 C-band is smaller compare to other altimeter (such as POS3). It leads to noisier C-band retrievals for Sentinel-6A.

The map of the C-band SWH differences is presented in figure 84, left panel. We observe a strong correlation to SWH values, as confirmed on the difference plotted function of ERA-5 SWH (figure 84, right panel). The bias increases of 25.2 cm between 2 and 7 m wave and reaches up to -140 cm for very low SWH.

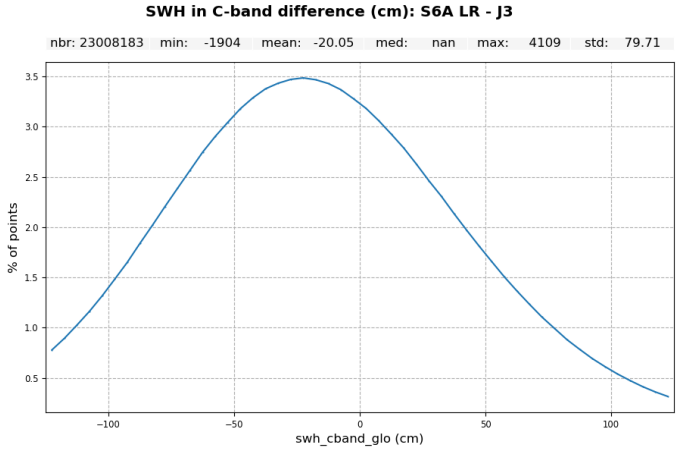

Figure 82 – Histogram of C-band SWH difference: Sentinel-6A LR minus Jason-3. Computed over the complete tandem period.

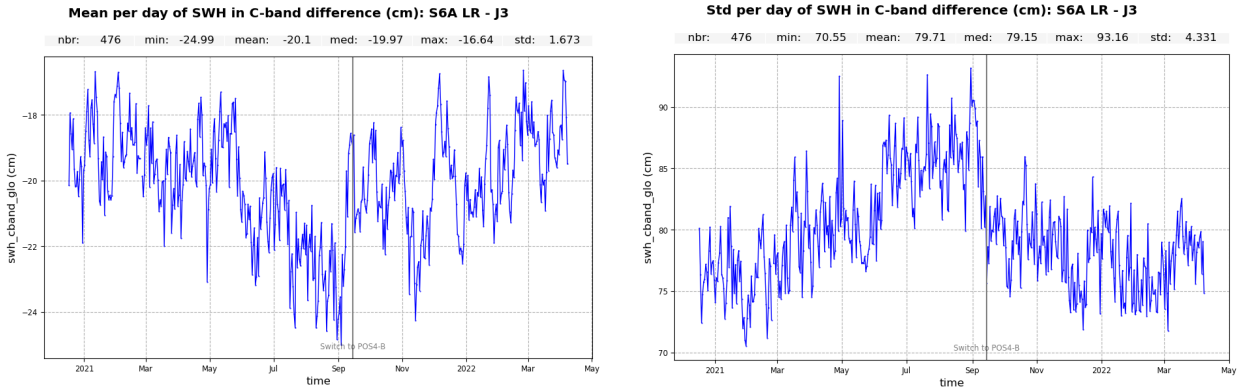

Figure 83 – Time monitoring of C-band SWH difference: Sentinel-6A LR minus Jason-3. Mean per day (left) and standard deviation per day (right) computed over the complete tandem period.

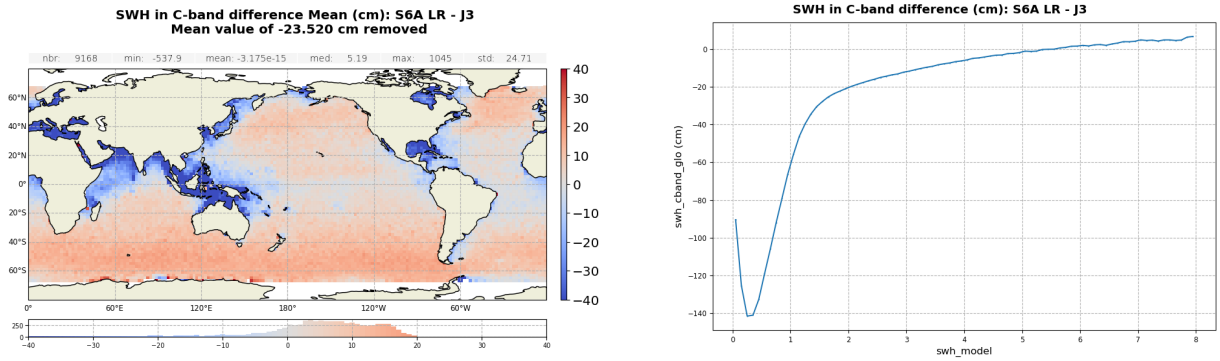

Figure 84 – C-band SWH difference: Sentinel-6A LR minus Jason-3 computed over the complete tandem period. Gridded map (left panel) and difference function of ERA5 SWH (right panel).

LR C-band Range

C-band range difference highlights the consitency between the two satellites with a bias of only 0.97 cm in average, which is of the same order as Ku-band range bias (0.76 cm). However, the standard deviation of the difference is higher for C-band: 12.1 cm versus 3.2 cm in Ku-band. This behavior is expected and due

to the reduced number of pulses in C-band.

The time monitoring of this difference is presented in figure 86. It shows the stability of the bias over POS4-A period. However, from the switch to the altimeter B-side, the bias seems to drift in time.

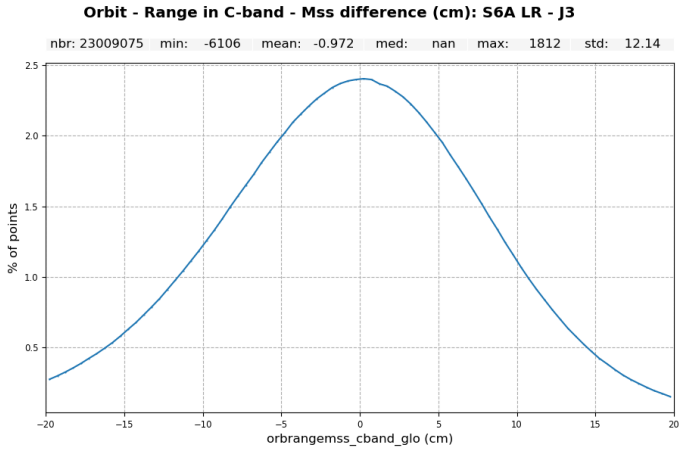

Figure 85 – Histogram of Orbit - C-band Range - MSS difference: Sentinel-6A LR minus Jason-3. Computed over the complete tandem period.

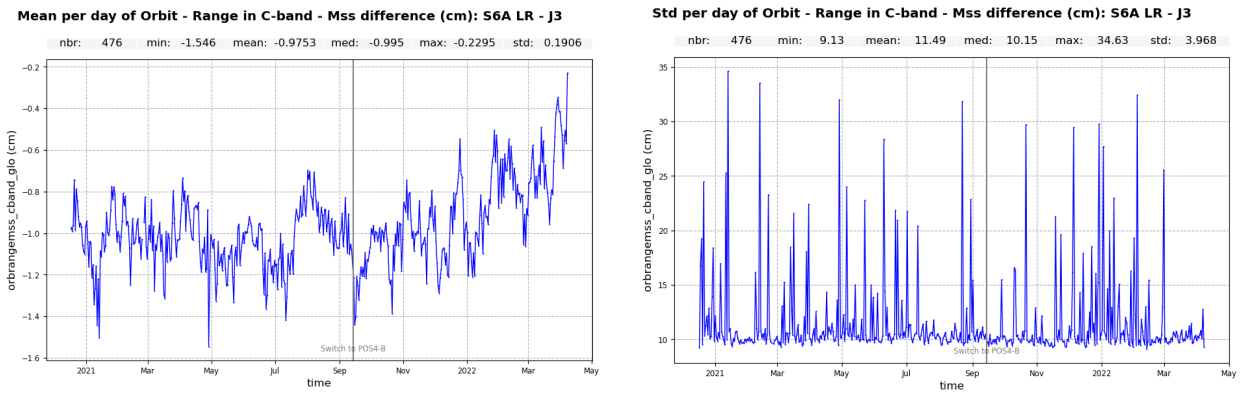

Figure 86 – Time monitoring of Orbit - C-band Range - MSS difference: Sentinel-6A LR minus Jason-3. Mean per day (left) and standard deviation per day (right) computed over the complete tandem period.

The map of C-band range differences is presented in figure 87, left panel. The main correlation is to the total electron content of the atmosphere, which can be explained by the C-band frequency difference between Sentinel-6A (5.41 Ghz) and Jason-3 (5.3 GHz) (the ionosphere impact depends on band frequency). Additionally, these differences might also be correlated to the sea state bias.

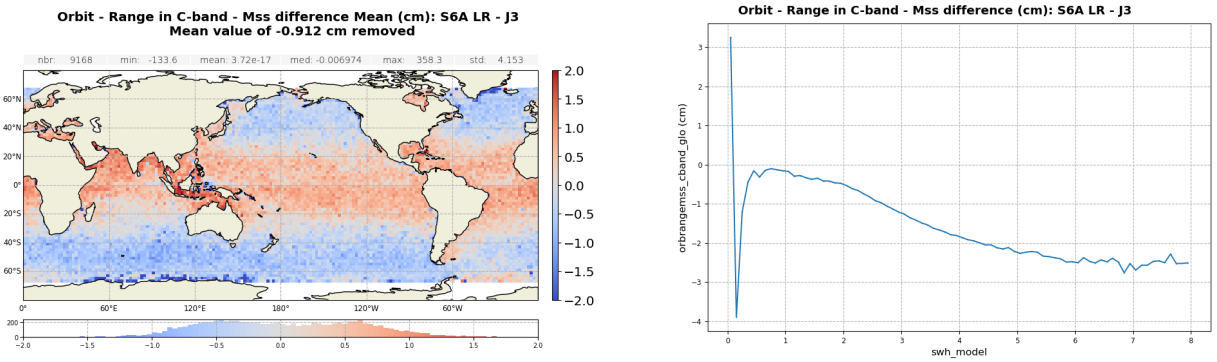

Figure 87 – Orbit - C-band Range - MSS difference: Sentinel-6A LR minus Jason-3 computed over the complete tandem period. Gridded map (left panel) and difference function of ERA5 SWH (right panel).

LR C-band Backscatter coefficient

Please note that the C-band sigma0 is not used in the SSHA computation process.

Figure 88 (left panel) shows the distribution of the differences in C-band sigma0 over the complete period, with a bias of -1.64 dB. On the right panel, the distribution is splitted between POS4 sides. Values are not identical: -1.66 dB for side A and -1.62 dB for side B. The time monitoring of these differences is presented in figure 89, with a visible drift before the POS4 switch to B-side.

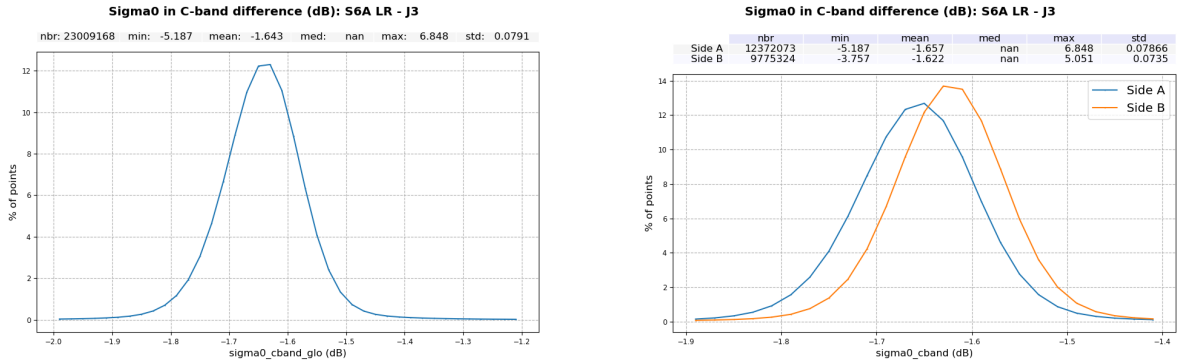

Figure 88 – Histogram of C-band backscatter coefficient difference: Sentinel-6A LR minus Jason-3. Computed over the complete tandem period (left panel) and over POS-4 side A and side B periods (right panel).

Map of C-band sigma0 difference is presented in figure 90, left panel. The differences are mostly located in low SWH areas.

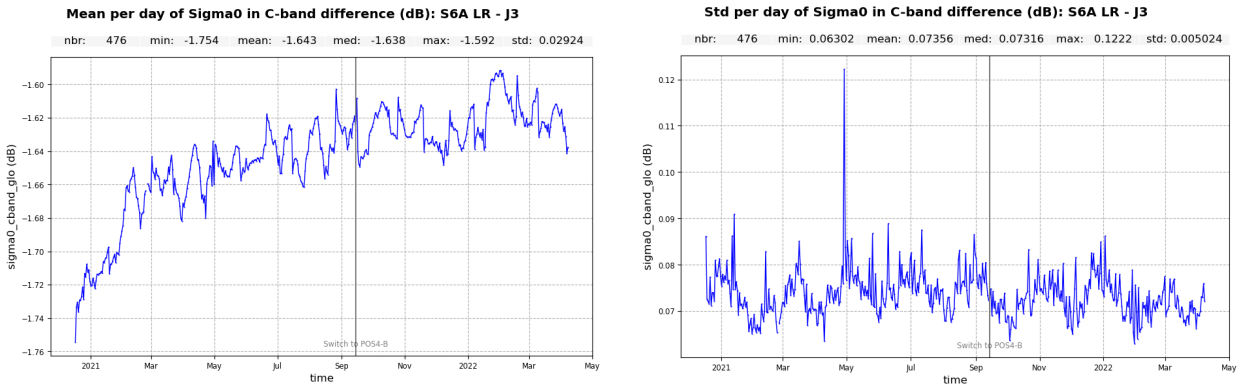

Figure 89 – Time monitoring of C-band backscatter coefficient difference: Sentinel-6A LR minus Jason-3. Mean per day (left) and standard deviation per day (right) computed over the complete tandem period.

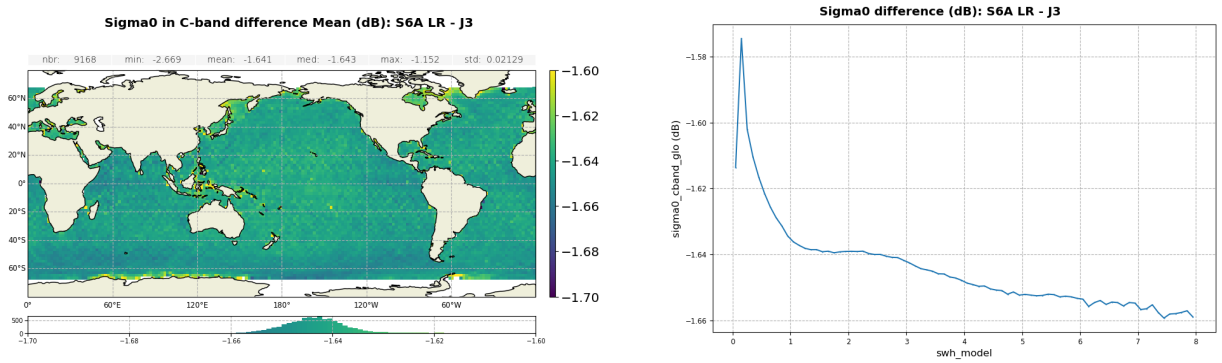

Figure 90 – C-band backscatter coefficient difference: Sentinel-6A LR minus Jason-3 computed over the complete tandem period. Gridded map (left panel) and difference function of ERA5 SWH (right panel).

LR C-band Sea State Bias

Sentinel-6A C-band SSB is computed using J3 GDR-F C-band algorithm with S6A LR Ku-band SWH and altimeter wind speed derived from LR Ku-band measurements as inputs. S6A and J3 C-band SSB are perfectly in line, with a bias below the mm (figure 91). The time monitoring of the SSB difference (figure 92) highlights a jump of 0.5mm at the POS4 B-side switch. This is due to Ku-band sigma0 and its calibration bias applied for the wind speed computation. For each POS4 side, the SSB bias is otherwise stable.

The corresponding map (figure 93) does not show any strong pattern nor clear correlation to sea state conditions.

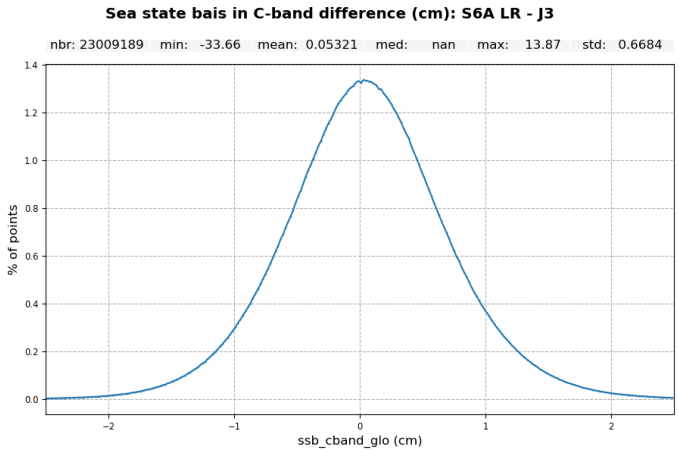

Figure 91 – Histogram of C-band SSB difference: Sentinel-6A LR minus Jason-3. Computed over the complete tandem period.

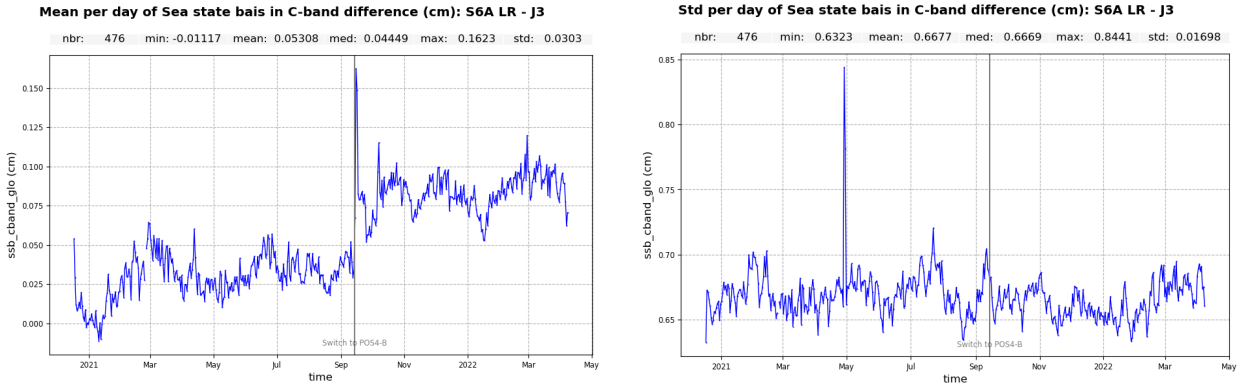

Figure 92 – Time monitoring of C-band SSB difference: Sentinel-6A LR minus Jason-3. Mean per day (left) and standard deviation per day (right) computed over the complete tandem period.

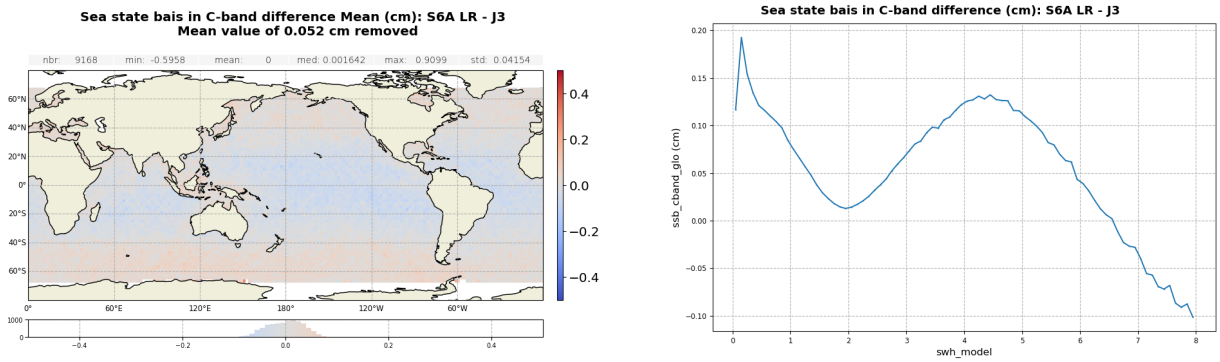

Figure 93 – C-band SSB difference: Sentinel-6A LR minus Jason-3 computed over the complete tandem period. Gridded map (left panel) and difference function of ERA5 SWH (right panel).

5.2.3. Altimeter ionosphere correction

Sentinel-6A altimeter ionosphere correction is derived from LR data, in Ku and C band, and more precisely

from ranges corrected from SSB.

In this section, the filtered altimeter ionosphere corrections from Sentinel-6A and Jason-3 are compared. Over the complete tandem phase, the bias between the two solutions is centred around -0.4 cm. The time monitoring of this bias (figure 95) shows a clear jump of -0.7 mm at the POS4-B switch. This value is small but the jump is clearly visible on the plot due to the stability of the bias over each POS4 side period. This jump is due to S6A Ku-band sigma0 change at the switch to POS4-B (see Figure 71). This change has not been taken into account in the altimeter wind speed computation, leading to jump in Ku-band and C-band SSBs and thus impacting the altimeter ionosphere correction.

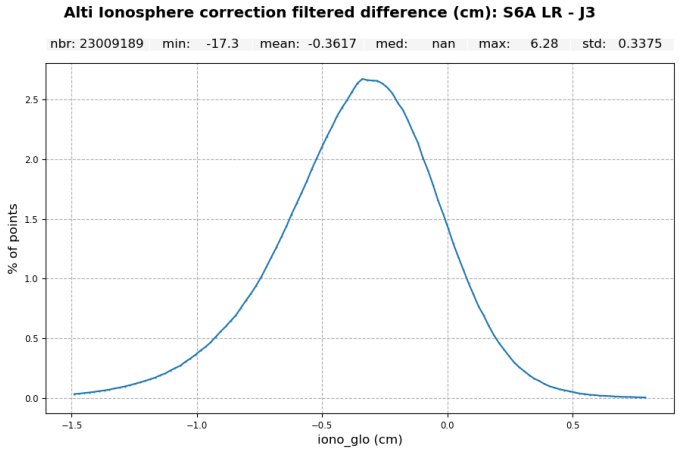

Figure 94 – Histogram of Altimeter Filtered Ionosphere correction difference: Sentinel-6A LR minus Jason-3. Computed over the complete tandem period.

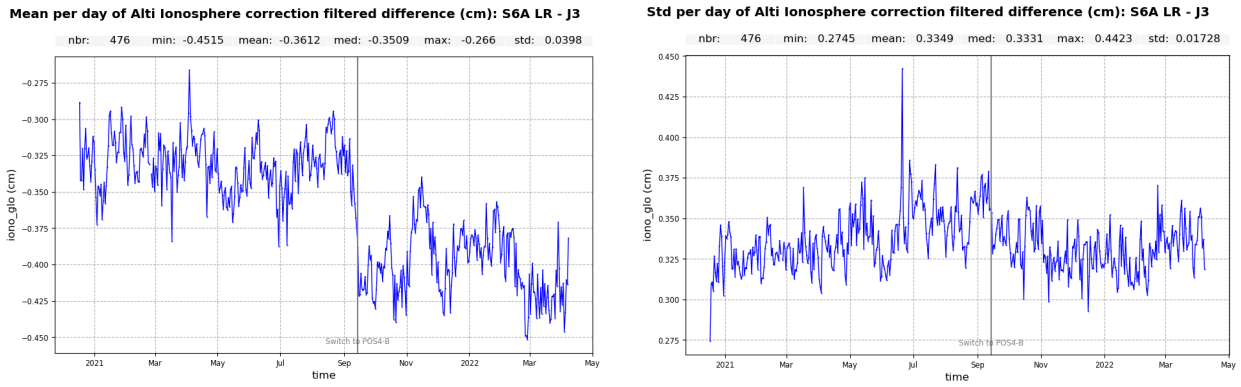

Figure 95 – Time monitoring of Altimeter Filtered Ionosphere correction difference: Sentinel-6A LR minus Jason-3. Mean per day (left) and standard deviation per day (right) computed over the complete tandem period.

The map of the filtered ionosphere correction differences is presented in figure 96, left panel. We observe a correlation with ERA-5 SWH (right panel) : -0.5 cm between 2 and 7m wave.

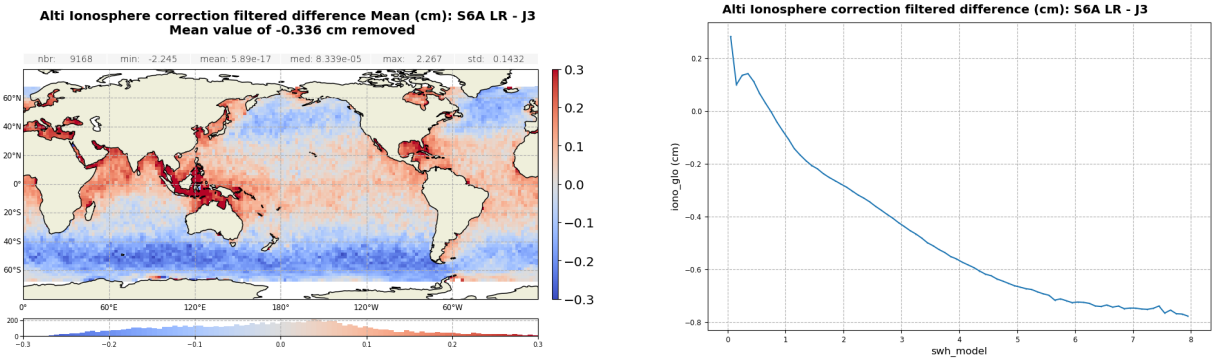

Figure 96 – Altimeter Filtered Ionosphere correction difference: Sentinel-6A LR minus Jason-3 computed over the complete tandem period. Gridded map (left panel) and difference function of ERA5 SWH (right panel).

5.2.4. LR SSHA

In this section, Sentinel-6A LR and Jason-3 SSHA are compared over the complete tandem flight. The average bias is of 1.17 cm, which is in line with the biases observed on SSHA parameters and summarized in table 4.

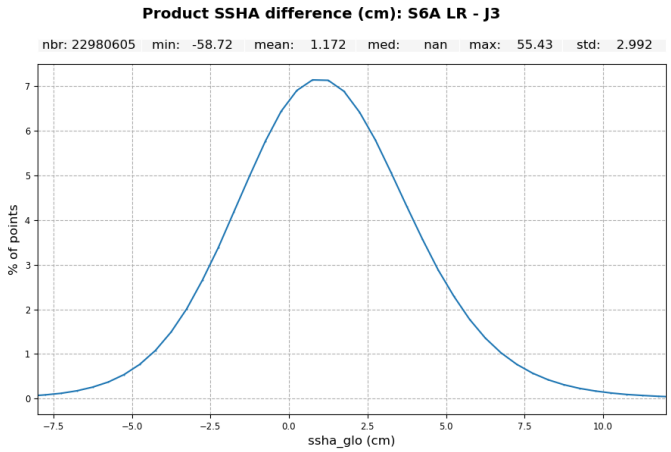

Figure 97 – Histogram of product SSHA difference: Sentinel-6A LR minus Jason-3. Computed over the complete tandem period.

Parameter	S6A LR - J3 bias
Orbit - Ku-band range - MSS	0.763 cm
Ku-band SSB	0.039 cm
Altimeter filtered ionosphere correction	-0.362 cm
AMR-C WTC	-0.084 cm
Sum	**1.17 cm**

Table 4 – Summary of the Sentinel-6A LR minus Jason-3 biases for the parameters used in the SSHA computation. Computed over the complete tandem flight. The sum is performed as [bias on orbit-range-mss] minus [the sum of the bias on the geophysical correction], as in the SSHA computation.

The time monitoring of this difference (figure 98) highlights two events:

- a jump of about +5 mm is visible after the satellite restart of 27-28 April 2021. This is partly caused by the jump in WTC (cf figure 62) of similar amplitude.
- a jump of about +2.5 mm is visible around the 20 January 2022. The origin is under investigation.

A SSHA recomputed with a model WTC (ECMWF) for both Sentinel-6A LR and Jason-3 is used for comparaison in figure 99. The use of model WTC reduces the jump of April 2021 to about 1.5mm. However, this SSHA bias presents larger oscillations. It is hard to say here if the second jump of January 2022 is also linked to Sentinel-6 AMR-C WTC or to Jason-3 AMR or from another source.

Using a GIM model ionospheric correction in addition to the model WTC, as presented in figure 100, does not significantly change the SSHA differences between the two missions, except for a constant bias.

It is important to note here that we do not see any jump in the monitoring at POS4 switch to B-side on September 14th 2021. It is because the jumps visible on the SSB and the ionosphere correction are partially cancelling themselves and because the SSHA difference has a standard deviation stronger than the jumps oberved. This standard deviation is stable in time and is centred around 3 cm (figure 101).

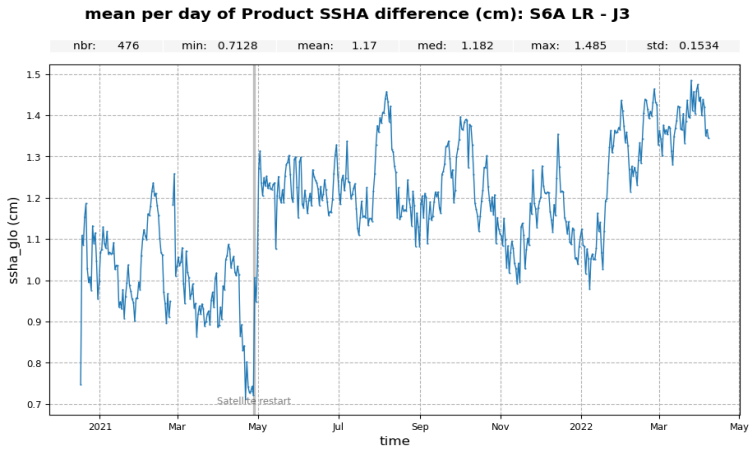

Figure 98 – Time monitoring of product SSHA difference: Sentinel-6A LR minus Jason-3. Mean per day computed over the complete tandem period.

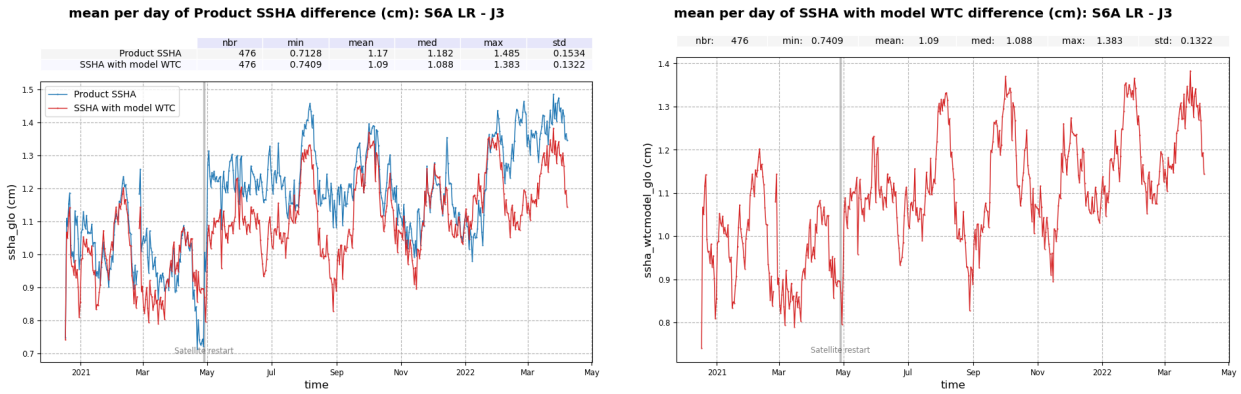

Figure 99 – Time monitoring of SSHA difference: Sentinel-6A LR minus Jason-3. Mean per day computed over the complete tandem period. Product SSHA in blue and SSHA recomputed with ECMWF WTC in red.

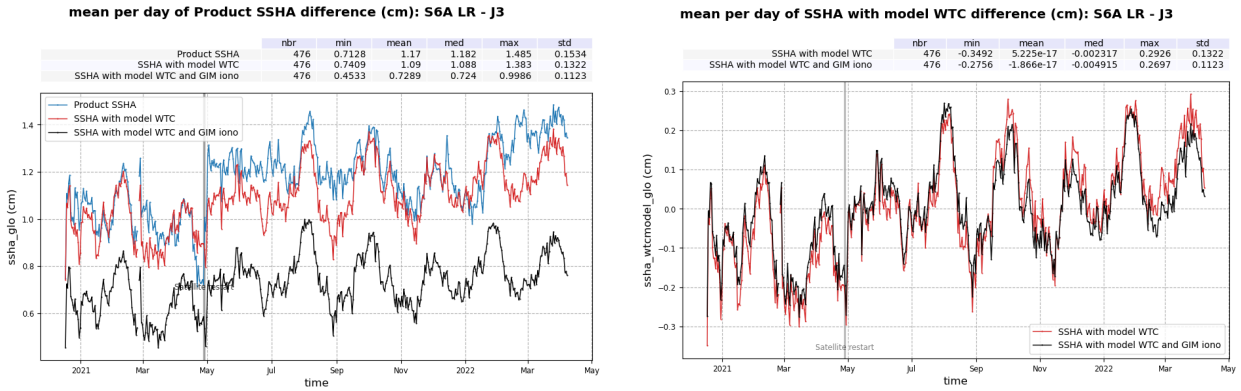

Figure 100 – Time monitoring of SSHA difference: Sentinel-6A LR minus Jason-3. Mean per day computed over the complete tandem period. Product SSHA in blue, SSHA recomputed with ECMWF WTC in red, and SSHA recomputed with ECMWF WTC and GIM ionosphere correction in black. On the left panel, mean values have been removed to allow a better comparison.

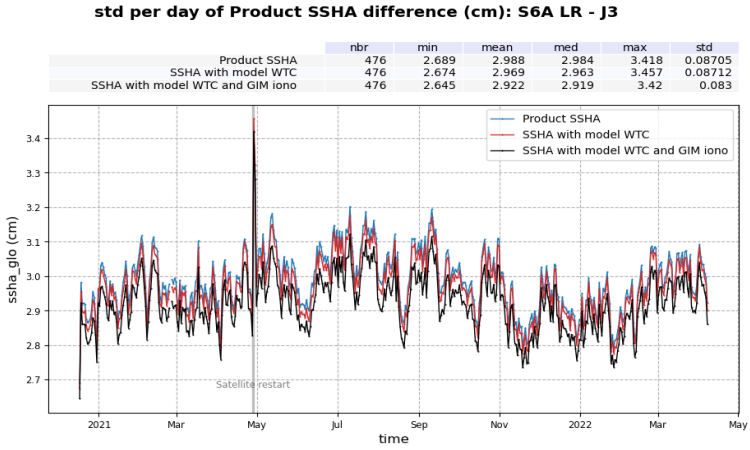

Figure 101 – Time monitoring of SSHA difference: Sentinel-6A LR minus Jason-3. Standard deviation per day computed over the complete tandem period. Product SSHA in blue, SSHA recomputed with ECMWF WTC in red, and SSHA recomputed with ECMWF WTC and GIM ionosphere correction in black.

The map of the SSHA differences (figure 102 left panel) highlights a clear correlation to SWH, as confirmed by the plot of the difference function of ERA-5 SWH (figure 102 left panel). The SSHA bias increases by 1.3 cm between 2 and 7m wave, which is in line with the behavior observed on the orbit-range-mss and ionosphere correction bias. Future numerical retracker should improve this behavior.

The equatorial band visible on the orbit-range-mss difference map is still observed on the SSHA difference map, with the same amplitude (see figure 68).

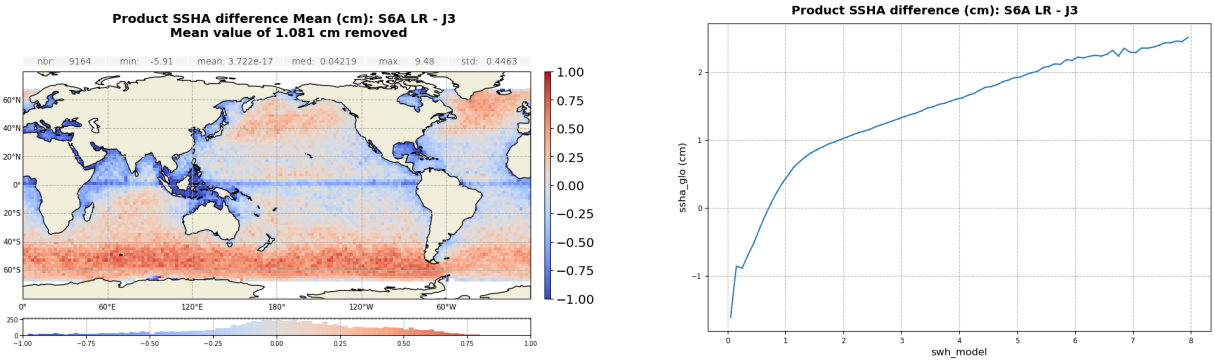

Figure 102 – Product SSHA difference: Sentinel-6A LR minus Jason-3 computed over the complete tandem period. Gridded map (left panel) and difference function of ERA5 SWH (right panel).

5.3. HR

In this section, Sentinel-6A HR data are compared to Jason-3.

5.3.1. HR SWH

The difference between S6A HR and Jason-3 SWH shows a bias of 22.1 cm in average (figure 103). This bias has been strongly reduced thanks to PB F06 (see section 2.1. for more details about the PB update), as it has already been shown in section 4.1.1.. The time monitoring of this difference (figure 104) shows a good stability and no behavior change at the switch to POS4-B.

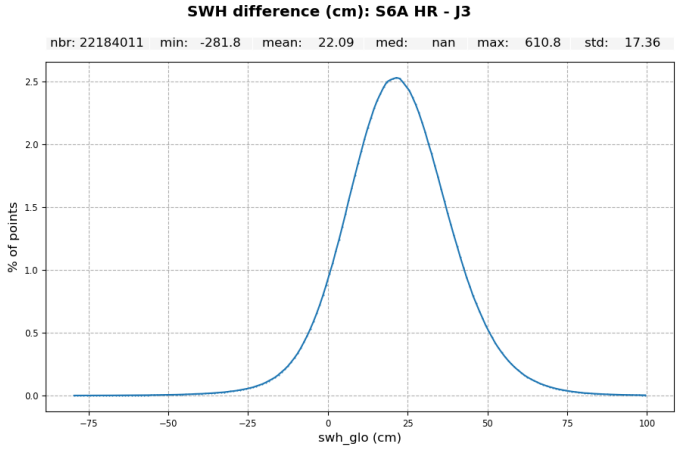

Figure 103 – Histogram of product SWH difference: Sentinel-6A HR minus Jason-3. Computed over the complete tandem period.

Looking at the corresponding map (figure 105 left panel), a correlation to SWH is observed. Such behavior was also observed before PB F06 update but has been strongly reduced. The bias is now of 18 cm at 2m-wave and reaches 40 cm at 6m-wave (figure 105 right panel).

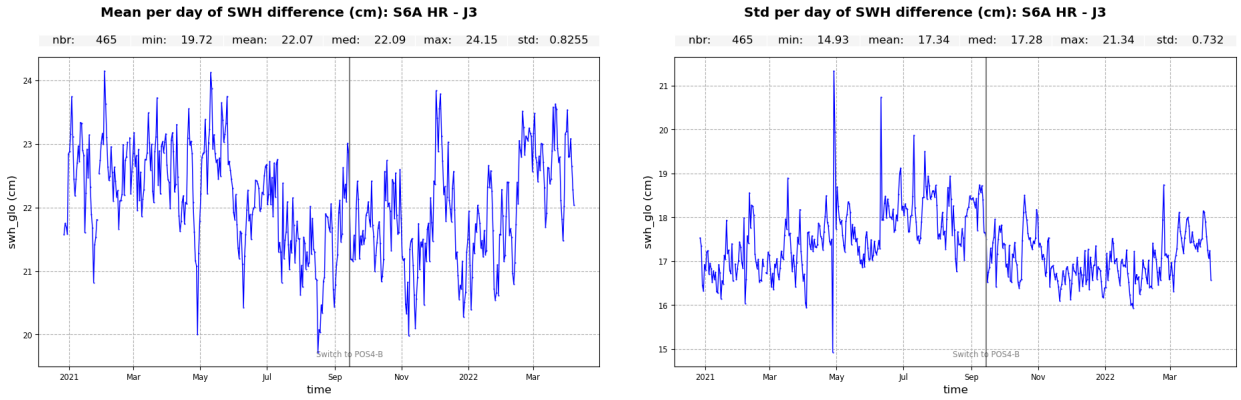

Figure 104 – Ku-band SWH difference: Sentinel-6A HR minus Jason-3. Mean per day (left panel) and standard deviation per day (right panel) computed over the complete tandem period.

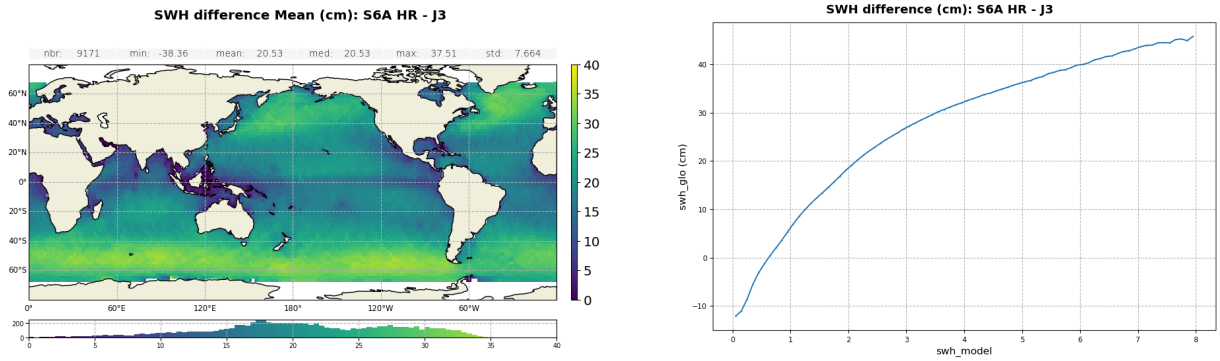

Figure 105 – Ku-band SWH difference: Sentinel-6A HR minus Jason-3 computed over the complete tandem period. Gridded map (left panel) and difference function of ERA5 SWH (right panel).

5.3.2. HR Range

In this section, HR range is compared to Jason-3 range, using the same method as for LR range comparison in previous section. The bias between the two retrievals is small (-1.2 cm, figure 106) and is stable in time (figure 107). However, due to the skewness difference between Sentinel-6A HR and Jason-3 processings, a strong correlation to sea state condition is observed, as shown on figure 108.

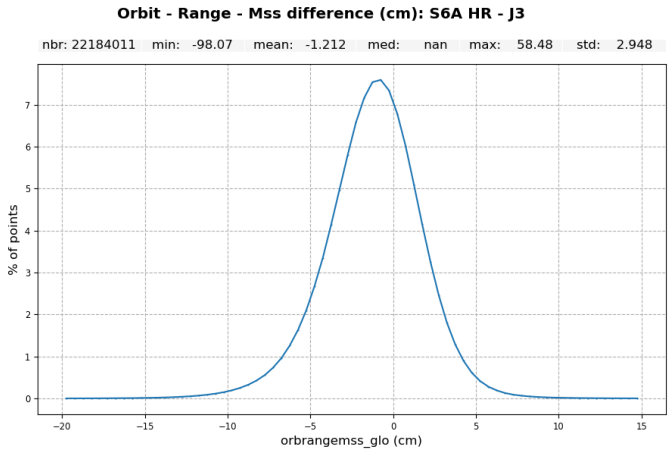

Figure 106 – Histogram of product Orbit - Ku-band Range - MSS difference: Sentinel-6A HR minus Jason-3. Computed over the complete tandem period.

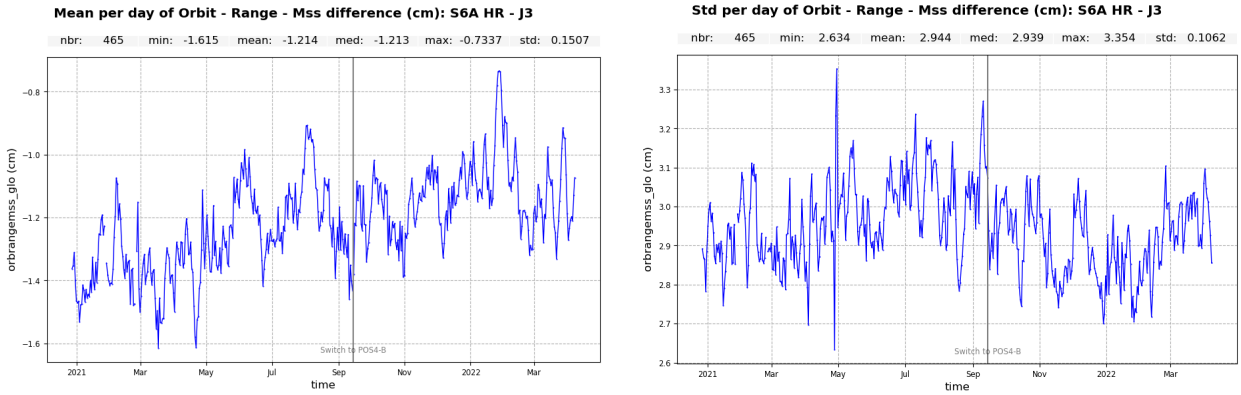

Figure 107 – Orbit - Ku-band Range - MSS difference: Sentinel-6A HR minus Jason-3. Mean per day (left panel) and standard deviation per day (right panel) computed over the complete tandem period.

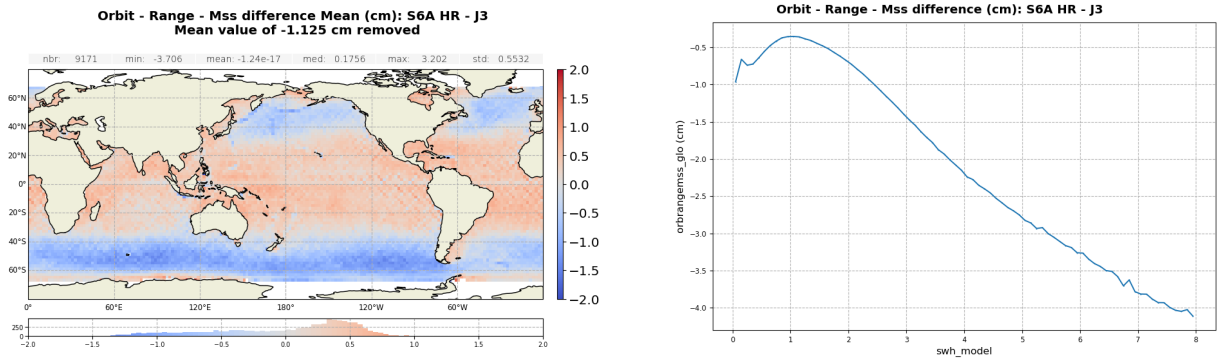

Figure 108 – Orbit - Ku-band Range - MSS difference: Sentinel-6A HR minus Jason-3 computed over the complete tandem period. Gridded map (left panel) and difference function of ERA5 SWH (right panel).

5.3.3. HR Backscatter coefficient

The comparison of S6A HR and J3 sigma0 hilghlights a difference centred around 4.41 dB in average over the complete tandem flight (figure 109 left panel). As for LR data, a small bias difference is observed between POS4-A and POS4-B. The bias equals to 4.4 dB for side A and 4.43 for side B. This change can also be observed in the time monitorings (figure 110).

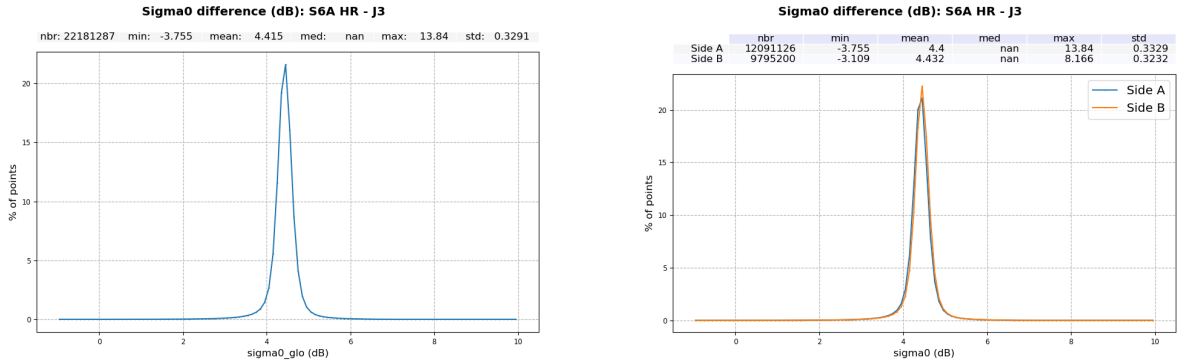

Figure 109 – Histogram of Ku-band Backscatter coefficient difference: Sentinel-6A HR minus Jason-3. Computed over the complete tandem period (left) and computed over Side A and Side B periods (right).

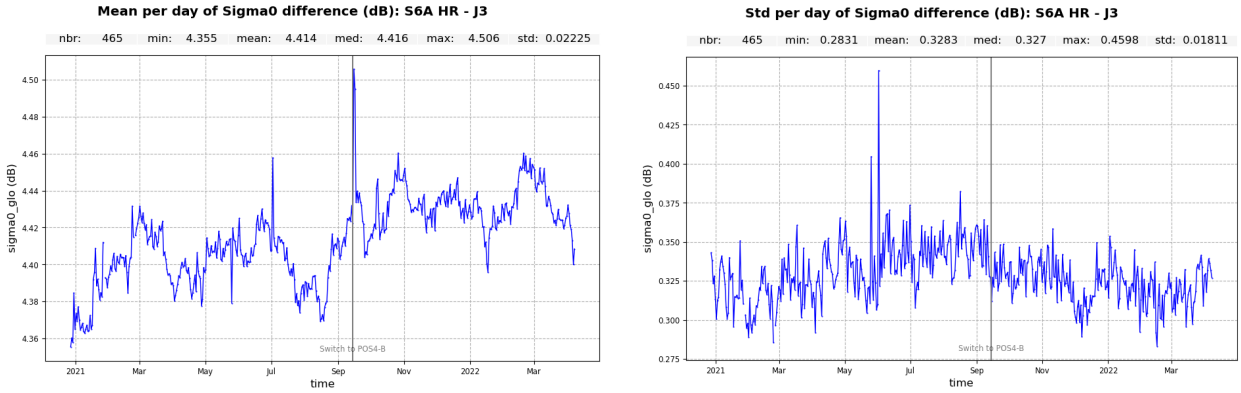

Figure 110 – Ku-band Backscatter coefficient difference: Sentinel-6A HR minus Jason-3. Mean per day (left panel) and standard deviation per day (right panel) computed over the complete tandem period.

The map of the sigma0 differences is presented in figure 111 (left panel). A correlation to SWH is observed, mainly for low SWH values (below 1 m), as confirmed with the right panel.

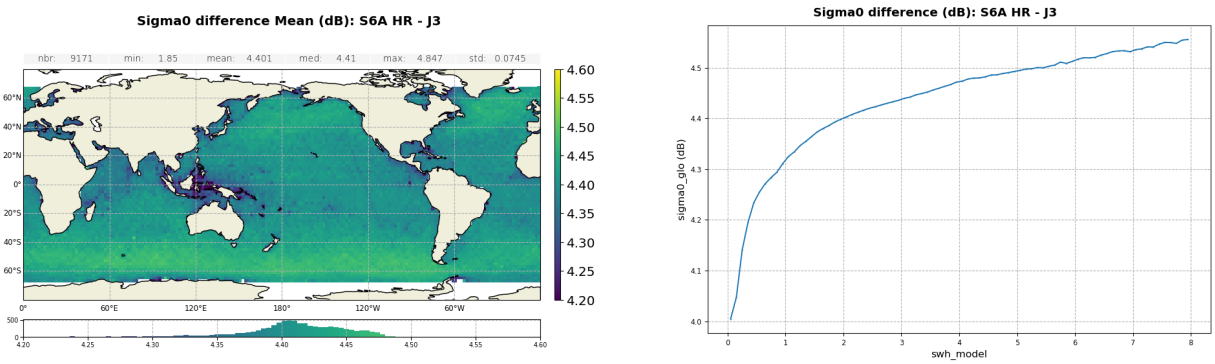

Figure 111 – Ku-band Backscatter coefficient difference: Sentinel-6A HR minus Jason-3 computed over the complete tandem period. Gridded map (left panel) and difference function of ERA5 SWH (right panel).

5.3.4. HR Wind-Speed

The altimeter wind speeds derived from Sentinel-6A HR and Jason-3 data are in line, with an average bias centred around only -5 cm/s (figure 112). Due to S6A HR sigma0 evolution at the switch to POS4-B, a small bias change can be observe in the time monitoring (figure 113). It is not as strong as what is observed on S6A LR data, but similarly to LR, we still recommend to update the HR sigma0 calibration bias used for HR wind speed computation for the next S6A reprocessing campaign.

For Sentinel-6A HR wind speed computation, the calibration bias applied on HR sigma0 should be:

- for POS4-A : -4.34 dB (= -4.4 + 0.06)
- for POS4-B : -4.26 dB (= -4.32 + 0.06)

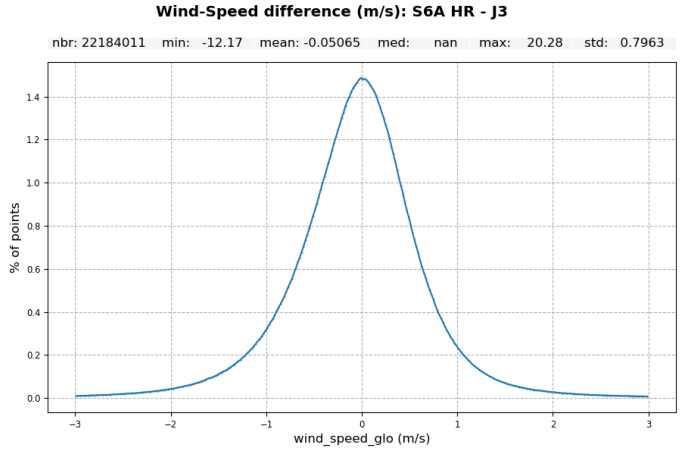

Figure 112 – Histogram of Altimeter Wind-Speed difference: Sentinel-6A HR minus Jason-3. Computed over the complete tandem period.

The map of the wind speed differences is presented in figure 114 (left panel). A correlation with SWH is still visible, as confirmed with the right panel.

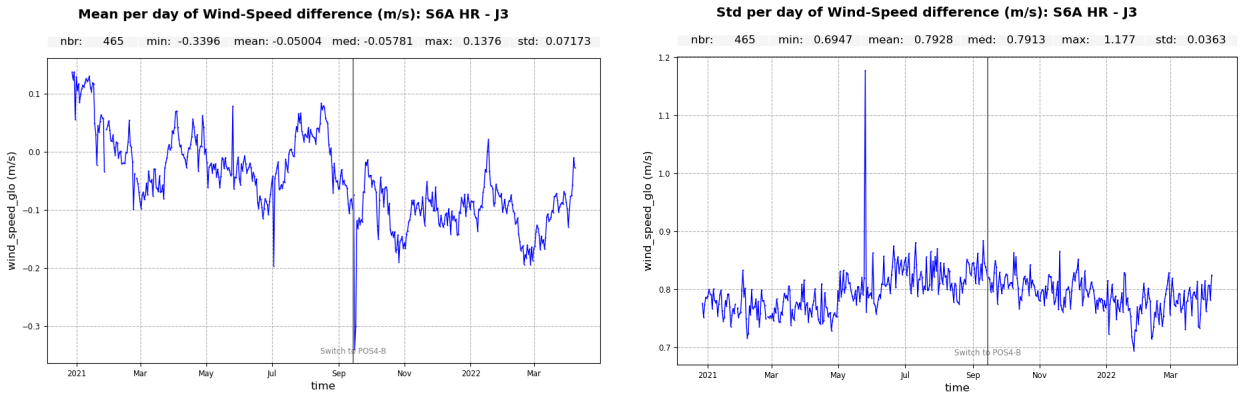

Figure 113 – Altimeter Wind-Speed difference: Sentinel-6A HR minus Jason-3. Mean per day (left panel) and standard deviation per day (right panel) computed over the complete tandem period.

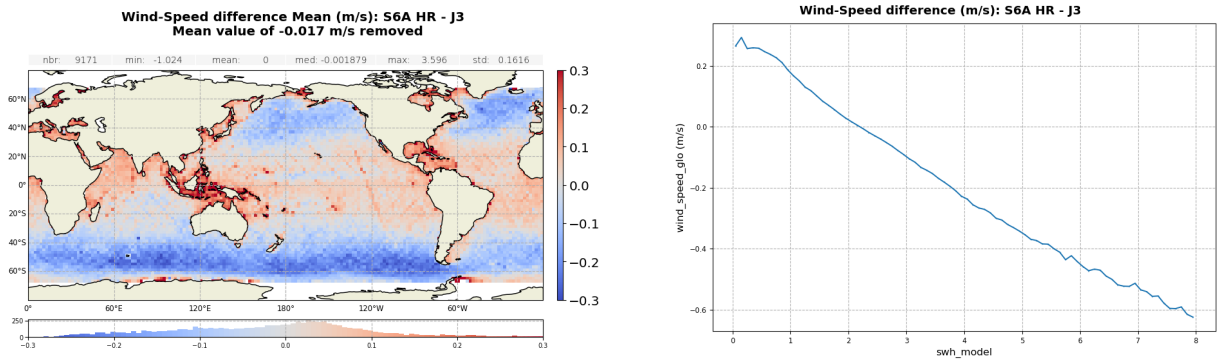

Figure 114 – Altimeter Wind-Speed difference: Sentinel-6A HR minus Jason-3 computed over the complete tandem period. Gridded map (left panel) and difference function of ERA5 SWH (right panel).

5.3.5. HR Sea State Bias

Comparison of SSB between S6A HR and J3 highlights the consistency of the two solutions, with a bias centred around -7 mm (figure 115). Because of its small impact on HR wind speed, the switch to POS4-B does not seems to impact the HR SSB retrieval: no jump are observed in the time monitoring, only a small reduction of the noise in the standard deviation monitoring is visible. The variations visible at the beginning of June 2021 are linked to SWH (see figure 104).

The map of the SSB differences is presented in figure 117 (left panel). A clear correlation to sea state condition is observed. It is important to note here that the SSB algorithm used for HR SSB computation is the same as for LR data, i.e. Jason-3 GDR-F Ku-band algorithm. This algorithm is not adapted to HR data. It can be the cause of the patterns observed here.

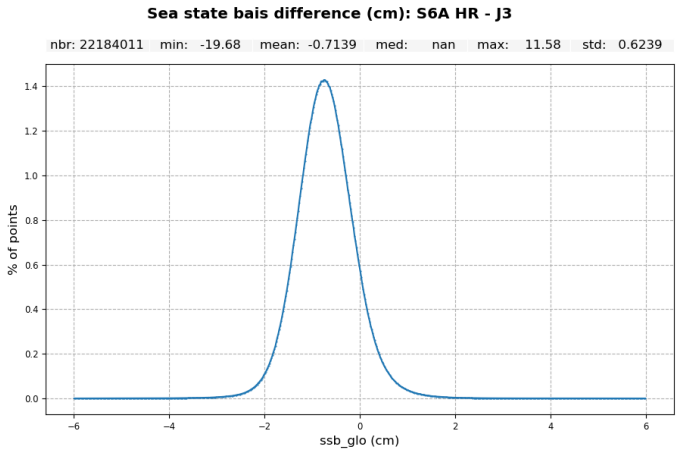

Figure 115 – Histogram of Ku-band SSB difference: Sentinel-6A HR minus Jason-3. Computed over the complete tandem period.

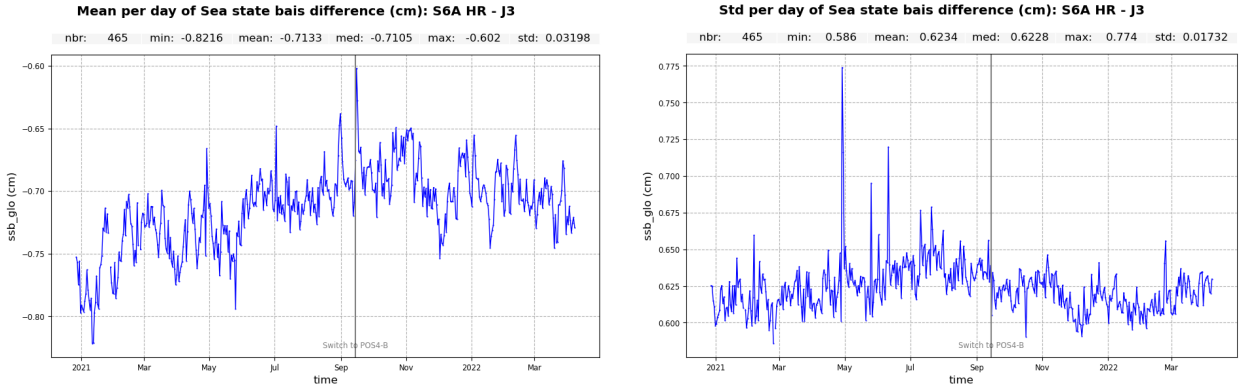

Figure 116 – Ku-band SSB difference: Sentinel-6A HR minus Jason-3. Mean per day (left panel) and standard deviation per day (right panel) computed over the complete tandem period.

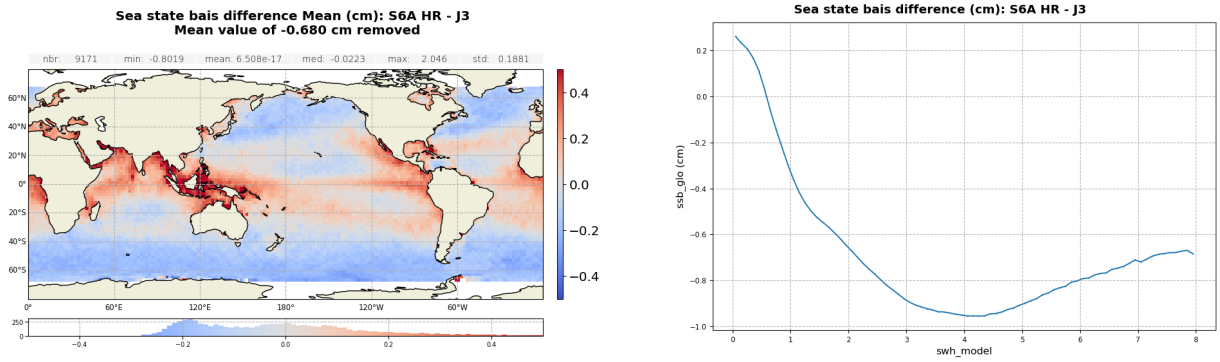

Figure 117 – Ku-band SSB difference: Sentinel-6A HR minus Jason-3 computed over the complete tandem period. Gridded map (left panel) and difference function of ERA5 SWH (right panel).

5.3.6. HR SSHA

In this section, we compared the SSHA derived from HR S6A data and J3 data. In terms of global bias, the

two solutions are perfectly in line (figure 120).

However, as for LR SSHA analysis, the temporal monitoring (figure 119) highlights two events on the 27-28 April and mid-February 2022, with a potential link to S6A or J3 radiometer WTC (see section 5.2.4. for more details). The jumps observed here are of the same amplitudes as for LR SSHA.

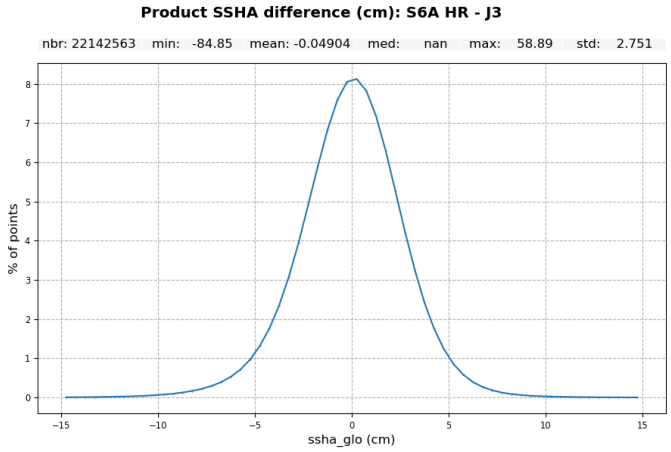

Figure 118 – Histogram of Product SSHA difference: Sentinel-6A HR minus Jason-3. Computed over the complete tandem period.

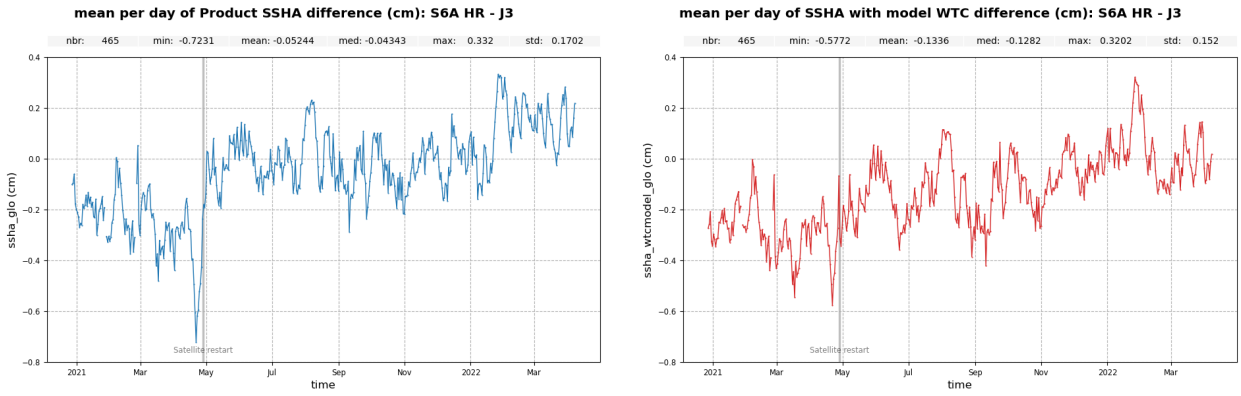

Figure 119 – Mean per day of SSHA difference: Sentinel-6A HR minus Jason-3. For product SSHA (left panel) and for SSHA recomputed using WTC from ECMWF model (right panel) computed over the complete tandem period.

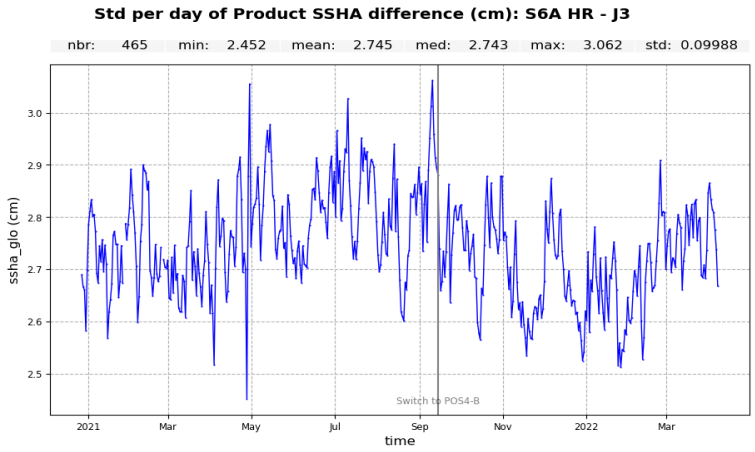

Figure 120 – Product SSHA difference: Sentinel-6A HR minus Jason-3. Standard deviation per day computed over the complete tandem period.

The map of SSHA differences highlight a strong correlation to sea state condition, mainly due to the skeweness difference between Jason-3 and Sentinel-6 HR processings but also to the impact of ocean vertical velocity on HR data, not fully corrected with PB F06.

As for LR data, an equatorial band of about 5 mm is visible. This behavior is most likely coming from Jason-3.

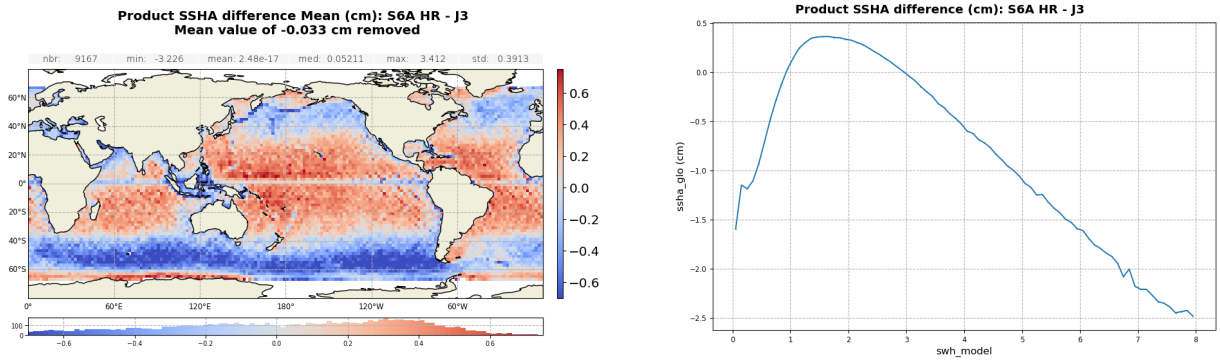

Figure 121 – Product SSHA difference: Sentinel-6A HR minus Jason-3 computed over the complete tandem period. Gridded map (left panel) and difference function of ERA5 SWH (right panel).

6. GMSL

Sentinel-6A satellite is taking over the responsibility as the reference mission to continue the long-term record of sea-surface height measurements started in 1992 by the Topex-Poseidon satellite and then by the Jason series. The role of Copernicus Sentinel-6 Michael Freilich is not only to extend the so-called Global Mean Sea Level (GMSL) climate record, but also to monitor the changing height of the sea surface with greater precision than before. As first, dedicated tandem phase with previous satellite Jason-3 ensure precise calibrations of the GMSL Sentinel-6A record.

In this section, we present the derivation of the GMSL offset and its uncertainty between Jason-3 and Sentinel-6A for its LR mode only. We also discuss the behavior of the GMSL difference timeseries between the two satellite to highlight potential residuals discrepancies.

For this analysis, Jason-3 GDR-F data has been used with the AVISO L2P standards.

6.1. Side A

Figure 122 presents the GMSL over POS4-A period for both the operational (left panel) and reprocessed (right panel) datasets. Thanks to the reprocessing, the GMSL difference with respect to Jason-3 is more stable. Still, a jump at cycle 17 is observed. It is concomitant with Sentinel-6A restart occuring on the 27-28 April 2021. This jump is also visible on S6A SSHA comparison to J3 and might comes from radiometer WTC (see sections 4.2., 5.1. and 5.2.4. for more details).

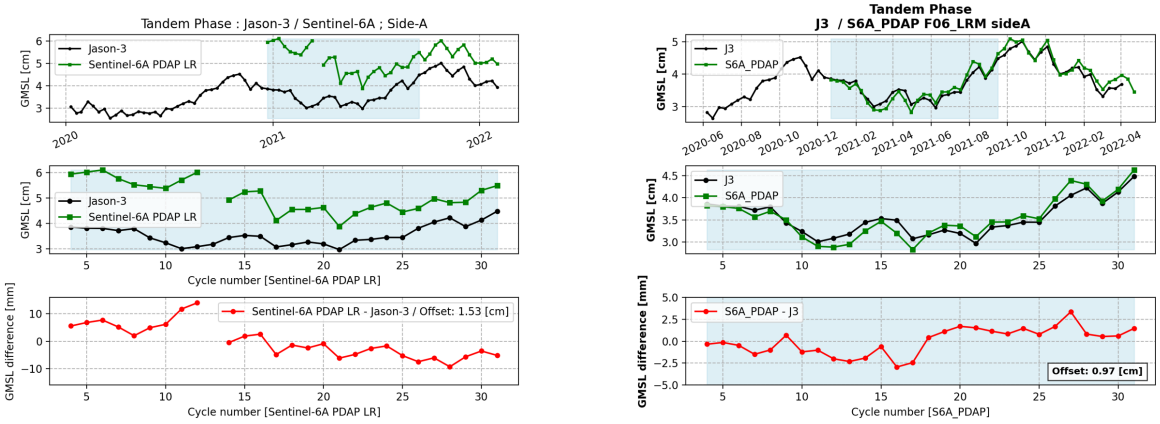

Figure 122 – Jason-3 (black) and Sentinel-6A (green) GMSL over the side A (top panel), the tandem phase (middle panel) and their differences over the side A tandem phase (bottom panel), for the operational dataset (left) and the reprocessed dataset of Sentinel-6A (right).

The GMSL offset between Jason-3 and reprocessed Sentinel-6A dataset is estimated to $9.7 \pm 0.3\,mm\,(1-\sigma)$ (see right panels of Figure 122 and Figure 123). Lower uncertainty is obtained as compared to the operational dataset ($1.5\,mm\,(1-\sigma)$ - not shown here) mainly due to correction of the time-tag issue correction deployed in PB F04 that cancels the trend that was observed previously (Figure 122 - bottom plot of left panel). The GMSL offset derivation and its uncertainty estimation is based on [5].

From Figure 123 (left panel), we still observed a significant GMSL drift between Jason-3 and Sentinel-6A ($4.2 \pm 2\,mm.yr^{-1}\,(1\,\sigma)$) that is mostly due to the jump at cycle 17 mentioned above.

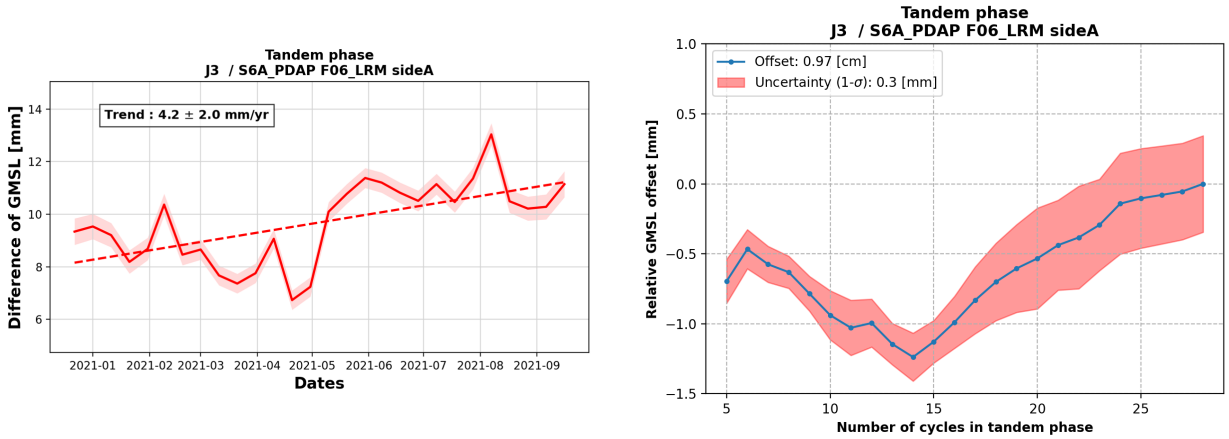

Figure 123 – Time series of GMSL difference between Jason-3 and Sentinel-6A over the side A tandem phase (left) and relative GMSL offset and its uncertainty between Jason-3 and Sentinel-6A as a function of the number of cycle used for the computation (right).

6.2. Side B

Figure 124 presents the GMSL over the side B for the reprocessed dataset, as well as the GMSL differences with respect to Jason-3 and their relative offset over the tandem phase. The stability between Jason-3 and Sentinel-6A has been improved after the switch (from 4.2 +/- 2.0 mm/yr to 2.6 +/- 2.6 mm/yr). No more significant drift is observed between Jason-3 and Sentinel-6A side-B GMSL (despite the large uncertainty due to the short time period). The uncertainty on the GMSL offset has also been improved from 0.3 mm to 0.2 mm ($1\,\sigma$). On the monitoring of the difference of GMSL with Jason-3, a change of behaviour can be seen during February 2022, which origin is under investigation. This behavior was also observed in the tandem phase analysis (see section 4.2., 5.1. and 5.2.4. for more details).

The difference of GMSL between Jason-3 and Sentinel-6A using ECMWF model WTC is presented on figure 125. With model WTC, the behaviour remains identical during the whole side B tandem phase. However, a periodic signal of about $3 - 4\,mm$ of amplitude is now appearing clearly. Similar behaviour has been observed during Topex/Jason-1 tandem phase (see Figure 1 of Guérou et al. (2022 - [5])) and is under investigation to better understand its origins (platforms thermal stability, vertical velocity, others).

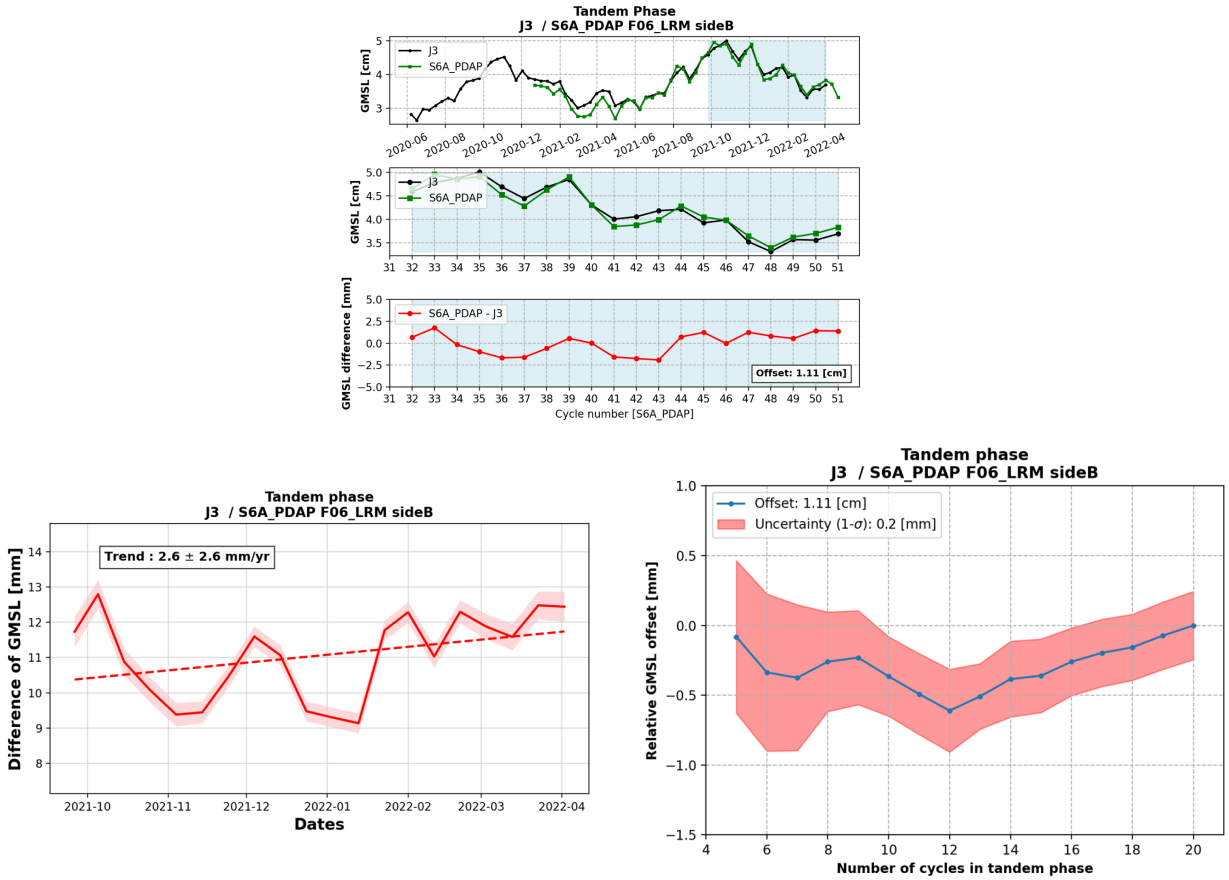

Figure 124 – Jason-3 (black) and Sentinel-6A (green) GMSL over the side B (top left panel), the tandem phase (middle left panel) and their difference over the side B tandem phase (bottom left panel) for the reprocessed dataset, difference of GMSL over the side B tandem phase (top right panel) and their relative GMSL offset (bottom right panel).

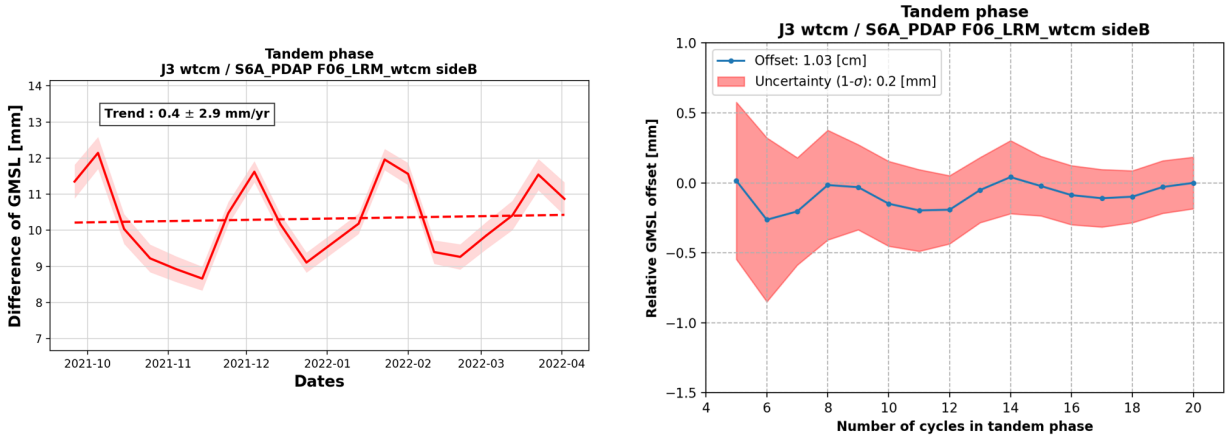

Figure 125 – Time series of GMSL difference between Jason-3 and Sentinel-6A over the side B tandem phase computed with wet tropospheric correction from ECMWF model (left) and relative GMSL offset and its uncertainty between Jason-3 and Sentinel-6A over the side B tandem phase as a function of the number of cycle used for the computation (right)

7. System requirements

In this section, the system requirements are verified for NTC data, in LR and in HR. Only reprocessed data are considered here.

7.1. LR

7.1.1. R-S-00260

Requirement	Status
For low-resolution ALT-NTC products, the standard deviation of the 1-second along-track averaged corrected low-resolution altimeter range measurements shall be less than 2.83 cm. Note: This requirement is based on the apportionment given in the table of the Sentinel-6 low-resolution altimetry error budget at the end of the document. Note: Like all performance requirements on the altimeter, unless specified otherwise, this specifies the maximum global RMS error over open ocean. Note: Note: A goal is 1.73 cm.	Not addressed in this report

Table 5 – R-S-00260

7.1.2. R-S-00270

Requirement	Status
For low-resolution ALT-NTC products, the noise of the 1-second along-track average of the low-resolution Ku-band altimeter range measurements shall be less than 1.5 cm at 2 m significant wave height. Note: the requirement is applicable after ground re-tracking. Note: The upper limit depends on SWH: 1.2 cm at 1 m SWH, 1.5 cm at 2 m SWH, 2.4 cm at 5 m SWH, and 3.2 cm at 8 m SWH. Note: A goal is 1.0 cm at 2 m SWH	**OK except for 1 m SWH limit**

Table 6 – R-S-00270

To estimate the noise of 1-second along-track average of the LR Ku-band altimeter range, we analyse "data_01/ku/range_ocean_rms" variable from LR products. It contains the standard deviation of 20 Hz measurements used for the compression to 1hz. To retrieve 1 Hz level of noise, this value is divided by $\sqrt{20}$.

The resulting 1 Hz level of noise averaged over the complete reprocessing period is plotted function of SWH on figure 126, left panel. As expected, S6A LR noise level is well below Jason-3 level and below the system requirement (black curve) over almost all the SWH spectrum. For 1 m wave, the level of noise is slightly above requirement with a value of 1.24 cm and an upper limit at 1.2 cm. Table 7 reports the level of noise

for the stated SWH values.

This noise level is stable in time, as shown on the cyclic monitoring of figure 126, right panel.

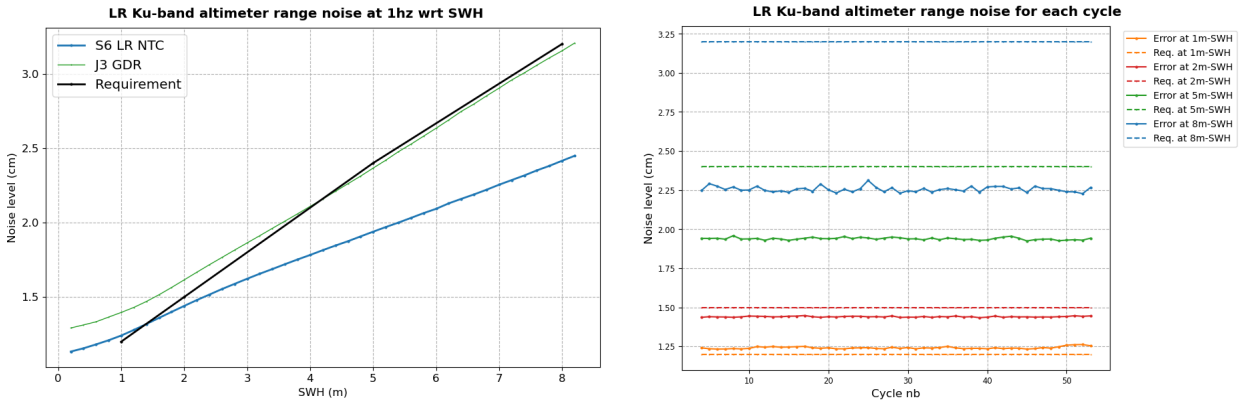

Figure 126 – 1 Hz noise of LR Ku-band altimeter range. Left panel: noise function of SWH for S6A LR and J3 computed over the complete reprocessing period; the black line represents the requirement thresholds. Right panel : noise level computed for each cycle and at 1, 2, 5 and 8 m-wave (solid lines) and the corresponding requirement levels (dashed lines).

SWH	Requirement	Noise level
1 m	**1.2 cm**	**1.24 cm**
2 m	1.5 cm	1.44 cm
5 m	2.4 cm	1.93 cm
8 m	3.2 cm	2.42 cm

Table 7 – 1 Hz noise of LR Ku-band altimeter range at 1, 2, 5 and 8 m-wave. Computed over the complete reprocessing period.

7.1.3. R-S-00280

Requirement	Status
For low-resolution ALT-NTC products, the noise of the 1-second along-track average of the C-band altimeter range measurements shall be less than 5.7 cm at 2 m significant wave height. Note: the requirement is applicable after ground re-tracking. Note: The upper limit depends on SWH: 4.5 cm at 1 m SWH, 5.7 cm at 2 m SWH, 9.1 cm at 5 m SWH, and 12.0 cm at 8 m SWH	**OK**

Table 8 – R-S-00280

Similarly to Ku-band, we analyse ”data_01/c/range_ocean_rms” variable from LR products to estimate the noise of 1-second along-track average of the LR C-band altimeter range.

The resulting 1 Hz level of noise averaged over the complete reprocessing period is plotted function of SWH on figure 126, left panel. As expected, S6A LR noise level is well below Jason-3 level and below the system requirement (black curve) over all the SWH spectrum. Table 9 reports the level of noise for the stated SWH values.

This noise level is stable in time, as shown on the cyclic monitoring of figure 127, right panel.

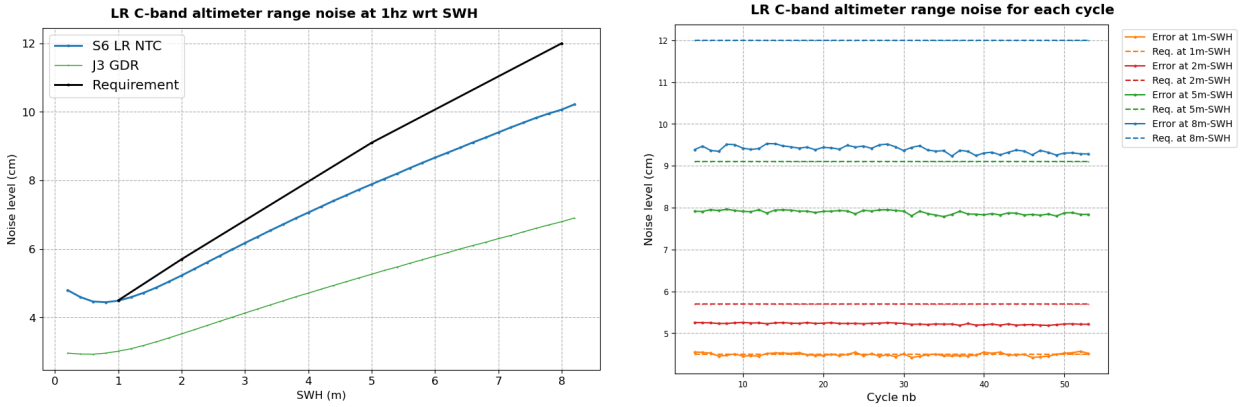

Figure 127 – 1 Hz noise of LR C-band altimeter range. Left panel: noise function of SWH for S6A LR and J3 computed over the complete reprocessing period; the black line represents the requirement thresholds. Right panel : noise level computed for each cycle and at 1, 2, 5 and 8 m-wave (solid lines) and the corresponding requirement levels (dashed lines).

SWH	Requirement	Noise level
1 m	4.5 cm	4.5 cm
2 m	5.7 cm	5.2 cm
5 m	9.1 cm	7.9 cm
8 m	12 cm	10.1 cm

Table 9 – 1 Hz noise of LR C-band altimeter range at 1, 2, 5 and 8 m-wave. Computed over the complete reprocessing period.

7.1.4. R-S-00290

Requirement	Status
For low-resolution ALT-NTC products, the contribution of the ionosphere correction error to the standard deviation of the 1-second along-track averaged corrected low-resolution altimeter range measurements shall be less than 0.5 cm. Note: Derived from C and Ku band and averaged over 200 km. Note: Like all performance requirements on the altimeter, unless specified otherwise, this specifies the maximum global RMS error over open ocean. Note: A goal is 0.3 cm	**OK**

Table 10 – R-S-00290

To quantify the contribution of the ionosphere correction error to the standard deviation of 1 Hz corrected LR range, several metrics are checked.

A first estimation of ionosphere correction error is performed by checking the noise between consecutive measurements. The results shows a very low level of noise, way below the mm (figure 128).

Comparison to Jason-3 ionosphere correction highlights a standard deviation ranging between 2 and 4.5 mm (figure 134 left panel). And finally, comparison to ionosphere correction derived from GIM model shows a standard deviation ranging between 3.5 mm and 1 cm (figure 134 right panel). These values are all within requirement.

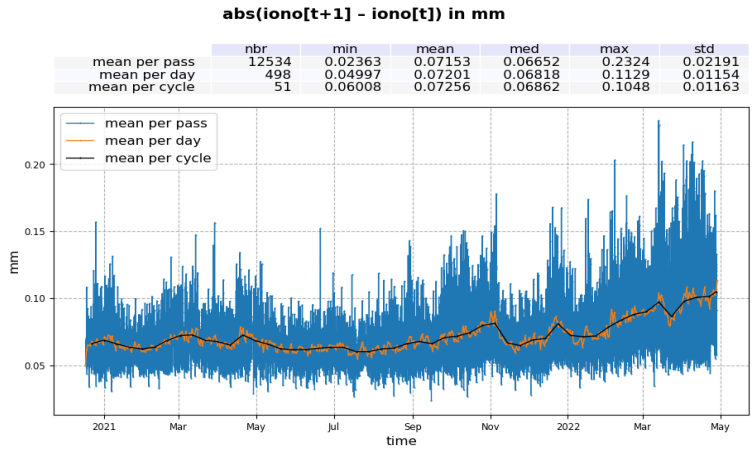

Figure 128 – Absolute value of consecutive filtred ionosphere correction measurement. Mean per pass (blue), mean per day (orange) and mean per cycle (black).

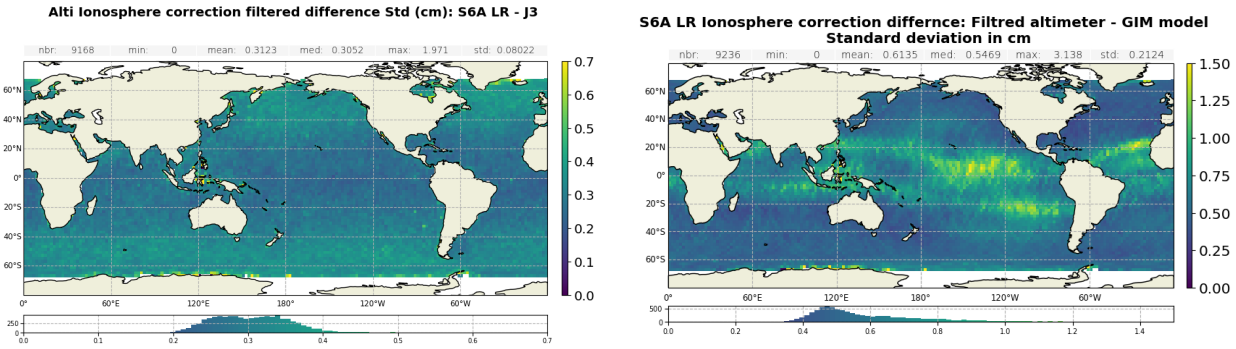

Figure 129 – Standard deviation gridded map of Altimeter Filtred Ionosphere correction difference. Left: Sentinel-6A LR minus Jason-3. Right: Altimeter Filtred minus GIM model (m). Computed over the completed reprocessed period

7.1.5. R-S-00300

Requirement	Status
For low-resolution ALT-NTC products, the contribution of the sea state bias error to the standard deviation of the 1-second along-track averaged corrected low-resolution altimeter range measurements shall be less than 2.0 cm. Note: Like all performance requirements on the altimeter, unless specified otherwise, this specifies the maximum global RMS error over open ocean. Note: A goal is 1.0 cm	**OK**

Table 11 – R-S-00300

As for ionosphere correction, a first estimation of the SSB error is performed by checking the noise between consecutive measurements. The results shows a low level of noise, below the cm (figure 130).

Comparison to Jason-3 SSB highlights a standard deviation ranging between 4.5 and 7.5 mm (figure 131). These values are within requirement.

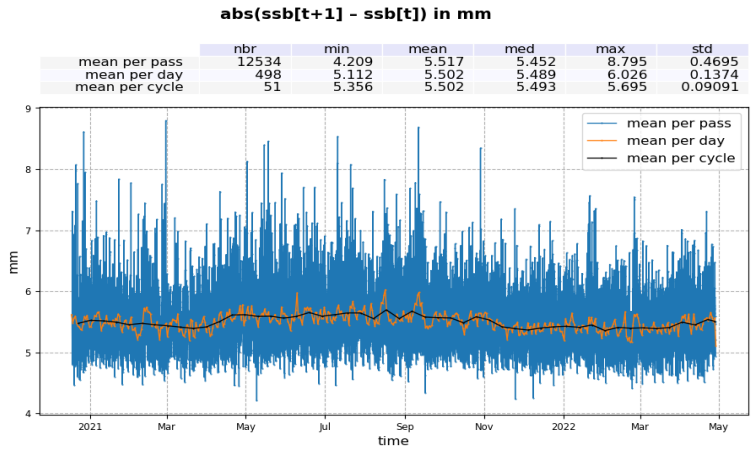

Figure 130 – Absolute value of consecutive LR sea state bias measurement. Mean per pass (blue), mean per day (orange) and mean per cycle (black).

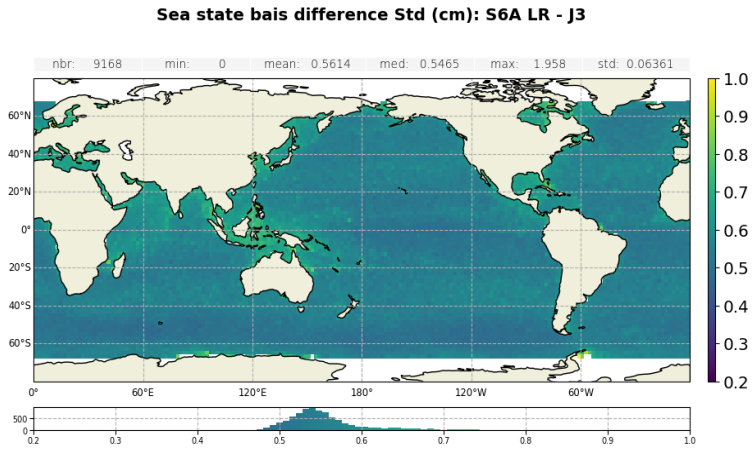

Figure 131 – Standard deviation gridded map of Ku-band SSB difference: Sentinel-6A LR minus Jason-3 computed over the complete tandem period.

7.1.6. R-S-00310

Requirement	Status
For low-resolution ALT-NTC products, the contribution of the dry tropospheric correction error to the standard deviation of the 1-second along-track averaged corrected low-resolution altimeter range measurements shall be less than 0.7 cm. Note: this requirement applies to the model to be used to calculate the dry troposphere model. Note: Like all performance requirements on the altimeter, unless specified otherwise, this specifies the maximum global RMS error over open ocean. Note: A goal is 0.5 cm	**OK**

Table 12 – R-S-00310

The dry troposphere correction model are identical between Jason-3 and Sentinel-6A products: same model and same estimation from model. Analysis have shown that the two retrievals are indeed perfectly in line (see figure 132).

System requirement for Jason-3 dry troposphere correction is the same as S6A present requirement and it has been shown that Jason-3 dry troposphere correction is compliant.

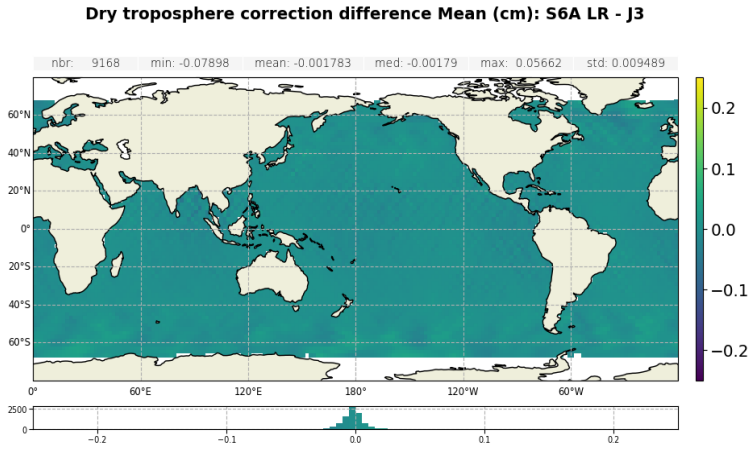

Figure 132 – Mean gridded map of dry tropospheric correction difference: Sentinel-6A LR minus Jason-3 computed over the complete tandem period.

7.1.7. R-S-00320

Requirement	Status
For low-resolution ALT-NTC products, the contribution of the wet tropospheric correction error to the standard deviation of the 1-second along-track averaged corrected low-resolution altimeter range measurements shall be less than 1.0 cm. Note: Like all performance requirements on the altimeter, unless specified otherwise, this specifies the maximum global RMS error over open ocean. Note: A goal is 0.8 cm	**OK**

Table 13 – R-S-00320

A first estimation of AMR-C WTC error is performed by checking the noise between consecutive measurements. The results shows a very low level of noise, below 2 mm (figure 133).

Comparison to Jason-3 AMR WTC highlights a standard deviation below 8 mm (figure 134). These values are within requirement.

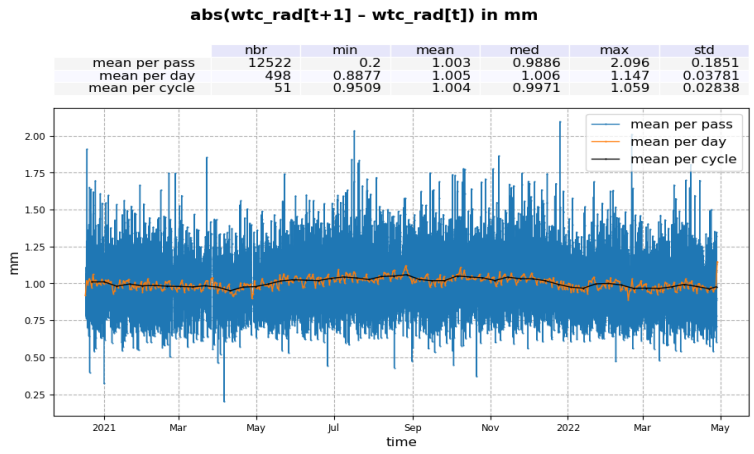

Figure 133 – Absolute value of consecutive AMR-C WTC measurement. Mean per pass (blue), mean per day (orange) and mean per cycle (black).

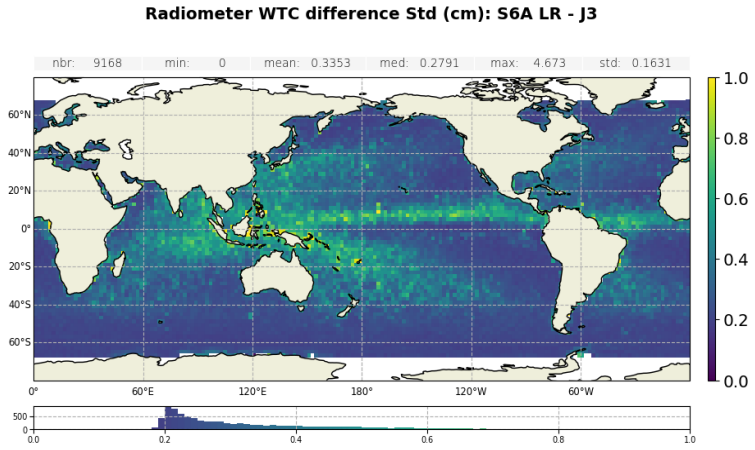

Figure 134 – Standard deviation gridded map of WTC difference: AMR-C Sentinel-6A LR minus AMR Jason-3. Computed over the completed reprocessed period

7.1.8. R-S-00330

Requirement	**Status**
For low-resolution ALT-NTC products, the standard deviation of the determination of the radial component of the orbit shall be less than 1.5 cm. Note: This requirement is applicable to the orbital solution derived from the combined set of data from DORIS, GNSS-POD and LRA. Note: Orbit errors have a larger than 1000 km length scale, significantly different from the 1 Hz altimetry noise. Nevertheless the orbit error is added in a RSS sense, presuming that the error is uncorrelated from cycle to cycle at the same location. Note: a goal is 1.0 cm	Not addressed in this report

Table 14 – R-S-00330

7.1.9. R-S-00340

Requirement	Status
For low-resolution ALT-NTC products, the standard deviation of the 1-second along-track averaged corrected low-resolution measurements of sea surface height shall be less than 3.20 cm. Note: This requirement is based on the apportionment given in the table of the Sentinel-6 low-resolution altimetry error budget at the end of the document. Note: Like all performance requirements on the altimeter, unless specified otherwise, this specifies the maximum global RMS error over open ocean. Note: A goal is 1.99 cm	**OK**

Table 15 – R-S-00340

To verify this requirement, the crossover analysis presented in section 4.3.2. is used. The standard deviation of corrected LR SSH difference is centred around 4.66 cm (see figure 58). It means that the error is of 3.29 cm (standard deviation divided by $\sqrt{(2)}$). This value is slightly above requirement.

However looking at a region with low variability, for example the pacific patch, the error is of 2.25 cm in average. On a cyclic basis, this error is always below the requirement limit of 3.2 cm as shown on figure 135.

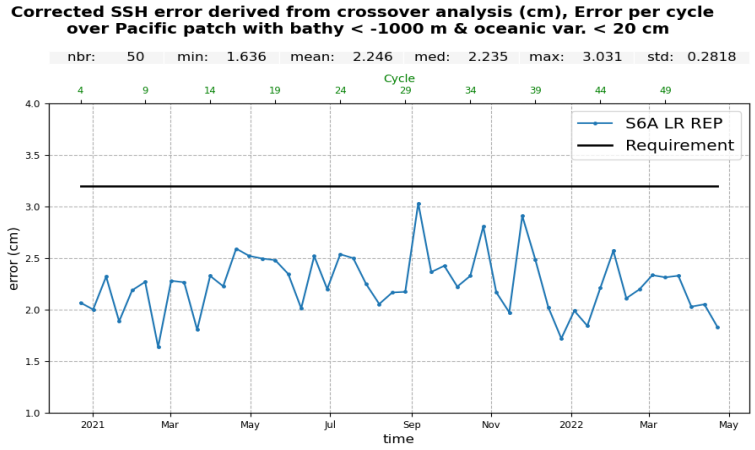

Figure 135 – Corrected LR SSH error derived from crossover analysis with a selection over Pacific patch (latitude in [-24.5°N; -3°N] and longitude in [220°E; 246°E]). The error equals to the standard deviation of the SSH difference divided by $\sqrt{(2)}$. Computed on a cyclic basis.

7.1.10. R-S-00350

Requirement	Status
For low-resolution ALT-NTC products, the uncertainty of 1-second along-track averaged low-resolution measurements of significant wave height in the range 0.5 to 8 m shall be less than 15 cm plus 5% of significant wave height. Note: This is based on the combination of noise and systematic error. Note: A goal is 10 cm plus 5% of significant wave height	**OK**

Table 16 – R-S-00350

LR Ku-band SWH are compared to SWH derived from ERA-5 model on figure 136. It shows a good consistancy between the two datasets, the difference being below requirement limit over the complete SWH spectrum.

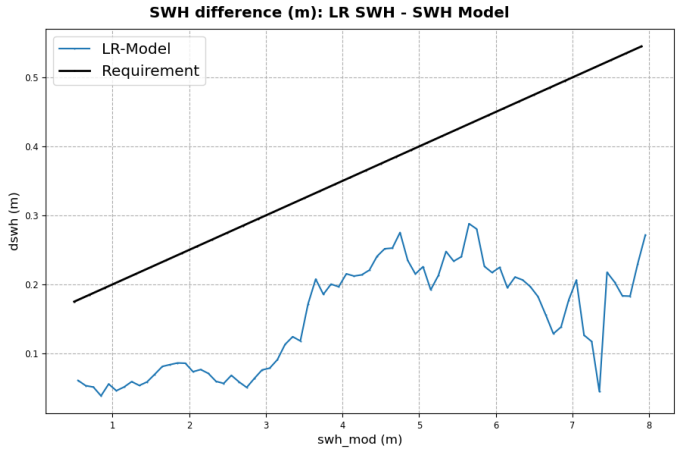

Figure 136 – SWH difference between Sentinel-6A LR data and ERA-5 SWH, plotted function of ERA-5 SWH. Computed over S6A cycle 30. Black lines represent requirement limits. Results are identical for all cycles.

7.1.11. R-S-00355

Requirement	Status
For low-resolution ALT-NTC products, significant wave heights shall be provided up to at least 20 m. Note: The measurement performance under high sea state conditions will be determined during commissioning	**OK**

Table 17 – R-S-00355

Figure 137 shows the maximum value per cycle of S6A LR SWH. The values are above 20 m, as expected.

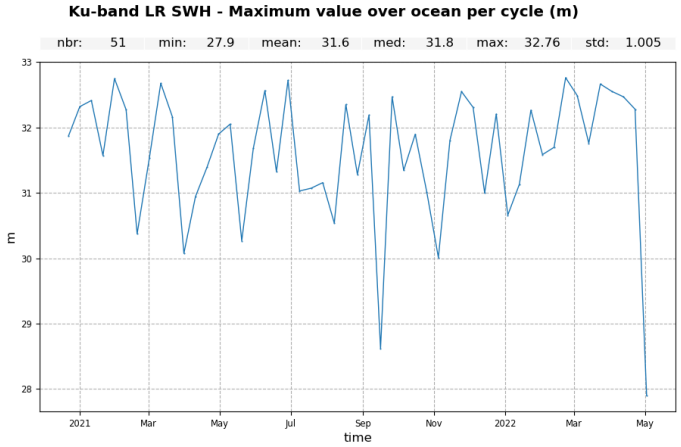

Figure 137 – Maximum value of Sentinel-6A LR SWH per cycle.

7.1.12. R-S-00360

Requirement	Status
For low-resolution ALT-NTC products, the uncertainty of 1-second along-track averages of 10 meter wind speed over ocean surfaces, derived from low-resolution altimeter measurements, shall be better than 1.5 m/s for wind speeds in the range 3 m/s to 20 m/s. Note: Wind speed refers to the wind (not neutral wind) speed at a reference height of 10 meters above the sea surface. Note: This wind speed accuracy requirement translates to an accuracy requirement on the backscatter. Note: A goal is 1.0 m/s	**OK**

Table 18 – R-S-00360

To verify the uncertainty of S6A LR altimeter wind-speed, a comparison to model is performed. The model wind speed used is derived from U and V components provided in L2 product (”data_01/wind_speed_mod_u” and ”data_01/wind_speed_mod_v”). Difference between altimeter and model wind speed is plotted on figure 138 function of model wind speed. Values are within requirement.

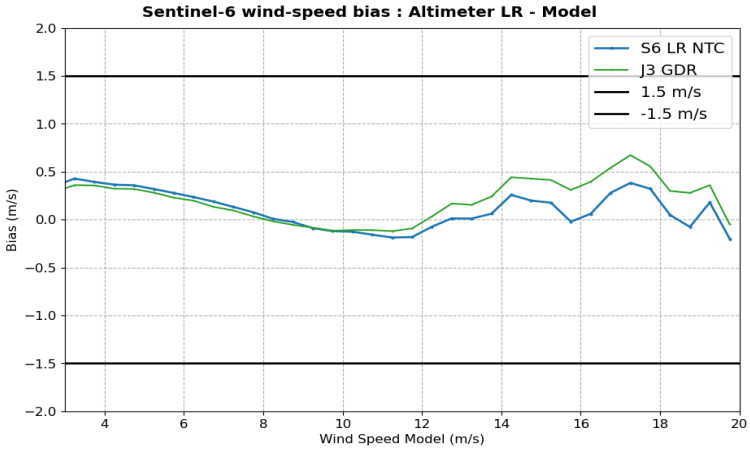

Figure 138 – Difference between Altimeter LR wind speed and model wind speed function of model wind speed. Computed over S6A cycle 30. Black lines represent requirement limits. Results are identical for all cycles.

7.1.13. R-S-00370

Requirement	Status
For low-resolution ALT-NTC products, the absolute accuracy of 1-second along-track averaged low-resolution measurements of normalised radar cross-section at Ku-band and vertical incidence, in the range 7 to 16 dB, shall be better than 0.3 dB. Note: This value (0.3 dB) is not the value at satellite level (1 dB), but it is achieved after external in-flight calibration to ensure coherence with other missions. In other words, 0.3 dB is the global value, what allows 1 dB at satellite level, to be compensated by the ground processing. Note: This requirement also sets limits on the accuracy of sigma0 attenuation correction to be supplied by the radiometer	Not addressed in this report

Table 19 – R-S-00370

The absolute accuracy of the LR sigma0 is not addressed in this report as there is currently no facility available to measure it. However, as discussed in section 5.2.1., the sigma0 bias with respect to Jason-3 is stable in time when considering independantly sides A and B, with a standard deviation of 0.12 dB.

7.2. HR

7.2.1. R-S-00680

Requirement	Status
For high-resolution ALT-NTC products, the standard deviation of the 1-second along-track averaged corrected high-resolution altimeter range measurements shall be less than 2.53 cm. Note: This requirement is based on the apportionment given in the table of the Sentinel-6 high-resolution altimetry error budget at the end of the document. Note: Note: Like all performance requirements on the altimeter, unless specified otherwise, this specifies the maximum global RMS error over open ocean. Note: Note: A goal is 1.49 cm.	Not addressed in this report

Table 20 – R-S-00680

7.2.2. R-S-00690

Requirement	Status
For high-resolution ALT-NTC products, the noise of the 1-second along-track average of the high-resolution Ku-band altimeter range measurements shall be less than 0.8 cm at 2 m significant wave height. Note: the requirement is applicable after ground re-tracking. Note: The upper limit depends on SWH: 0.7 cm at 1 m SWH, 0.8 cm at 2 m SWH, 1.3 cm at 5 m SWH, and 2.0 cm at 8 m SWH. Note: A goal is 0.5 cm at 2m SWH	**NOK**

Table 21 – R-S-00690

Similarly to LR, we analyse ”data_01/ku/range_ocean_rms” variable from HR products to estimate the noise of 1-second along-track average of the HR Ku-band altimeter range.

The resulting 1 Hz level of noise averaged over the complete reprocessing period is plotted function of SWH on figure 139, left panel. As expected, S6A HR noise level is well below Jason-3 and Sentinel-3A levels. However, S6A HR noise level is above requirement (black curve) for 5 m and 8 m wave upper limits. Table 22 reports the level of noise for the stated SWH values.

This noise level is stable in time, as shown on the cyclic monitoring of figure 139, right panel.

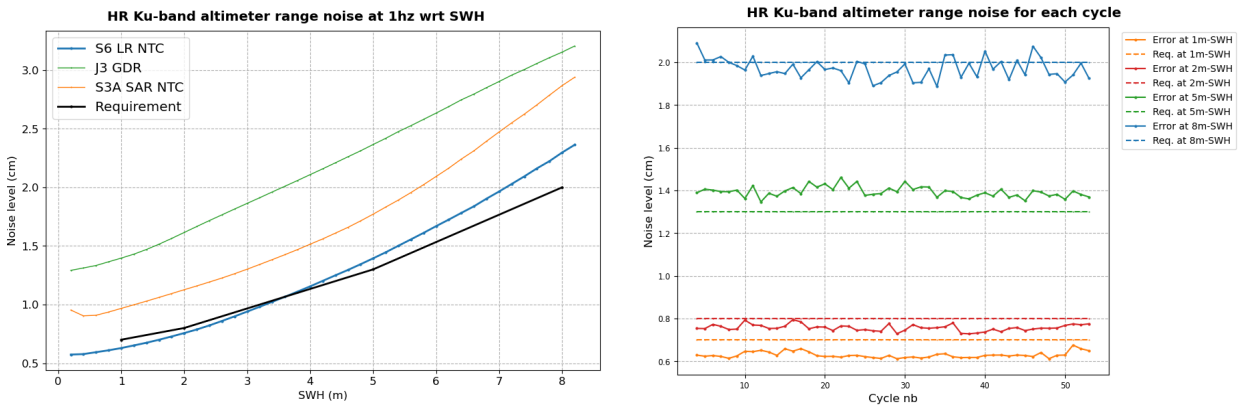

Figure 139 – 1 Hz noise of HR Ku-band altimeter range. Left panel: noise function of SWH for S6A HR and J3 computed over the complete reprocessing period; the black line represents the requirement thresholds. Right panel : noise level computed for each cycle and at 1, 2, 5 and 8 m-wave (solid lines) and the corresponding requirement levels (dashed lines).

SWH	Requirement	Noise level
1 m	0.7 cm	0.63 cm
2 m	0.8 cm	0.76 cm
5 m	**1.3 cm**	**1.39 cm**
8 m	**2.0 cm**	**2.30 cm**

Table 22 – 1 Hz noise of HR Ku-band altimeter range at 1, 2, 5 and 8 m-wave. Computed over the complete reprocessing period.

7.2.3. R-S-00700

Requirement	Status
For high-resolution ALT-NTC products, the contribution of the ionospheric correction error to the standard deviation of the 1-second along-track averaged corrected high-resolution altimeter range measurements shall be less than 0.5 cm. Note: Derived from C and Ku band and averaged over 200 km. Note: Like all performance requirements on the altimeter, unless specified otherwise, this specifies the maximum global RMS error over open ocean. Note: A goal is 0.3 cm	**OK, see section 7.1.4.**

Table 23 – R-S-00700

7.2.4. R-S-00710

Requirement	Status
For high-resolution ALT-NTC products, the contribution of the sea state bias error to the standard deviation of the 1-second along-track averaged corrected high-resolution altimeter range measurements shall be less than 2.0 cm. Note: Since the sea state bias model will have to be determined for the altimeter data itself, the error can only be evaluated based on day-2 processing. Note: Like all performance requirements on the altimeter, unless specified otherwise, this specifies the maximum global RMS error over open ocean. Note: A goal is 1.0 cm	**OK**

Table 24 – R-S-00710

As for LR data, a first estimation of HR SSB error is performed by checking the noise between consecutive measurements. The results shows a low level of noise, below the cm (figure 140).

Comparison to Jason-3 SSB highlights a standard deviation ranging between 4.5 and 8.5 mm (figure 131). These values are within requirement.

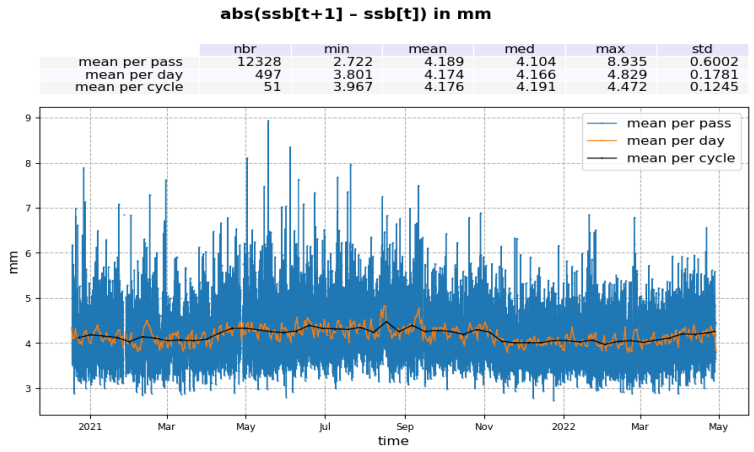

Figure 140 – Absolute value of consecutive HR sea state bias measurement. Mean per pass (blue), mean per day (orange) and mean per cycle (black).

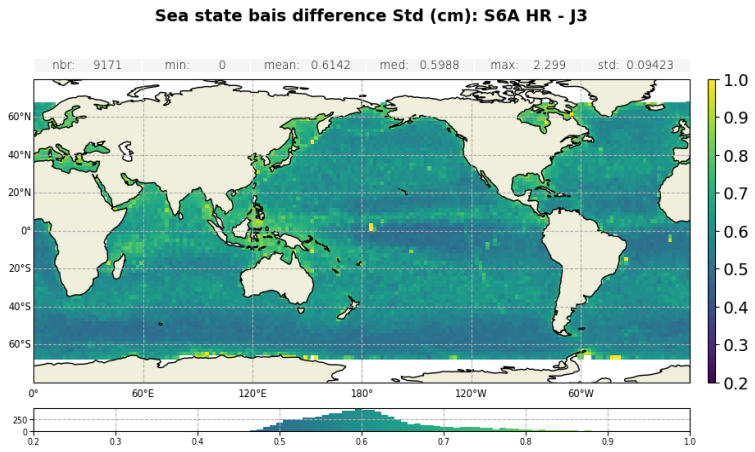

Figure 141 – Standard deviation gridded map of Ku-band SSB difference: Sentinel-6A HR minus Jason-3 computed over the complete tandem period.

7.2.5. R-S-00720

Requirement	Status
For high-resolution ALT-NTC products, the contribution of the dry tropospheric correction error to the standard deviation of the 1-second along-track averaged corrected high-resolution altimeter range measurements shall be less than 0.7 cm. Note: this requirement applies to the model to be used to calculate the dry troposphere model. Note: Like all performance requirements on the altimeter, unless specified otherwise, this specifies the maximum global RMS error over open ocean. Note: A goal is 0.5 cm	**OK, see section 7.1.6.**

Table 25 – R-S-00720

7.2.6. R-S-00730

Requirement	Status
For high-resolution ALT-NTC products, the contribution of the wet tropospheric correction error to the standard deviation of the 1-second along-track averaged corrected high-resolution altimeter range measurements shall be less than 1.0 cm. Note: Like all performance requirements on the altimeter, unless specified otherwise, this specifies the maximum global RMS error over open ocean. Note: A goal is 0.8 cm	**OK, see section 7.1.7.**

Table 26 – R-S-00730

7.2.7. R-S-00740

Requirement	Status
For high-resolution ALT-NTC products, the standard deviation of the determination of the radial component of the orbit shall be less than 1.5 cm. Note: This requirement is applicable to the orbital solution derived from the combined set of data from DORIS, GNSS-POD and LRA. Note: Orbit errors have a larger than 1000 km length scale, significantly different from the 1 Hz altimetry noise. Nevertheless the orbit error is added in a RSS sense, presuming that the error is uncorrelated from cycle to cycle at the same location. Note: A goal is 1.0 cm	Not addressed in this report

Table 27 – R-S-00740

7.2.8. R-S-00750

Requirement	Status
For high-resolution ALT-NTC products, the standard deviation of the 1-second along-track averaged corrected high-resolution measurements of sea surface height shall be less than 2.94 cm. Note: This requirement is based on the apportionment given in the table of the Sentinel-6 high-resolution altimetry error budget at the end of the document. Note: Like all performance requirements on the altimeter, unless specified otherwise, this specifies the maximum global RMS error over open ocean. Note: A goal is 1.80 cm	**OK**

Table 28 – R-S-00750

To verify this requirement, the crossover analysis presented in section 4.3.2. is used. The standard deviation of corrected HR SSH difference is centred around 4.49 cm (see figure 58). It means that the error is of 3.17 cm (standard deviation divided by $\sqrt{(2)}$). This value is slightly above requirement, but includes natural ocean variability.

However looking at a region with low variability, for example the Pacific patch, the error is of 2.04 cm in average. On a cyclic basis, this error is always below the requirement limit of 2.94 cm (figure 142), except for two cycles (19 and 24).

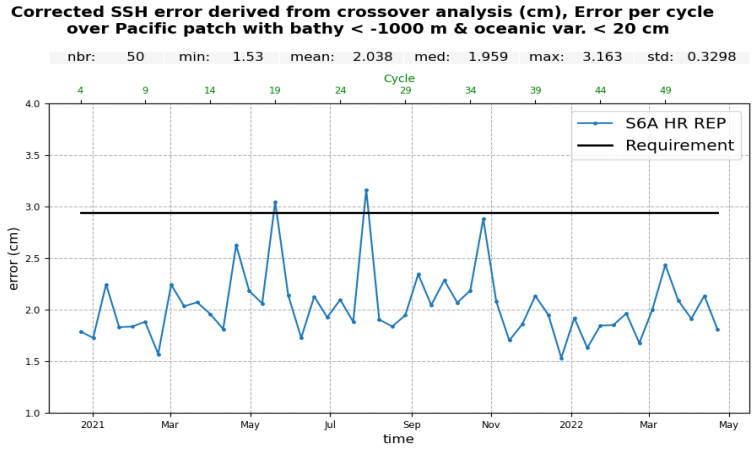

Figure 142 – Corrected HR SSH error derived from crossover analysis with a selection over Pacific patch (latitude in [-24.5°N; -3°N] and longitude in [220°E; 246°E]). The error equals to the standard deviation of the SSH difference divided by $\sqrt{(2)}$. Computed on a cyclic basis.

7.2.9. R-S-00760

Requirement	Status
For high-resolution ALT-NTC products, the uncertainty of 1-second along-track averaged high-resolution measurements of significant wave height in the range 0.5 to 8 m shall be less than 15 cm plus 5% of significant wave height. Note: This is based on the combination of noise and systematic error. Note: A goal is 10 cm plus 5% of significant wave height	**NOK**

Table 29 – R-S-00760

HR Ku-band SWH are compared to SWH derived from ERA-5 model on figure 143. Even with the PB F06 update, Sentinel-6A HR SWH are not compliant with requirement.

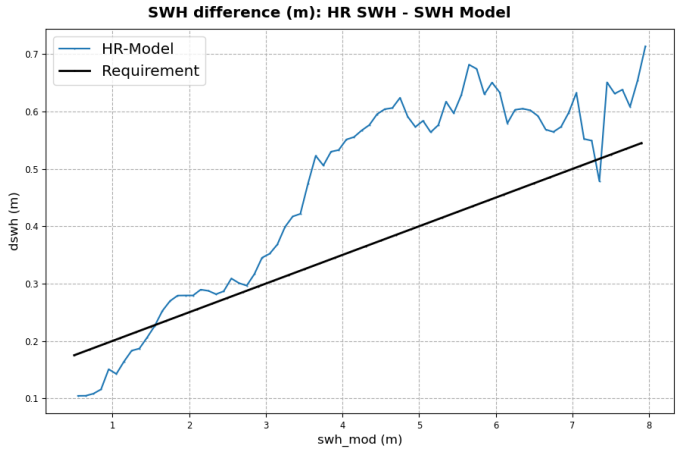

Figure 143 – SWH difference between Sentinel-6A HR data and ERA-5 SWH, plotted function of ERA-5 SWH. Computed over S6A cycle 30. Black lines represent requirement limits. Results are identical for all cycles.

7.2.10. R-S-00765

Requirement	Status
For high-resolution ALT-NTC products, significant wave heights shall be provided up to at least 20 m. Note: The measurement performance under high sea state conditions will be determined during commissioning	**OK**

Table 30 – R-S-00765

Figure 144 shows the maximum value per cycle of S6A HR SWH. It equals to 20 m for all cycles, which is consistant with the requirement.

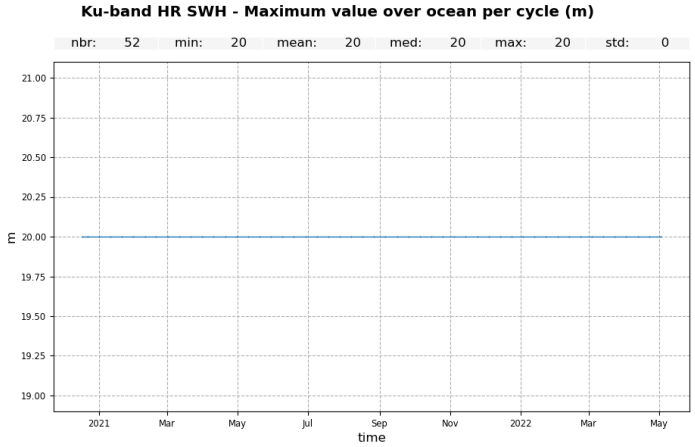

Figure 144 – Maximum value of Sentinel-6A HR SWH per cycle.

7.2.11. R-S-00770

Requirement	Status
For high-resolution ALT-NTC products, the uncertainty of 1-second along-track averages of 10 meter wind speed over ocean surfaces, derived from high-resolution altimeter measurements, shall be better than 1.5 m/s for wind speeds in the range 3 m/s to 20 m/s. Note: Wind speed refers to the wind (not neutral wind) speed at a reference height of 10 meters above the sea surface. Note: This wind speed accuracy requirement translates to an accuracy requirement on the backscatter Note: A goal is 1.0 m/s	**OK**

Table 31 – R-S-00770

As for LR, a comparison to model is performed to verify the uncertainty of S6A HR altimeter wind-speed. Difference between altimeter and model wind speed is plotted on figure 145 function of model wind speed. Values are within requirement.

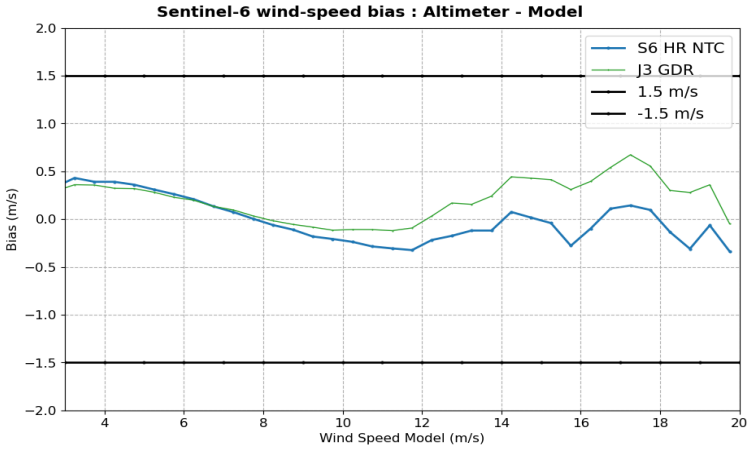

Figure 145 – Difference between Altimeter HR wind speed and model wind speed function of model wind speed. Computed over S6A cycle 30. Black lines represent requirement limits. Results are identical for all cycles.

7.2.12. R-S-00780

Requirement	Status
For high-resolution ALT-NTC products, the absolute accuracy of 1-second along-track averaged high-resolution measurements of normalised radar cross-section at Ku-band and vertical incidence, in the range 7 to 16 dB, shall be better than 0.3 dB. Note: This value (0.3 dB) is not the value at satellite level (1 dB), but it is achieved after external in-flight calibration to ensure coherence with other missions. In other words, 0.3 dB is the global value, what allows 1 dB at satellite level, to be compensated by the ground processing. Note: This requirement also sets limits on the accuracy of sigma0 attenuation correction to be supplied by the radiometer	Not addressed in this report

Table 32 – R-S-00780

The absolute accuracy of the HR sigma0 is not addressed in this report as there is currently no facility available to measure it. However, as discussed in section 5.3.3., the sigma0 bias with respect to Jason-3 is stable in time when considering independantly sides A and B, with a standard deviation of 0.33 dB.

8. Conclusion

An overview of the impact of Sentinel-6A F06 reprocessing over ocean has been presented in this report. This reprocessing present the first opportunity to assess Sentinel-6A data performance with an homogeneous Processing Baseline version over the complete mission lifetime. The results presented here testify of the improvement in stability and overall mission performance of Sentinel-6A LR and HR data.

The Processing Baseline used for this reprocessing (F06) brought a major improvement on HR data, with a reduction of 17 cm on HR SWH bias. The consistency of HR SWH with respect to LR SWH and to Jason-3 SWH has then been improved. The impact is also visible for the other altimeter HR estimated variables (range, sigma0), reducing the correlation to SWH of their biases with respect to LR data. It is important to note that the impact of the ocean vertical velocity on HR data has not been totally suppressed by this update but strongly reduced.

Thanks to the reprocessing, both the mean and the standard deviation of SSH difference at crossover is more stable in time and reduced, down to 4.66 and 4.45 cm for respectively LR and HR standard deviation, which is a very good performance.

POS4 switch between A and B side on 14/09/2021 has only shown impact on the backscatter coefficient (in LR and HR). Its value slightly varies between the altimeter sides, impacting the altimeter wind-speed, sea state bias and ionosphere correction retrievals. In this report, we recommand new values for the sigma0 calibration bias for next reprocessing, in order to improve the consitency between POS4-A and -B. Except from that, the transition between the two altimeters is perfectly smooth.

LR reprocessed data are in line with Jason-3 with a bias in SWH of only -1.3 cm and in range of only 0.8 cm. The total SSHA bias with respect to Jason-3 is also excellent, only 1.17 cm. The correlation to SWH in range should be improved thanks to future numerical retracker. Mispointing derived from Sentinel-6A LR retracking presents a small mis-centring, with a value centred around 0.0126 degree^2.

HR mode is impacted by the remaining effect of ocean vertical velocity and by the absence of skewness parameter in its processing. Future addition of skewness parameter in the HR processing along with numerical retracker and ocean vertical velocity correction should improve these results in the future.

Tandem flight analysis has shown the existence of an equatorial band in SSHA (with and without geophysical corrections) differences between Sentinel-6A and Jason-3. This band has an amplitude of 5 mm for both LR and HR data. Investigations point to Jason-3 as the origin. The root cause is yet to be found.

Despite the excellent performances of Sentinel-6A, two events reduce their stability over time:

- A loss of stability in the SSHA difference with respect to Jason-3 and in the GMSL is observed at the satellite restart occuring on 27-28 April 2021. It is concomitant with an event on AMR-C WTC (- 4 mm). The potential link between this restart and the event observed on AMR-C WTC is yet to be identified.
- Another event more spread over time, occuring beginning of 2022, impacts also the SSHA and GMSL stability. The origin of such behavior is under investigation (Sentinel-6A AMR-C, Jason-3 AMR, other).

The compliance status to system requirements shows once again the excellent quality of Sentinel-6A data, especially for LR dataset. In HR, two requirements are not fufilled yet:

- R-S-00690: 1 Hz noise of HR range is above requirements for 5 and 8 m SWH upper limits.

- R-S-00760: due to the remaining impact of ocean vertical velocity on HR data, HR SWH uncertainty is above requirement.

9. References

References

[1] Sentinel-6A user handbook available at https://eumetsatspace.atlassian.net/wiki/spaces/SEN6/overview

[2] Sentinel-6A product notice at https://www.eumetsat.int/media/48237

[3] Jason-3 product handbook available at https://www.aviso.altimetry.fr/fileadmin/documents/data/tools/hdbk_j3.pdf

[4] Changes in ECMWF model, web page: https://www.ecmwf.int/en/forecasts/documentation-and-support/changes-ecmwf-model

[5] Guérou, A., Meyssignac, B., Prandi, P., Ablain, M., Ribes, A., and Bignalet-Cazalet, F.: Current observed global mean sea level rise and acceleration estimated from satellite altimetry and the associated uncertainty, EGUsphere [preprint], https://doi.org/10.5194/egusphere-2022-330, 2022.